A STUDY OF CONFORMATION IN DISUBSTITUTED CYCLOHEXANES

by

Michael G. Roderick, B.Sc., P.G.C.E.

A thesis submitted during April 1986, in part fulfilment of the requirements for the award of M.Phil degree by the C.N.A.A. describing work carried out in the Department of Science at The Polytechnic of Wales.

INDEX

ACKNOWLEDGEMENTS

I would like to thank:

Dr.J.R. Dixon, my Director of Studies and Dr.P.S. McIntyre, my (Academic) Supervisor, for their encouragement throughout this work.

Mr.S. Reade, NMR Technician, and all other Technicians who gave me help.

Mrs. M. Lambert for typing this thesis.

Finally, as much of this thesis was written at home, I would like to thank Bethan and our children Gareth, Huw and Nia for bearing with me and the mountain of books and papers that have threatened to take over our dining room.

A STUDY OF CONFORMATION IN DISUBSTITUTED CYCLOHEXANES

by

Michael G. Roderick, B.Sc., P.G.C.E.

ABSTRACT

It is well known that the intermolecular hydrogen bonding is concentration and temperature dependent. It is also well known that ^1H chemical shift of a hydroxyl proton is dependent on concentration and temperature. ^1H NMR has been used to study hydrogen bonding in solution.

It was found previously by Becker, Liddel and Schoolery that at very high dilution in CCl_4, the chemical shift of the hydroxyl group in ethanol is directly proportional to the concentration. This was also found by Ouellette et al for cyclohexanol in CCl_4. The present author has extended this work to disubstituted cyclohexanol systems like trans-2-aminocyclohexanol, and the methylcyclohexanol isomers, in CCl_4 or $CDCl_3$ depending on the solubility of the solutes. The chemical shift at infinite dilution has been found to give an indication of an intramolecular hydrogen bond and the chemical slope to give a measure of the strength of the intermolecular H bond.

The effect of a lanthanide shift reagent on cyclohexanol, cyclohexylamine and the methyl cyclohexanols was looked at in a quantitative way.

Carbon-13 T_1 values were determined for the methylcyclohexanol isomers by Inversion Recovery Method and the results were compared with the Freeman-Hill Method. ^{13}C or ^1H T_1 values were used to give an estimate of the strength of intermolecular hydrogen bonding in the methylcyclohexanols.

The axial and equatorial chemical shifts of the proton of cyclohexanol and the methylcyclohexanol isomers were measured at around 190 K and also the position of resonance at 300 K.

1 INTRODUCTION

1.1 STEREOCHEMISTRY OF RING SYSTEMS

1.2 HYDROGEN BONDING

1.3 NMR

1.1 STEREOCHEMISTRY OF RING SYSTEMS

The five membered ring system

In the planar form cyclopentane has very little angle strain (the internal angle in a regular pentagon being 108^{o}, which is very close to the tetrahedral angle of 109^{o} 28′). However there is substantial eclipsing strain between adjacent hydrogen atoms, and hence it turns out that, by puckering the cyclopentane ring, more energy is gained through staggering the hydrogen atoms than is lost by the consequent increase in the angle strain in the molecule. As a result cyclopentane has the puckered forms shown below rather than the planar form shown.

Figure 1

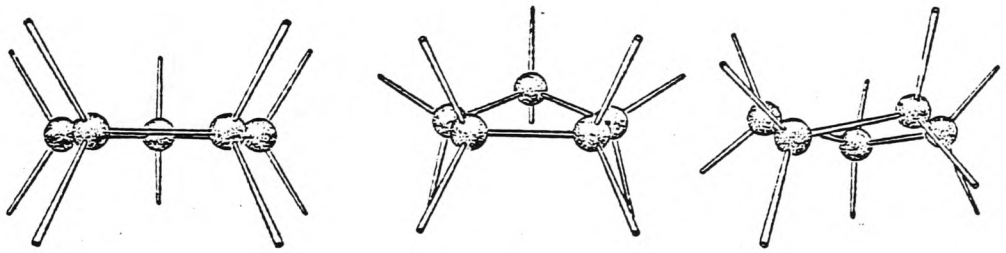

Envelope Half-chair

Planar Puckered

Cyclopentane

The shape of the ring is not fixed; the individual carbon atoms move up and down at right angles to the average plane of the ring in such a manner as to cause the irregularity or puckering to move around the ring in what has been termed by Pitzer[1] as "pseudorotation". Although in substituted cyclopentanes, one or the other, of the puckered forms may have greater stability, the conformational energy changes in the cyclohexane system are far more extreme, as will be

shown later, i.e. compared to the six membered system the cyclopentane system is fairly rigid.

The six membered ring system

It was pointed out by Sachse[2] in 1892 and later reviewed by Mohr[3] in 1918 that two puckered, i.e. non-planar models of cyclohexane could be constructed in which the valence bonds of all the carbons were at the tetrahedral angle, 109° 28′, to each other and which were therefore free of angle strain. These are a rigid or chair form and a mobile form which can readily be distorted into a variety of shapes, some of which resemble a boat. See Figure 2 below.

Figure 2

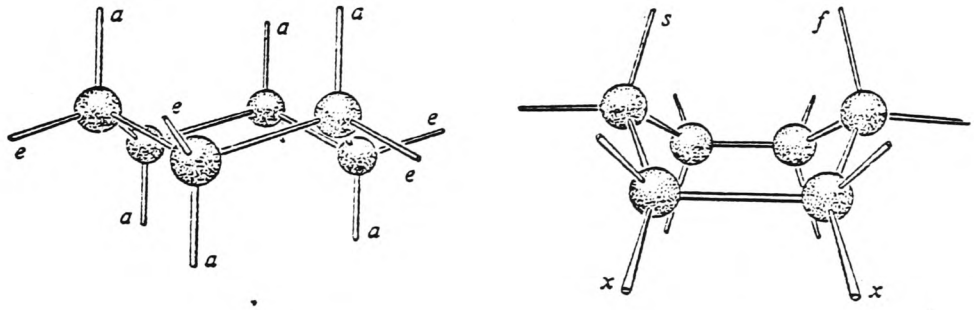

Chair

a Axial bonds
e Equatorial bonds

Boat

x-x Pair of eclipsed bonds
s-f Bowsprit-flagpole interaction

In the chair shaped molecule there are two types of bonds, namely those pointing up and down called axial (a), and those pointing sideways which are called equatorial (e).

In the chair form, not only is there no angle strain but there is no bond opposition (eclipsing) strain either and hence the potential energy is at a minimum (see point (a) in potential energy diagram shown in Figure 3).

When the bottom part of the chair is bent upward (or the back bent downward), the chair is transformed into a boat. However, during the transformation, some angular distortion is required because several bonds have to be rotated at the same time, and hence the molecule passes through a form of high potential energy point 'b' in Figure 3.

The height of this potential barrier has been determined by NMR[4] and is found to be of the order of 40 kJ mol^{-1}. However, at room temperature, this barrier is not high enough to prevent rapid interconversion.

In the boat form although there is no angle strain there is bond opposition strain involving the four pairs of hydrogens at the side of the boat i.e. one pair being x-x in Figure 2. There is also strain due to the interference of the pair of hydrogens shown in Figure 2 as s-f which are only 0.18 nm apart (the sum of the van der Waals radii of two hydrogens being 0.24 nm). This is sometimes called the "bowsprit-flagpole interaction." As a result of this the boat is considerably less stable than the chair. But by distorting the model in such a way as to pass from one boat to another, one obtains forms in which bowsprit-flagpole interactions and eclipsings of adjacent hydrogens are somewhat alleviated (see Figure 4). Hence in the energy diagram (Figure 3) these forms (sometimes called "skew-boat or twist forms") correspond to the energy minimum at point (c) with the true boat being at point (d). The difference in energy between the chair form and the flexible form has been estimated[5,6], to be of the order of 22 kJ mol^{-1}.

Figure 3

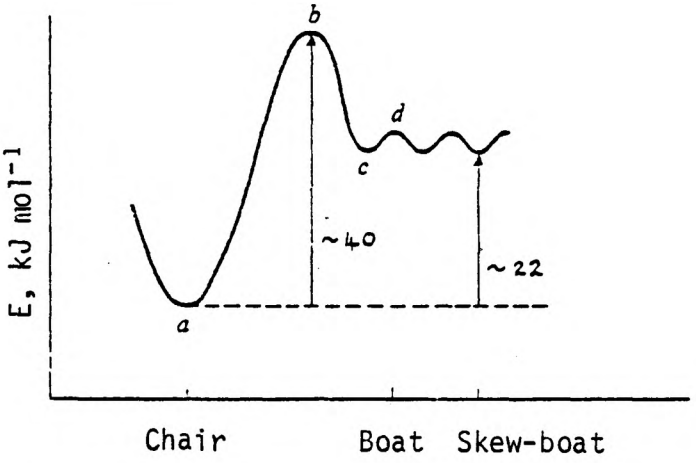

Potential energy of cyclohexane as a function of conformation

Figure 4

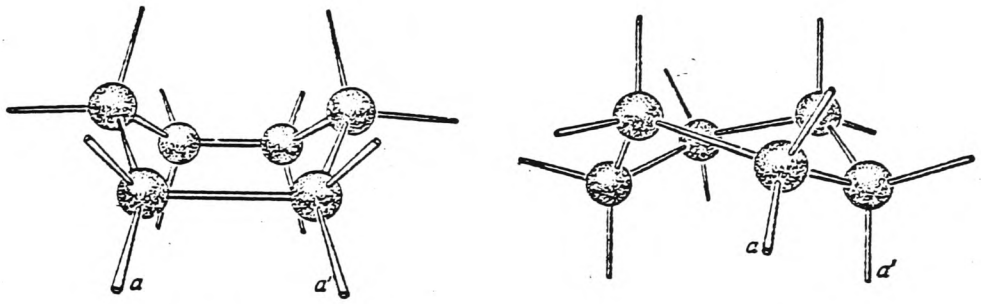

(a) Boat

(b) Skew-boat

Monosubstituted Cyclohexanes

Substituents attached to axial and equatorial bonds are customarily called axial and equatorial substituents respectively. However it has been shown previously that an equatorially substituted chair can be readily converted into a flexible form (see Figures 2 and 4), and this, in turn, can be similarly converted into another chair in which the substituent is now axial.

Figure 5

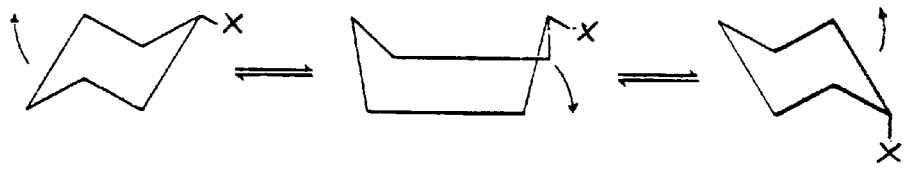

Equatorial (e) Present in very small concentration Axial(a)

Figure 5 shows the interconversion of chair forms of monosubstituted cyclohexane.

The two isomers (a) and (e) in Figure 5, are conformational isomers, or conformers. The difference in potential energy between them can be estimated from an inspection of the models. The axial isomer (a), has two interactions of the type present in the gauche form of butane (these are shown in heavy lines in Figure 5). No such interactions are present in the equatorial isomer (e).

The potential energy difference between the axial and equatorial forms, of course, depends upon the nature of the substituent, X and where X = OH the value[7] is given as 2.5 to 3.5 kJ mol^{-1}. The potential energy of cyclohexanol as a function of conformation is shown in Figure 6.

Figure 6

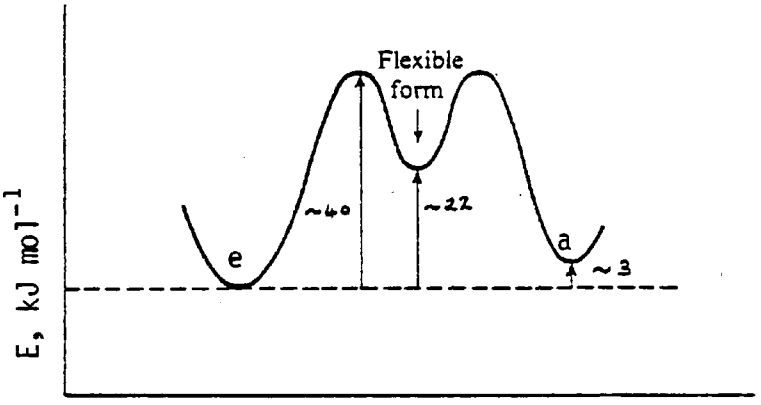

Disubstituted Cyclohexanes

On introducing a second substituent into the cyclohexane ring, diastereoisomeric forms are introduced i.e. one cis and the other trans. The disubstitution can be 1,2-, 1,3- and 1,4- and all three will exist in cis and trans forms. For simplicity, these may be written in a planar form (Figure 7), e.g. 1,2- disubstituted cyclohexane.

Figure 7

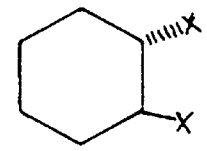

trans-isomer

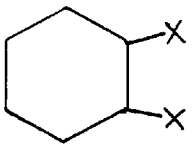

cis-isomer

However, as the cyclohexane ring is not planar, one needs to consider these isomers in the chair forms.

Figure 8

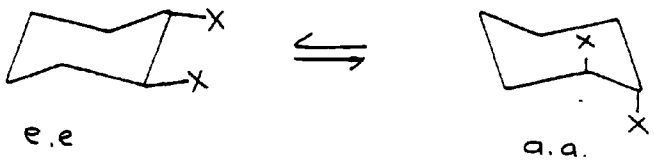

trans-isomer

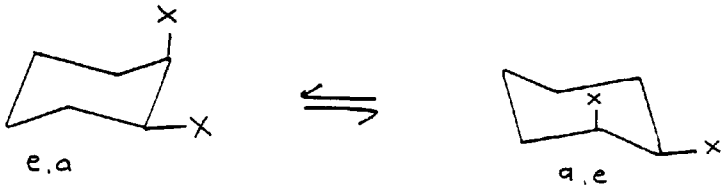

cis-isomer

It is worthwhile, here, looking at the cis and trans forms of 1,3- and 1,4- disubstitued cyclohexanes.

Figure 9 1,3- disubstituted cyclohexane (cis)

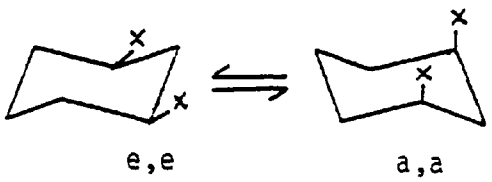

cis-isomer

Figure 10 1,3- disubstituted cyclohexane (trans)

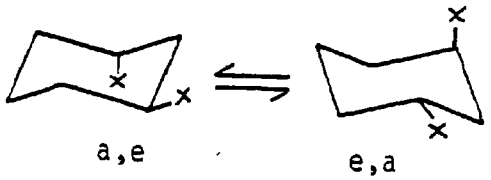

trans-isomer

Figure 11 1,4- disubstituted cyclohexane (cis)

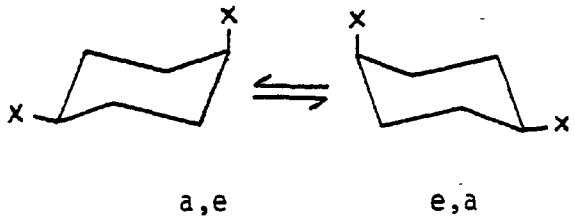

cis-isomer

Figure 12 1,4- disubstituted cyclohexane (trans)

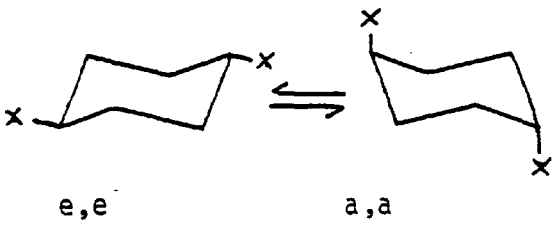

trans-isomer

It can be seen (Table 1) that the most stable conformer is the one where the interaction energy is lowest, indicated by the least number of interactions in this case.

TABLE 1

Isomer	Conformation	Number Gauche	Interaction kJ mol^{-1}
cis-1,2	e,a	3	11.3
	a,e	3	
trans-1,2	e,e	1	3.75
	a,a	4	15.0
cis-1,3	a,a	4	22.5 *
	e,e	0	0
trans-1,3	e,a	2	7.5
	a,e	2	
cis-1,4	e,a	2	7.5
	a,e	2	
trans-1,4	e,e	0	0
	a,a	4	15.0

In this table X = CH_3 in the conformers, and these are the number of butane gauche interactions. It would be expected that a similar sort of situation would occur when one X = OH although the CH_3 group is larger than the OH group.

Also, additional interaction between -OH groups must be considered, i.e. hydrogen bonding.

* includes diaxial methyl-methyl interaction.

1.2 HYDROGEN BONDING

The criteria for the existence of H-bonds are somewhat more clear cut than for other intermolecular interactions. Some convenient criteria for the existence of hydrogen bonding are listed below:

1. H-bonding occurs between a proton donor group A-H and a proton acceptor group B, where A is an electronegative atom, O, N, S, halogen and the acceptor group is a lone electron pair of an electronegative atom, or an orbital of a multiple bond system. Generally a hydrogen bond can be characterised as a proton shared by two lone electron pairs.
2. H-bonding is a distinctly directional and specific interaction. It is more localised than any other type of weak intermolecular interaction. Where the acceptor group is a π electron orbital, H-bonding is probably no more directed than a typical charge transfer complex such as that between iodine and benzene.
3. The total H-bond length R(A....B) is equal to or less than the sum of the van der Waal's radii of atoms A and B, that is the total bond length contraction caused by H-bond formation is equal to or is greater than twice the van der Waal's radius of the hydrogen atom.
4. The enthalpy of H-bonds generally falls in the range 4-40 kJ mol^{-1}. Intermolecular interactions other than H-bonding also fall within this range.
5. H-bonding is an association phenomenon. It causes a decrease in the total number of free molecules and an increase in the average molecular weight (except in the case of intramolecular hydrogen bonding where the H-bond exists in the monomer state). See Figure 14.

6. In H-bonding a specific covalent A-H group interacts with a specific acceptor site. The A-H bond is thereby weakened but not broken, and the properties of the acceptor group are also affected. All molecules can be conveniently classified into four groups with respect to their ability to participate in H-bonding; as was classified by Pimentel and McClellan[8], Table 2.

TABLE 2

Type	Description	Examples
I	Molecules with one or more donor groups (acids) and no acceptor groups.	Haloforms, highly halogenated compounds, alkynes.
II	Molecules with one or more acceptor groups (bases) and no donor groups.	Ketones, ethers, esters, alkenes, aromatics, tertiary amines, nitriles, isonitriles.
III	Molecules with both donor and acceptor groups.	Alcohols, water, phenols, inorganic and carboxylic acids, primary and secondary amines.
IV	Molecules with neither donor or acceptor groups.	Saturated hydrocarbons, tetrachloramethane, carbon disulphide.

Hydrogen bonding molecules are divided into type I, II and III. Molecules incapable of H-bonding form type IV. The latter includes compounds which are used as the so-called inert solvents in studies of H-bonded molecules. (In fact no completely inert solvent can exist, since dissolving takes place only through some interaction between solute and solvent molecules, but these 'inert' solvents exert minimal solvent effects).

Type I plus type II molecules form H-bonded complexes frequently in a simple ratio, 1:1. The strength of the hydrogen bonding depends primarily on the relative acidity of I and the basicity of II. The system trichloromethane-propanone is a typical example:

$Cl_3C\text{-}H + (CH_3)_2C{=}O$ $\qquad$ $Cl_3C\text{-}H \cdots O{=}C(CH_3)_2$

Hydrogen bond

The bonding in trichloromethane is worth noting as it was found necessary to use it as a solvent in the work carried out.

Type III molecules can self-associate by H-bonding with themselves. Two types of H-bonded complexes may be formed.

Intermolecular

This is the widest general class of H-bonding which involves the association of two or more molecules of the same or different substances. The resulting H-bonded complexes are not usually limited to dimeric linkages, but may produce chains, rings or three dimensional networks.

Figure 13

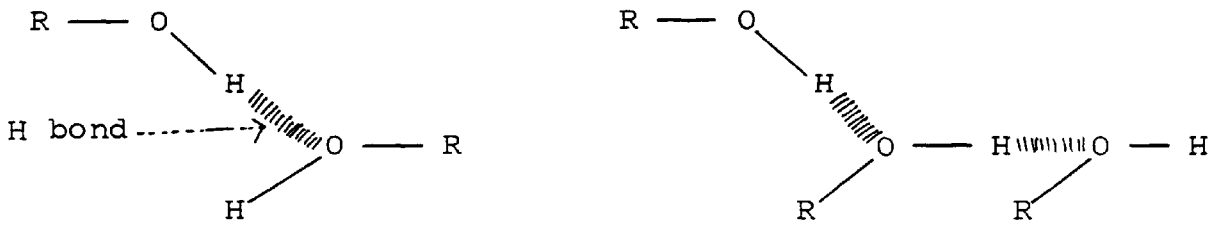

open / linear dimer and trimer.

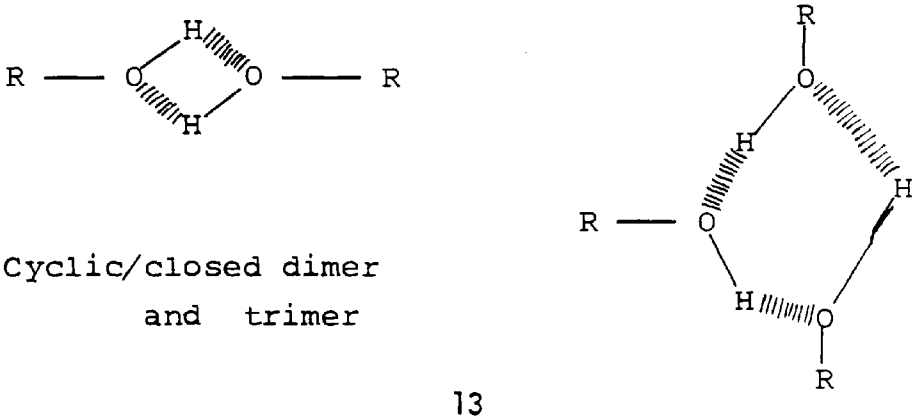

Cyclic/closed dimer and trimer

Because of the number and complexity of the molecular species possible in such systems, experimental results are difficult to interpret. Great simplification can generally be achieved through the use of the inert solvent, i.e. type IV. Dilution of a solution of self associated type III molecule by an "inert" solvent shifts the self association equilibria to the left, towards monomeric species. At sufficiently low concentrations (10^{-2} to 10^{-3} mol dm^{-3}) the type III molecules may be completely associated (this behaviour applies only to intermolecular H-bonding, since the extent of intramolecular H-bonding is little influenced by dilution with inert solvent).

Also, with molecules of type III, it should be noted that temperature will exert a great effect on the amount of association present, i.e. an increase in temperature will increase the thermal motion of the molecules and hence can break down the H-bonding (note again that this has the greatest effect on intermolecular H-bonding as opposed to intramolecular H-bonding).

Hence it is worthwhile stating that there are three main criteria which will affect H-bonding, namely:

I. Solvent

II. Concentration

III. Temperature

Thus in order to carry out any experimental work on H-bonding, it is necessary to keep two of the factors constant while varying the third.

In work with the aminocyclohexanols the temperature and solvent were kept constant while the concentration was varied.

Intramolecular

This other broad class contains those substances which have donor and acceptor sites within the same molecules; i.e. H-bond is formed between groups within the same molecule. This process was first called chelation, because of its pincer-like action resembling the closing of a crab's claw. However this picturesque model is lost in proteins and larger molecules so the more general term "intramolecular hydrogen bonding" is used.

Figure 14

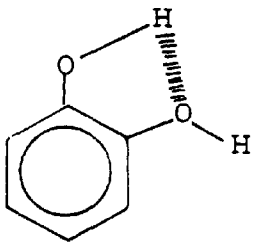

Catechol

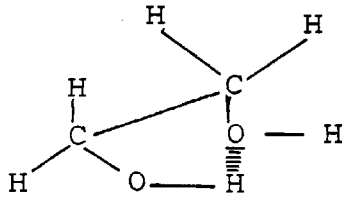

Ethylene Glycol

The strength of H-bonding depends upon the relative acidities and basicities of the donor and acceptor sites and in the case of intramolecular H-bonds, on the special arrangement present.

When molecules of type I or II are added to type III molecules, several H-bonding equilibria can coexist. In the case of type I plus type III molecules, the donor group of the type I molecules must compete with that of the type III molecule for the acceptor site(s) in the latter. This competition generally leads to a decrease in the extent of the self association of type III molecules and the formation of one or more new H-bonded complexes between the two types of molecules.

1.3 EFFECT OF HYDROGEN BONDING ON SPECTROSCOPIC MEASUREMENTS PROTON MAGNETIC RESONANCE

The formation of a hydrogen bond A-H ··· B modifies the electron density around the proton of the A-H group and hence its shielding. In most cases the PMR absorption is displaced downfield (lower magnetic field), causing a hydrogen bonding shift which is added to the existing chemical shift. Therefore the hydrogen bonding shift is usually negative, with the exception of some cases involving aromatic molecules.

There are several contributions to the H-bonding shift:

1. The electronic structure of the A-H group is distorted by the presence of the proton acceptor group B. The electric field of the latter tends to draw the H away from the bonding electrons of the A-H bond and to reduce the electron density in the immediate vicinity of H. The contribution of this effect to the H-bonding shift is always negative, since the deshielding of the H will cause its resonance signal to occur at lower magnetic fields than on the absence of B.
2. Another contribution is also provided by group B. The secondary magnetic field at the proton due to electron currents in the group B will be non-zero when the electron cloud of group B is not spherically symmetrical and is therefore magnetically anisotropic. This contribution can be either positive or negative, but will be positive if the principal symmetry axis of B is along the A-H axis (i.e. increased shielding, requiring a stronger magnetic field). This contribution is not large, generally of the order of 0.6 ppm. When B is an aromatic ring, a large positive contribution can occur.
3. A related effect is one that can be ascribed to the relative orientations of groups A-H and B. If A-H acts as a donor to a group B with the molecular axis of the two at the same angle, then

the axial symmetry required for the presence of contribution 2 will be partially removed and the paramagnetic high field shift will be reduced. This will appear as a shift to low field on association. Such an effect may be important in hydrogen bonding interactions where the A-H group associates with the π bonding electrons of another group, e.g.

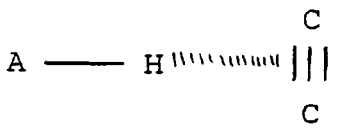

Generally contribution 1 is the principal one, and has been ascribed simply by Schneider, Bernstein and Pople[9] to two phenomena:

(a) partial withdrawal of the proton from its electronic environment by the electronegative acceptor atom

(b) inhibition of electronic circulation about the proton by the electric field of the electronegative atom.

Hence in the case of an -OH group the relative position of its resonance indicates to a greater or lesser extent of H-bonding, a high field shift corresponding to less H-bonding. With some reservation this is a good approximation, although electronic screening, steric hindrance and inductive effects should not be overlooked completely.

High resolution PMR spectroscopy is very useful in the study of H-bonding phenomena in liquids and solutions. In solutions concentrations are limited to about 0.01 $mol.dm^{-3}$ or more, in order to provide a sufficient number of protons for a measurement. Hydrogen-bonded shifts are clearly revealed when the PMR spectra of H-bonded species such as alcohols or amines are measured as a function of temperature and concentration in "inert" solvents.

The following diagram shows the appearance of the PMR spectrum of liquid ethanol and its progressively more dilute solutions in CCl_4. The positions of the methyl triplet and the methylene quartet are affected very little by dilution. The OH signal, however, moves from approximately 5 ppm downfield from TMS in pure ethanol to approximately 1 ppm in 0.1 mol.dm^{-3} solutions of ethanol in CCl_4.

Figure 15

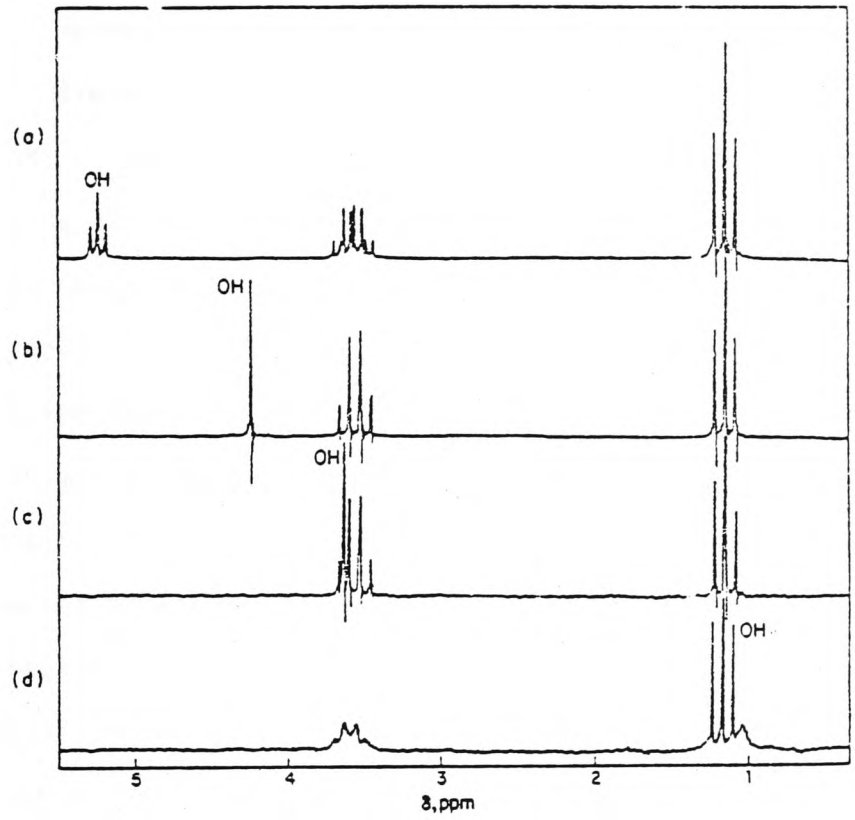

PMR spectra of ethanol at 60 MH_z and 40^{o}C

(a) Liquid ethanol
(b) 2.2 mol.dm^{-3} ethanol in CCl_4
(c) 1.1 mol.dm^{-3} ethanol in CCl_4
(d) 0.11 mol.dm^{-3} ethanol in CCl_4

all with TMS standard

In pure ethanol the OH resonance is a triplet and the CH_2 resonance is more complex than a quartet because of coupling between OH and CH_2 protons. The increase in shielding of the -OH proton, indicated by the shift of the -OH resonance to higher magnetic field with decrease in concentration is due to the dissociation of H-bonded (self associated) alcohol complexes.

It might be expected that in self associated hydroxylic compounds, individual -OH resonances would be observed for non-H-bonded hydroxyl groups in monomers, as well as for H-bonded hydroxyl groups in cyclic and open dimers, trimers and n-mers and so on. In PMR the signal of the proton is the weighted average of all the protons in their environments in the free as well as the associated forms. The time required for the resonance measurement (the time of spin orientation on the magnetic field, about 10^{-2} to 10^{-3} sec.) is long compared to the life-times of H-bonded species which is 10^{-12} to 10^{-13} sec., because of the very rapid formation and breaking of H-bonds in solution. In a time of the order of 10^{-3} sec. the H of an A-H group will participate in many H-bonds with neighbouring molecules. Accordingly it will experience at each concentration an averaged out environment which will depend on the number and kind of proton donor species present. In the case of self associated systems this fact decreases the usefulness of PMR as a method of investigating the nature of the H-bonded dimers and n-mers and their equilibria. However in cases where there is only one type of proton donor H-bonded to acceptor molecules in 1:1 complexes, the PMR method is a very powerful method for studying H-bonding.

The main method used to obtain the unassociated value of the chemical shift is the method explained above for ethanol (i.e. successive dilution) and extrapolating the results to infinite dilution. This method

undoubtedly introduces some error in the H-bond shifts, however comparisons can be made for data collected under similar conditions.

In the above, the type of H-bonding discussed is intermolecular and successive dilution down to almost infinite dilution will ensure the presence of the monomer. However, in the case of an intramolecular H-bond, it is not affected by dilution and hence the -OH resonance will appear at a much lower magnetic field due to the deshielding effect, i.e. at finite dilution, in the case of association (i.e. intermolecular H-bonding) the -OH groups will be 'free' whereas in the case of intramolecular H-bonding the -OH groups will <u>not</u> be free.

A fact worth noting is that intramolecular hydrogen bonds tend to be bent rather than linear.

Here it is well worth mentioning the work carried out by Becker, Liddel and Shoolery[10], in which they made a detailed study of the ethanol -OH dilution shift in CCl_4 solution, with particular attention to the behaviour at low concentrations of ethanol.

Their results are shown below.

Figure 16

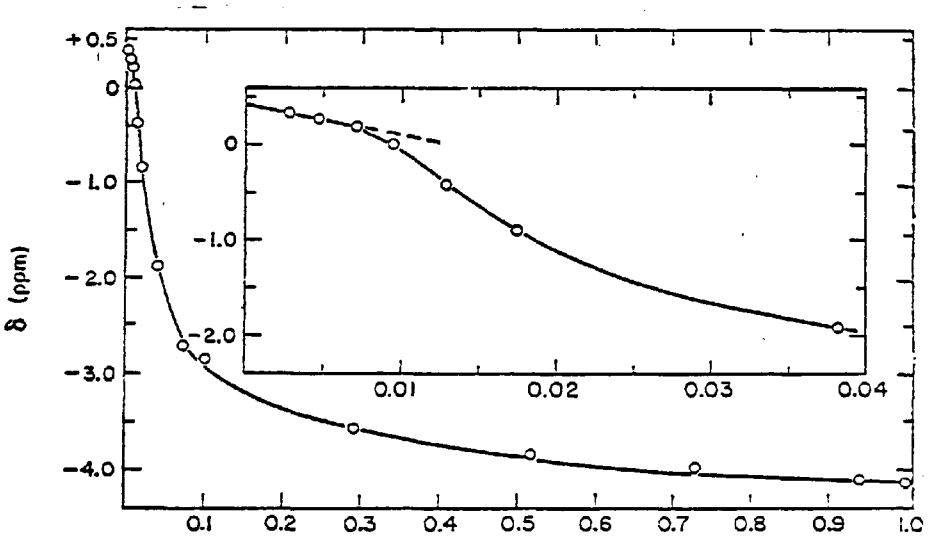

Figure 16 shows the chemical shift of hydroxyl-proton resonance versus ethanol concentration in CCl_4 at room temperature. The chemical shift reference point is the methyl group resonance of ethanol.

The general shape of the curve, including the reversal in curvature at N near 0.015 is of the form to be expected for a system of monomers, dimers and high polymers. The value of δ m, the limiting chemical shift, corresponding to the -OH resonance of the monomer, can then be obtained by extrapolation to N = 0.

At very low concentrations of ethanol, the -OH proton shift is influenced almost entirely by the monomer-dimer equilibrium. The limiting slope of the dilution curve, i.e. from approximately N = 0.015 to infine dilution, gives some very useful information.

Intermolecular and Intramolecular Hydrogen Bonding in Ring Systems (PMR)

The dependance of chemical shift on concentration has been studied by Ouellette, Booth and Liptak[11], and they showed the graph obtained by plotting concentration versus chemical shift to have the same general shape as the curve obtained for ethanol (Figure 16). The graph gives a linear slope in the region 0.02 to 0.002 mole fraction range.

A similar curve was obtained with cyclohexanol.

In cyclohexanol only one hydroxyl group is present and hence only intermolecular H-bonding can occur.

Hence the results given for the limiting chemical shift are a measure of the monomeric hydroxyl proton at infinite dilution and are a standard set for the absence of intramolecular hydrogen bonding.

A similar set of conclusions can be applied to the results with cyclohexylamine.

When an amino and a hydroxyl group are both introduced into a cyclohexane system the possibility for intramolecular hydrogen bonding will exist.

Dilution has a great effect on intermolecular H-bonding but not on intramolecular H-bonding. Hence when intramolecular H-bonding is present in a compound the hydroxyl resonance position (limiting chemical shift) would be expected to be much larger, i.e. further downfield from TMS than that of a free hydroxyl proton.

In order to test this the concentration versus chemical shift plots of 1-amino-1-hydroxymethylcyclopentane should have inter and intramolecular hydrogen bonding.

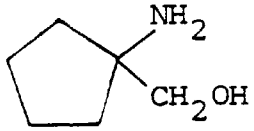

Similar experiments were carried out with trans-2-aminocyclohexanol.

trans-2-Aminocyclohexanol

As a result of the chemical shift versus concentration technique using cyclohexanol, cyclohexylamine and 1-amino-hydroxymethylcyclopentane methanol for comparison, it is possible to predict the conformation of trans-2-aminocyclohexanol.

Consider the possible conformations of the isomer.

Figure 17

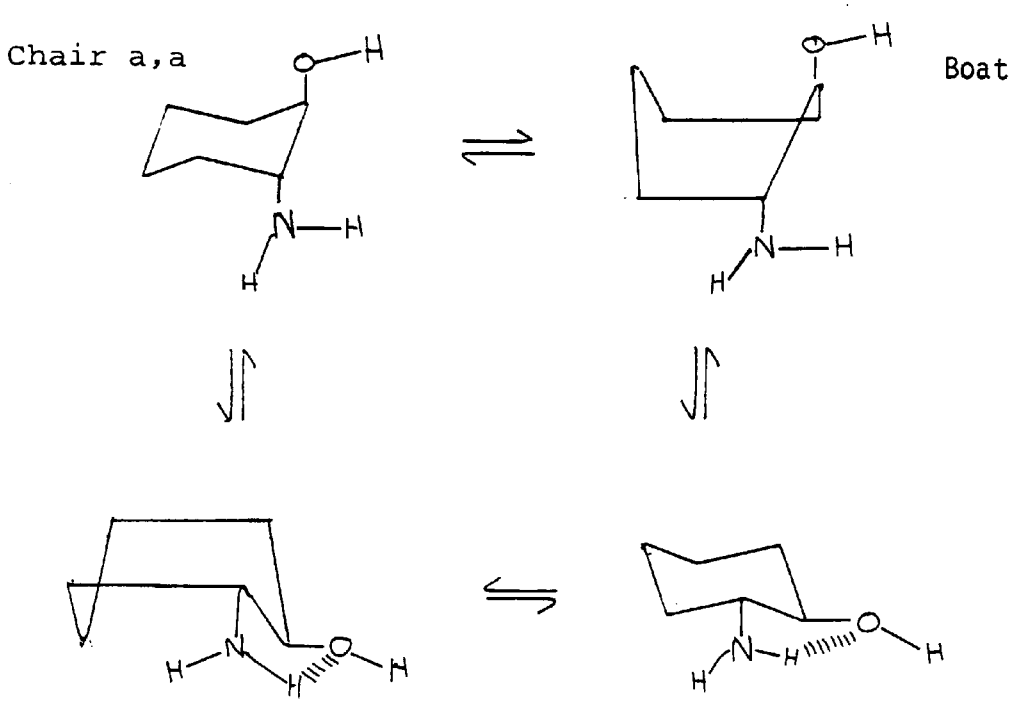

From Figure 17 it can be seen that in the chair conformer the hydroxyl and amino groups are diaxial which is energetically unfavoured whereas in the alternate chair the two groups are diequatorial which is energetically favoured.

The results seem to indicate that the trans isomer forms an intramolecular H-bond.

Conformational Analysis with Lanthanide Shift Reagents

The usefulness of NMR in the study of large hydrocarbon compounds has been severely limited by insufficient resolution. Although this deficiency has been partially overcome by the development of higher frequency spectrometers the situation still remains unsatisfactory since considerable structural information usually remains buried in a featureless methylene methine envelope common to such systems. However the addition of a shift reagent like Europium-tris(1,1,1,2,2,3,3.-heptafluoro-7,7,-dimethyl,-4,6,octadionate) causes a shift in the NMR resolutions of the protons to high field. It is believed that a co-ordination complex is formed between an -OH or $-NH_2$ on the molecule and the shift reagent. There is a different chemical shift on the addition of increased amounts of the shift reagent.

In these experiments approximate deuteriochloroform resonance positions for various protons in cyclohexanol and cyclohexylamine can be obtained by extrapolation of the concentration lines to their origin. Also if resulting $CDCl_3$ values for the different protons are subtracted from corresponding values obtained by extrapolating in the opposite direction to a point where the molar ratio of complex to solute is one, a paramagentic induced shift for different solute protons is determined.

The experiments were carried out by dissolving cyclohexanol and $Eu(fod)_3$ deuteriochloroform at room temperature 19^oC.

For cyclohexanol the proton chemical shifts were taken.

For cyclohexylamine the C^{13} chemical shifts were taken.

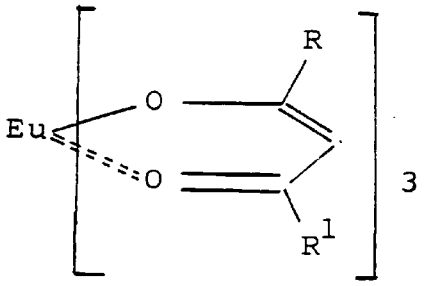

If R = R_1 = tert Bu, Eu(DPM)$_3$
If R = tert Bu, R^1 = CF_3, Eu(PTA)$_3$
If R = tert Bu, R^1 = CF_2 CF_2 CF_3, Eu(fod)$_3$

Eu(fod)$_3$ is Europium-tris(1,1,1,2,2,3,3.-heptafluoro-7,7,-dimethyl, -4,6,octadionate).

M_r = 1037.5

C_{30} H_{30} Eu F_{21} O_6

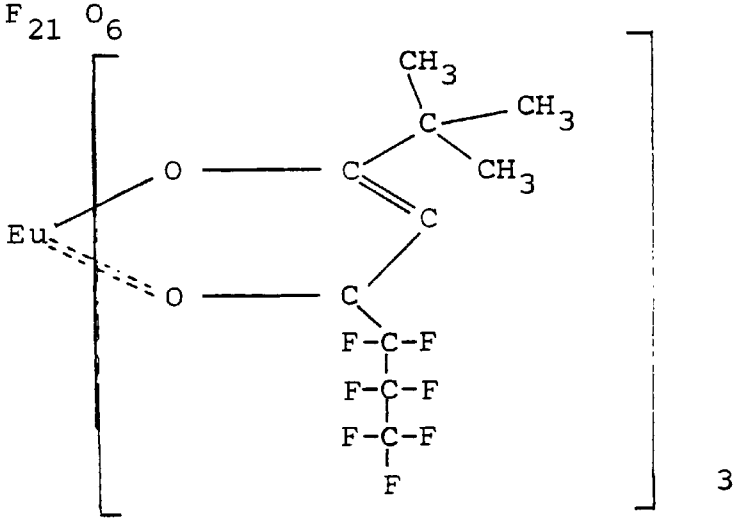

Eu(fod)$_3$ has better solubility in many inert solvents.

The Conformational Preference of the Hydroxyl Group in Cyclohexanol[12a] and the Methylcyclohexanol Systems

NMR spectroscopy can be used to study molecular changes, in particular exchange of atomic positions that take place on what is called the "NMR Time Scale." This covers processes that take place between about once a second and a million times a second. It is so called because these processes are too slow to be caught by electron, neutron or X-ray diffraction or electron vibrational spectroscopy, but too fast to be studied by conventional kinetic methods. Consider cyclohexane, the protons in cyclohexane have two distinct environments:

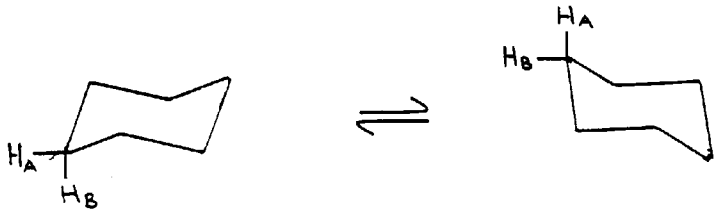

The flipping of the cyclohexane ring occurs too fast at room temperature to see the two separate kinds of proton since each axial proton becomes an equatorial one and vice versa. The protons exhibit an average environment and the signal is a sharp singlet. As the sample is cooled down, the flipping becomes slower and the axial and equatorial protons can be distinguished; first the resonance broadens and then at low enough temperature the spectrum consists of two resonances. The axial and equatorial protons spins are coupled together and are also coupled to other protons on the ring, resulting in broad second order peaks.

Consider cyclohexyl bromide, here we can obtain quantitative information from NMR spectra. Again at room temperature there is rapid interconversion between the two chair forms shown below:

Figure 18

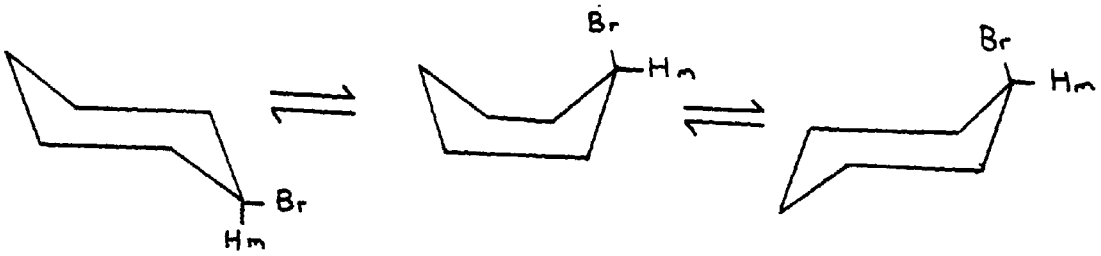

At 273 K the spectrum looks like this:

Figure 19

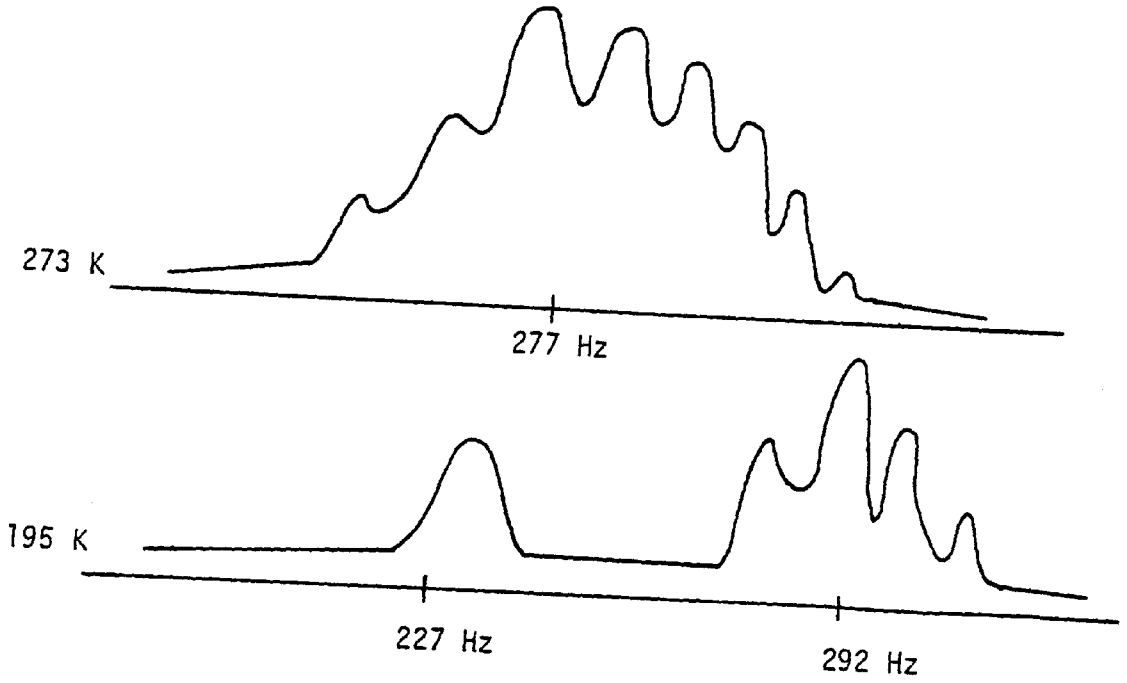

At 195 K we can see separate absorptions for axial and equatorial methine protons centred in 227 and 292 Hz wrt $CHCl_3$.

Figure 20

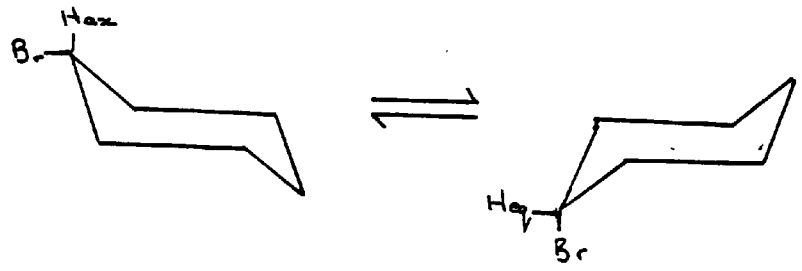

The relative amount of axial to equatorial H can be determined by integration at 195 K.

At room temperature however, the position of equilibrium is likely to be different and can not be measured since there is only a weighted mean resonance (say Z Hz). However, since it is an averaged position, the proportions can be obtained by linear interpolation between the axial and equatorial shifts which is known from the low temperature measurements.

Y Hz corresponds to 100 % axial conformer

X Hz corresponds to 0 % axial conformer 100 % equatorial

Z Hz corresponds to $\frac{Z-X}{Y-X}$ x 100 of axial conformer at room temperature

This then gives a value for the equilibrium constant = $\frac{Heq}{Hax}$ at temperature TK where Hax is the conformer with the Br equatorial.

The difference for the Gibb's Function at TK can be obtained from:

$$\Delta G^0 = -RT\ln K_{eqm}$$

Examination of the NMR spectrum of cyclohexanol in a 50:50 mixture of deuteriochloroform and carbon disulphide at around 190 K revealed two resonances.

Figure 21

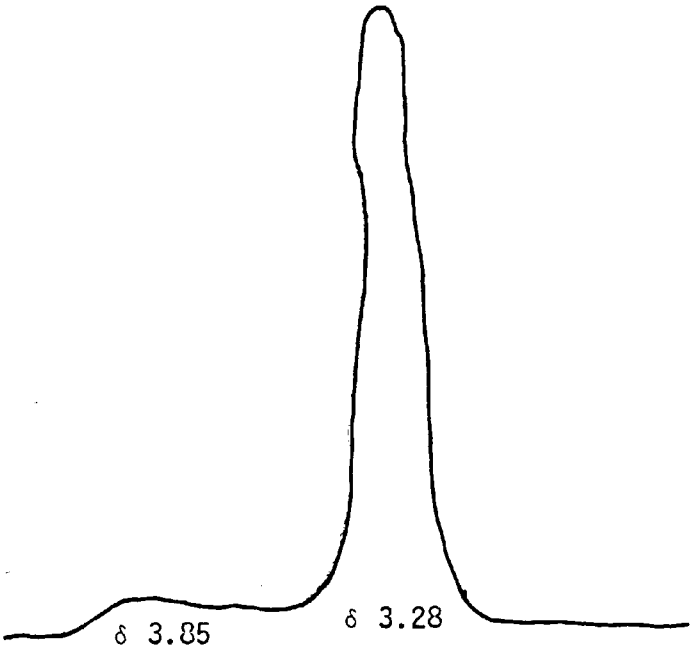

A Axial (δ 3.28) and equatorial (δ 3.85) resonances of the proton in cyclohexanol at 190 K

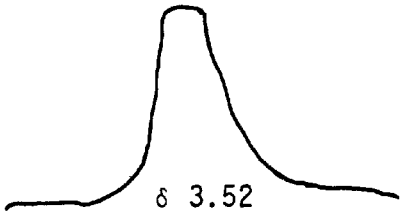

B Average resonance position of the proton in cyclohexanol at 300 K

Background Theory of NMR

NMR in Perspective

The development of nuclear magnetic resonance spectroscopy (NMR) ranks among the most important advances in chemical physics during the period since its origins in the late 1940's. Few other spectroscopic methods have enjoyed such spectacular development and offered such a direct and detailed insight into events at the molecular level. In recent years the volume of literature on NMR has grown on a truly massive scale and virtually every branch of chemistry has received new impetus as a consequence. Its importance is reflected in the rapidly growing number of applications, which cover such broad fields as organic and inorganic chemistry and, more recently, biochemical and biomedical sciences.

With the advent of commercially available multinuclear pulsed NMR apparatus and the role of ^{1}H and ^{13}CMR, the organic chemist has acquired a versatile and extremely powerful tool for compound analysis. Indeed it was a technological lag which held up the rapid development of this spectroscopic field, in that instrument design could not keep pace with the theoretical ideas, particularly during the 1960's. However, with the amazing surge in the development of computer technology and the importance of software, the technologists were able to incorporate analogue to digital convertors into existing instruments to assist in spectral analysis. It was thus a short step before the ideas of pulsed excitation and Fourier-Transformation (FT) became realities. Thanks to the capabilities of computers, chemists involved in NMR now talk in terms of two dimensional spectra and their analysis.

Basic Concepts

The fundamental concepts on which the theory of NMR spectroscopy rests was suggested by Pauli[12b] in 1924. His discovery of hyperfine structure in atomic spectra led him to suggest that certain nuclei possess angular momentum and thus a magnetic moment which interacts with the atomic orbital electrons. His idea was later confirmed by spectroscopic work which enabled values of the angular momentum and moment to be determined for many nuclei. When subjected to a magnetic field such magnetic moments take up specific orientations and thus it is possible to observe transitions occurring between the nuclear energy levels associated with these orientations by irradiation with energy of a suitable frequency. This is the crux of all NMR spectroscopic techniques.

Magnetic Properties of Nuclei

These properties of nuclei are somewhat analagous to those of orbital and intrinsic moments of the electron. From quantum mechanics the components of the nuclear angular momentum in any direction may take values $\frac{mh}{2I}$, where h is Planck's constant, and m is the discrete spin variable whose range consists of 2I + 1 values.

$m = -I, (-I-1), \ldots\ldots, (I-1), I$

I = spin quantum number

I is an integer for nuclei with even mass number and $\frac{1}{2}$ integer for nuclei with odd mass number, e.g.

^{1}H, ^{19}F, ^{13}C, $I = \frac{1}{2}$

^{2}H, ^{14}N, ^{12}C, $I = 1$

From classical physics, a rotating sphere of mass M and charge e will have a magnetic moment given by magnetic moment, $\mu = \frac{Pe}{2M}$.

Thus for a nucleus $\mu_a = \frac{gPe}{2M_nC}$ Eqn (1)

where M_n = mass of nucleus

g = nuclear g factor (positive or negative depending on nucleus)

P = angular momentum

μ_a = magnetic moment of nucleus

C = velocity of light (3×10^8 ms^{-1})

e = charge of an electron ($-1.6 \times 10^{-19}C$)

The direction in which this moment acts is called the

Magnetic Axis

For all nuclei with an even mass number and an even atomic number, $\mu_a = 0$, that is, neutron proton pairs nullify spin effects. Such nuclei will have no NMR spectra

Angular momentum of a nucleus may also be obtained from quantum theory.

$$P = \frac{h}{2\pi} \; I\,(I+1)^{\frac{1}{2}} \qquad \text{Eqn (2)}$$

Elimination of P from equation (1) yields:

$$\mu_a = \frac{geh}{4\pi M_n C} \; I\,(I+1)^{\frac{1}{2}} \qquad \text{Eqn (3)}$$

Therefore $\mu_a = g\mu_N \; I\,(I+1)^{\frac{1}{2}}$ Eqn (4)

where μ_N is the nuclear magneton.

The nuclear g factor, sometimes referred to as the Lande or splitting factor, is a measure of the spin and orbital motion of the particle in relation to its angular momentum.

Figure 22

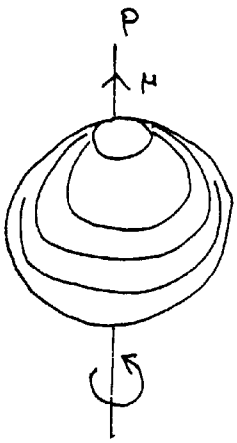

(a) Classical model of a spinning charged particle

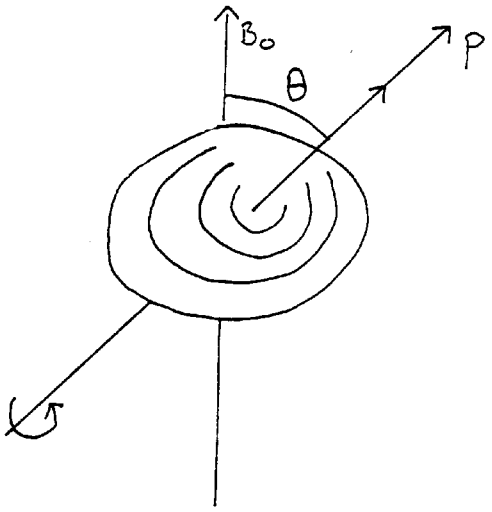

(b) Larmor Precession of Nuclear Spin Axis about the direction of the applied field, B_o

In order to analyse the behaviour of a nucleus in a magnetic field, it is convenient to consider the nucleus as a bar magnet with a magnetic moment as given in equation (4). Thus, when placed in a magnetic field, it will tend to align itself with the field according to classical concepts of magnetism [13,14]. However, since nuclei are actually spinning, it is essential to consider and account for the principle of Conservation of Angular Momentum. Thus, the nucleus will possess the properties of a gyroscope, that is, it will precess about the field direction. This precession is usually called the LARMOR PRECESSION - which has a definite frequency of precession known as the LARMOR FREQUENCY.

Now the potential energy (V) of the nuclear magnetic in a field, B_o Tesla, is given by:

$$V = -\mu_a B_o \cos\theta = -\mu_b B_o \qquad \text{Eqn (5)}$$

where μ_b = component of μ_a in the direction of the field θ = angle between magnetic axis and B_o.

As there are always 2I + 1 possible values of m (i.e. the number of possible orientations of the nuclear magnetic in the applied field), then this statement can be utilised in a consideration of the actual moment along the field.

As a consequence, the actual moment along the field μ_H, is restricted to:

$$\mu_H = \frac{ge}{2M_nC} \cdot \frac{mh}{2}$$

$$\text{i.e. } \mu_H = \mu_N gI$$

$$\text{therefore } \mu_H = \mu \cdot \mu_N \qquad \text{Eqn (6)}$$

where $\mu = gI$ = the magnetic moment of the nucleus and thus obviously varies for all nuclei as g varies. This magnetic moment will determine the sensitivity of any particular nucleus to radiation. An illustration of the variation of μ with g and I is shown in the following Table for selected nuclei:

TABLE 3

Nucleus	Factor	Spin I	Magnetic Moment $\mu = gI$
^{1}H	5.585	$\frac{1}{2}$	1.913
^{4}He	0	0	0
^{7}Li	2.171	$\frac{3}{2}$	3.257
^{9}Be	-0.785	$\frac{3}{2}$	-1.1718
^{13}C	1.405	$\frac{1}{2}$	0.702
^{19}F	5.256	$\frac{1}{2}$	2.628

For a particular energy transition the energy change can be expressed as:

$$\Delta V = g \mu_N B_o$$

and this then is the energy required to reverse the direction of the magnet in the field. Thus, if transitions occur between these energy levels, then the frequency of the absorbed (and emitted) light will be:

$$\nu = \frac{g \mu_N B_o}{h} \quad \text{as} \quad \nu = \frac{V}{h} \quad \text{and} \quad \hbar = \frac{h}{2\pi} \qquad \text{Eqn (7)}$$

$$\text{therefore} \quad \nu_o = \frac{\gamma B_o}{2\pi}$$

where γ is the magnetogyric ratio and this quantity again varies from nucleus to nucleus.

Hence $\gamma = \frac{g\,\mu_N}{\hbar} = \frac{\mu}{I\hbar}$ Eqn (8)

The frequency ν_0 is the Larmor frequency. It is now clear that the theory is based on a resonance phenomenon, that is, in order to observe a spectrum the nucleus involved must be irradiated with light (electromagnetic radiation) of frequency equal to the Larmor frequency of that nucleus.

The Resonance Phenomenon

The NMR phenomenon relies on the nuclear interaction between the nuclear moment μ which precesses about B_0 at the Larmor frequency ν_0 (see Figure 22) and a small magnetic induction B_1, perpendicular to B_0 and rotating about B_0 at frequency, ν, in the same direction as μ. In practice, B_1, is a linear radio frequency (RF) field oscillating in the x or y direction.

Figure 23

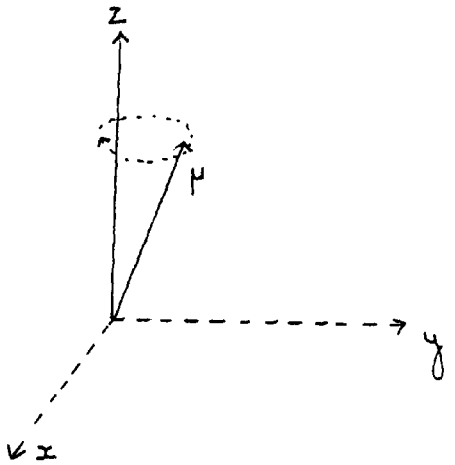

Precession of a nuclear magnetic moment μ, in a magnetic field B_0

However, such a field may be considered as equivalent to a pair of circulating polarised components, rotating in the X-Y plane with equal angular velocities but opposite directions. Only the component which rotates in the same direction as the magnetic moment, μ, is able to influence its motion. Resonance is attained when the frequency of B_1 exactly equals ν_0.

$$\nu = \nu_0 = \frac{\gamma B_0}{2\pi} \qquad \text{Eqn (9)}$$

Hence in order to observe the resonance of protons orientated by a magnetic field B_0 of 2.35 T, there must be an applied field, as calculated from above, an RF field of B_1 of $\nu = \nu_0 = 100\ MH_E$.

In energy terms, it can be considered that a field of B_1 of frequency ν induces transitions between the nuclear spin levels (see Figure 23) when its energy, $h\nu$, equals the energy difference is given by:

$$\Delta \varepsilon = \gamma \frac{h}{2\pi} B_0 \qquad \text{Eqn (10)}$$

between adjacent levels, when condition in Eqn (9) is fulfilled.

Quantum Mechanical Description of NMR

At this stage of the development of the theory it is important to grasp the explanation of NMR phenomena put forward by quantum mechanical theory.

When a nucleus of magnetic moment, μ, is placed in a magnetic field the Hamiltonian for the system is given by:

$$H = \mu B_0 \qquad \text{Eqn (11)}$$

and since $\mu = \gamma \frac{h}{2\pi} I$ from Eqn (8)

then $$H = \gamma \frac{h}{2\pi} B_0 I \qquad \text{Eqn (12)}$$

The expectation values of the Operator I are m, hence the expectation energy levels of the system are:

$$\varepsilon = \gamma \hbar m B_0 \qquad \text{Eqn (13)}$$

In order to induce transitions between the energy states, a perturbation of some kind must be introduced. A suitable perturbation is the application of an oscillating magnetic field, and the necessary direction of this field can be decided from the properties of the spin operators and eigen functions appropriate to a nucleus spin I.

The resultant equation as a solution of time dependent perturbation theory[15], gives an expression for the probability W^1 of a transition between the two levels when an oscillating field is applied along the axis:

$$W^1 = \gamma^2 B_1^2 |\alpha|Iz|\beta|^2 = 0 \qquad \text{Eqn (14)}$$

where α and β are spin eigen functions.

Here transitions can not be induced with this arrangement of the steady and oscillating magnetic fields.

If an oscillating field is applied along the X axis:

$$(\alpha|Ix|\beta) = \tfrac{1}{2}\hbar \qquad \text{Eqn (15)}$$

and a similar finite transition probability is obtained if the oscillating field is regarded as applied along the Y axis.

The change in energy when a transition takes place is:

$$\Delta \varepsilon = \gamma \hbar B_0 \qquad \text{Eqn (16)}$$

thus the frequency of the magnetic field must be:

$$\nu = \frac{\Delta \varepsilon}{\hbar} = \frac{\gamma B_0}{2\pi} \qquad \text{Eqn (17)}$$

which is the resonance condition.

For the general case of a nucleus of spin I the transition probability between two energy levels m and m^1 is given by:

$$W^1 = \gamma^2 B_1^2 |T_m|I_X|T_{m'}|^2 \qquad \text{Eqn (18)}$$

which is non-zero only when $m = m^1 \pm 1$, that is, transitions between nuclear energy levels are governed by the selection rule $\Delta m = \pm 1$.

Transition probabilities for the general case of a nucleus of spin I have also been calculated by a perturbation method.

Population of Spin States and the Effect of the Boltzmann Distribution

Most problems encountered in carbon-13 NMR spectroscopy were, in some way, associated with the sensitivity of the spectrometer. NMR is known to be an intrinsically insensitive technique when compared to U.V./visible or I.R. spectroscopy. This is so for two basic reasons:

1. The energy difference $\Delta \varepsilon$ between the ground state and excited states is comparatively small, and, consequently
2. The population differences are also small.

The phenomenon of population differences may be studied by considering the Boltzmann distribution laws and firstly looking at the analogous situation in optical spectroscopy.

The absorption coefficients obtained in optical spectroscopy are independant of the intensity of the radiation source. Normally a rapid return is made from the excited state to the ground state, the liberated energy being dissipated as heat. In NMR spectroscopy, the intensity of radiation may weaken the absorption signals or cause them to disappear entirely. The situation is a consequence of the isolation of a nucleus from its surrounding lattice. In the case of a liquid, the nucleus may remain isolated for a few seconds while this can be extended to hours

for solids at low temperature. However, fluctuating magnetic fields associated with either inter or intra molecular motion in the sample will have components at the resonance frequency and they will induce a return to the ground state. While for most of the electromagnetic spectrum the probability of stimulated emission (or absorption) induced by irradiation is usually negligible, for NMR it is usually large and in comparison the probability of spontaneous emission is negligible (the excited state would have a lifetime of about 10^{18} years for hydrogen nuclei). Because of this irradiation with an intense radio-frequency field would rapidly equalise the population of energy levels. A dynamic equilibrium would be set up between the levels but no absorption would be detected.

If there is a Boltzmann distribution of nuclei among the spin states, a net absorption of energy may be observed on application of a low intensity of radiation at the resonance frequency. For an assembly of weakly coupled identical nuclei of spin value, $\frac{1}{2}$, the energy levels derived for an isolated nucleus may be applied to the assembly as a whole. It must be assumed that nuclei do not interact with any other part of the system. When there is thermal equilibrium throughout the assembly then the relative population of the two energy levels is given by:

$$\frac{N_2}{N_1} = \exp \frac{-\Delta \varepsilon}{KT} \qquad \text{Eqn (19)}$$

where N_2 and N_1 are the number of nuclei in the high and low energy levels respectively; K is the Boltzmann constant and T the absolute temperature.

But by equation (16) it may be said:

$$\Delta \varepsilon = \gamma \hbar B_0$$

$$\text{Hence } \frac{N_2}{N_1} = \exp - \frac{\gamma \hbar B_o}{KT} \qquad \text{Eqn (20)}$$

$$\text{Therefore } \frac{N_2}{N_1} = \exp \frac{2 \mu B_o}{KT}$$

For small values of the argument in the exponential approximation:

$$e^{-X} = 1-X$$

may be employed to show that the fractional excess population in the lower level is:

$$\frac{N_1 - N_2}{N_1} = \frac{2 \mu B_o}{KT} \qquad \text{Eqn (21)}$$

Thus, for H, which has a large magnetic moment, in a field of 1.4 Tesla, this fractional excess is only 1×10^{-5} at room temperature.

On examination of equation (2) the desirability of the main magnetic field being as large as possible becomes apparent: not only are the energy levels more widely spread but also the sensitivity is increased. The observation of NMR absorption depends on the net absorption of energy by this small excess of population. With continued absorption the fractional excess dwindles. The ratio of spin populations may still be described by a Boltzmann factor but now there is a corresponding rise in temperature. For this purpose, T is defined as the spin temperature and the spin system may be regarded as undergoing radio-frequency heating.

It is interesting in that when radio-frequency cooling occurs and there is an excess of nuclei in the higher level (i.e. cooling gradient), then the spin temperature may have negative values. This is an odd concept, but one which has been accounted for with reference to the first and second laws of thermodynamics[16].

The probabilities of a given nucleus being in either the upper or lower states are:

$$\tfrac{1}{2}\left(1 - \frac{\mu B_o}{KT}\right) \text{ and } \tfrac{1}{2}\left(1 + \frac{\mu B_o}{KT}\right) \text{ respectively.}$$

Because of the unequal distribution of nuclei there will be a resultant macroscopic moment per unit volume in the direction of the main magnetic field. The mean nuclear moment in this direction is given by:

$$\bar{\mu} = \mu\left[\tfrac{1}{2}\left(1 + \frac{\mu B_o}{KT}\right) - \tfrac{1}{2}\left(1 - \frac{\mu B_o}{KT}\right)\right]$$

$$\text{therefore } \bar{\mu} = \frac{\mu^2 B_o}{KT} \qquad \text{Eqn (22)}$$

The very small population differences, as derived from the Boltzmann Law earlier, are a main restricting factor in NMR spectroscopy. Typically it is found that the population difference is about 3 or 4 in 10^6, which is a very different situation than that of U.V. or I.R. spectroscopy. Another main cause of the inherent low sensitivity of the NMR equipment lies in the long lifetime of the excited states (10^{-3} to 10^3 seconds). This severely limits the power applicable to induce a transition. If too large a power level is chosen then a situation where the spin populations of the upper and lower energy levels become equalised or saturated is rapidly attained. This means that energy can be observed no longer by the NMR system. For this reason it can be expected that only very faint signals will occur for detection.

On the other hand, since spontaneous emission can be excluded as a process contributing to restoring equilibrium populations, the only

mechanism counteracting radio-frequency (RF) perturbation is relaxation or, more precisely, spin lattice relaxation (see later discussion). The two time dependant processes affecting spin populations may be represented diagrammatically as shown below.

Figure 24

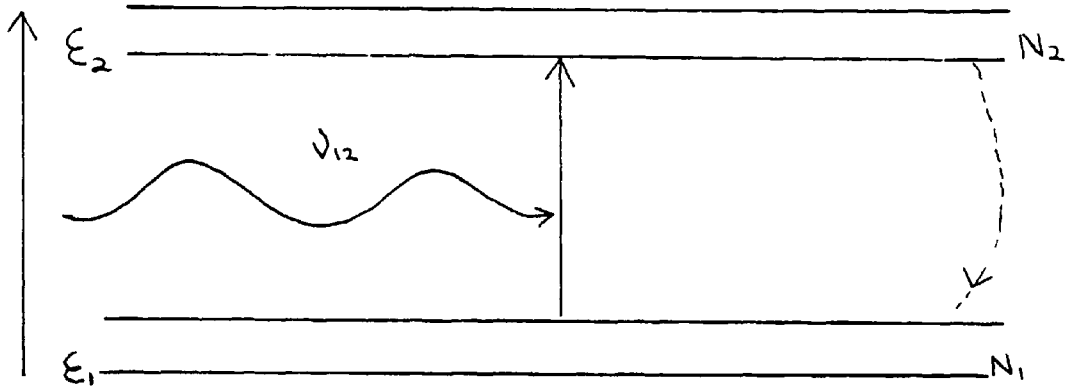

In Figure 24 nuclear energy (Zeeman) levels ε_1 and ε_2 with equilibrium spin populations N_1 and N_2 respectively. Irradiation at the Larmor resonance frequency ν_{12} promotes spurs from ε_1 to the ε_2 level whilst spin lattice relaxation (dashed line) tends to re-establish Boltzmann populations.

As evident from equation (22), the energy difference between the nuclear Zeeman levels is proportional to the magnetogyric ratio, which is a characteristic constant of a nuclear species.

At this stage it must be borne in mind that the sensitivity is proportional to γ^3, and knowing this relationship it can be referred closely to the sensitivity of ^{13}C nuclei and protons ^{1}H.

Knowing that $\frac{\gamma(^1H)}{\gamma(^{13}C)} \sim 4$, ^{13}C is less sensitive than proton by a factor of 64, assuming an equal number of nuclei. However, the natural abundance of ^{13}C is only 1.11 %, which further reduces the sensitivity by almost two orders of magnitude. Some relevant physical properties

relating to ^{13}C and ^{1}H nuclei are displayed in the following Table:

TABLE 4

	^{13}C	^{1}H
Relative abundance	1.11	99.8
Spin I (in multiples of h)	$\frac{1}{2}$	$\frac{1}{2}$
Magnetic Moment (in multiples of nuclear magneton)	0.70216	2.7927
Larmor Frequency ν_o (at 2.34 T)	25.2 MH_z	100 MH_z
Relative sensitivity of nuclei	1/64	1
Relative sensitity at natural abundance	1/5800	1

Time and Frequency Domains

Before examining the responses of the spin system to different types of excitation it may be useful to recall the correspondence between the time domain and the frequency domain. The important area in NMR is the specific nuclear magnetic frequencies exhibited by a particular sample, that is, a knowledge of frequency domain is required. With continuous wave NMR, the information may be dealt with directly in the frequency domain. However, pulsed NMR yields the same information only in the time domain. This was an infuriating early blockade to pulse spectroscopy development, as this time domain information is not easily intelligible, particularly for large molecules. Thus, pulsed spectroscopy had a slow development until a method of converting the time was available.

The method applied to interconvert the two domains is a purely mathematical one, the process of Fourier Transformation. The process

enables the conversion of a time function f(t), into the corresponding frequency function, F(w):

$$F(w) = \int_{\infty}^{\infty} f(t)\, e^{-iwt}\, dt \qquad \text{Eqn (23)}$$

and also the inverse relationship holds:

$$F(t) = \frac{1}{2\pi} \int_{\infty}^{\infty} F(w)\, e^{iwt}\, dw \qquad \text{Eqn (24)}$$

Although the above mathematical formulae may be immediately recognisable as equations used in Fourier analysis in mathematics, their importance or usage in pulsed NMR spectroscopy was not made obvious until 1966[17].

The immediate and long-range applications of Fourier Transform spectroscopy may be assessed by the immense quantity of publication on the subject and its applications and with the advent of small commercial computers, FT NMR has become routine. Computer programs for the Fourier Transformer were devised during the pioneering work[17] and a simplified block diagram of such a program may be:

Figure 25

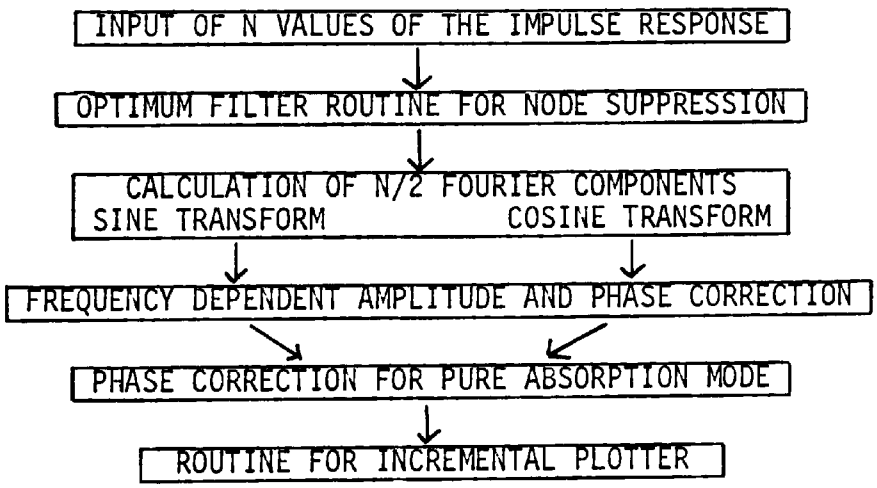

Experimental Methods for Finding T_1

Two main methods were attempted for determining the spin-lattice relaxation time T_1.

They were:

1. Inversion Recovery.

2. Freeman-Hill Inversion Recovery.

For a set of non-interacting identical spin $\frac{1}{2}$ nuclei, an exponential relaxation of the longitudinal relaxation is predicted from Equation (29) and the relaxation rate:

$$T_1^{-1} \text{ is defined as } T_1^{-1} = 2w\alpha\beta \qquad \text{Eqn (25)}$$

where α and β are energy levels, w = transition probability.

For two loosely coupled nuclei of spin $\frac{1}{2}$, A and X, the variation of the magnetisation depends on the possible transitions, according to:

$$\frac{dMzA}{dt} = -(2w_1^A + wo + w_2)(MzA - MoA) - (w_2 - wo)(Mzx - Mox) \qquad \text{Eqn (26)}$$

$$\frac{dMzx}{dt} = -(2w_1^X + wo + w_2)(Mzx - Mox) - (w_2 - wo)(MzA - MoA) \qquad \text{Eqn (27)}$$

That is, the variation of magnetisation with time is no longer described by a single exponential, and hence T_1 cannot be defined as in earlier theory. But if the cross relaxation term $(w_2 - wo)$ is negligible, exponential behaviour characterised by relaxation rates:

$$(T_1A) \text{ and } (T_1X)^{-1}$$

is expected as:

$$(T_1A)^{-1} = 2w_1^A + wo + w_2 \qquad \text{Eqn (28)}$$

$$(T_1X)^{-1} = 2w_1^X + wo + w_2$$

For more than two loosely coupled spins, relaxation laws analogous to Equation (28) may be written by summing pair interactions between A and each of the other spins. Again it must be borne in mind that the model neglects cross relaxation/correlation between the pairs. So even in small molecules, relaxation of these equivalent protons of a rapidly rotating methyl group is expected to be non-exponential. In most practical cases single exponential recoveries of carbon magnetisations are obtained to a reasonable degree in proton decoupled spectra and cross correlation effects are neglected. Denoting Mo as the equilibrium magnetisation of the observed nuclei a general differential equation is usually applied to the analysis of the results.

$$\frac{dMz}{dt} = - \frac{Mz - Mo}{T_1} \qquad \text{Eqn (29)}$$

$$\text{integrating } Mo - Mz = -Ke^{\frac{-t}{T_1}} \qquad \text{Eqn (30)}$$

where K depends on the initial conditions of the experiment.

The general principle of the relaxation experiment is to subject the nuclei to a burst or pulse of non-selective radio-frequency which nutates the equilibrium spin magnetisation, Mo, through a known flip angle, and allow the system to revert to its equilibrium position, sampling its progress at given intervals. The two methods used work on this basic principle but varying different parameters are introducing slight modifications.

The following figure illustrates the effect of such a RF pulse on the spin magnetisation vector and it illustrates the exponential plot of (Mo - Mz) versus time.

Figure 26

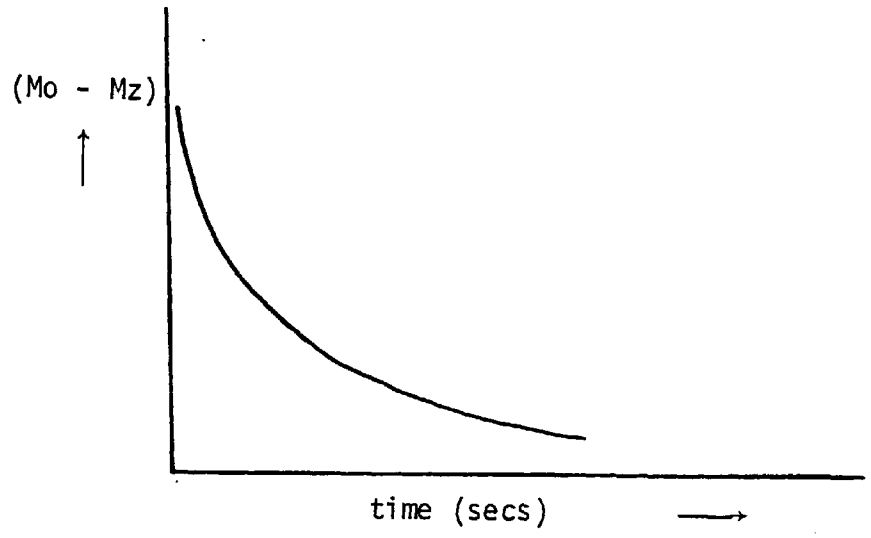

From the above, Equation (30) modifies to:

$$(Mo - Mz) = Mo(1 - \cos\theta)\, e^{-\frac{t}{T_1}} \qquad \text{Eqn (31)}$$

and it may be seen that when $t = T_1$ the system has relaxed by;

e^{-1} i.e. 63 % of Mo

when $t = 2T_1$, $e^{-2} \simeq 86$ %

$t = 3T_1$, $e^{-3} \simeq 95$ %

$t = 4T_1$, $e^{-4} \simeq 98$ %

$t = 5T_1$, $e^{-5} \simeq 99.3$ %

Hence, in order to obtain the most meaningful information, a time equivalent to at least five times the T_1 value of the longest T_1 in the molecule must be allowed before the system is pulsed again, this time is called the Pulse Delay (PD***). This exerts constraints on experimentation time. The pulse delays used were between 40 to 60 seconds. The experiment time will then depend upon the number of times the system will be pulsed during the experiment; usually, for a given

interval during the relaxation of the magnetisation vector the system is pulsed several times with the FID's sampled at that interval after each pulse being added and then time averaged in order to observe the mean effect. The pulse sequence of an experiment is thus very important and a pulse sequence of an experiment may be given as:

$$\left[\text{Pulse - t - sample pulse - } \overset{\text{Store}}{\text{FID}} \text{ - } 5T_1 \text{ (PD)}\right]_n$$

What is happening here is that the system is being pulsed to nutate Mo through to Mz, at a fixed flip angle. The system is allowed to relax back to Mo, but during relaxation at given time intervals denoted by t the FID is sampled. At that interval, t, the collection of one FID may not be a sufficient or satisfactory representation of the Mz at that point, so the system is allowed to relax fully, pulsed again and sampled again at that given t. The process may be repeated as many times as necessary, denoted by the number of accumulations or scans in order to have sufficient information to obtain a satisfactory time-averaged representation of Mz at t . The experiment is lengthened further by varying t between 5 and 10 different values, in order to plot a graph given by Equation (32). Equation (32) is the semi-logarithmic plot of Equation (30) where the value ln (Mo - Mz)/2Mo is plotted against time to give a slope of $-\frac{1}{T}$

$$\ln \frac{Mo - Mz}{2Mo} = \frac{-t}{T_1} + K \qquad \text{Eqn (32)}$$

(Compare $y = mx + C$)

Figure 27

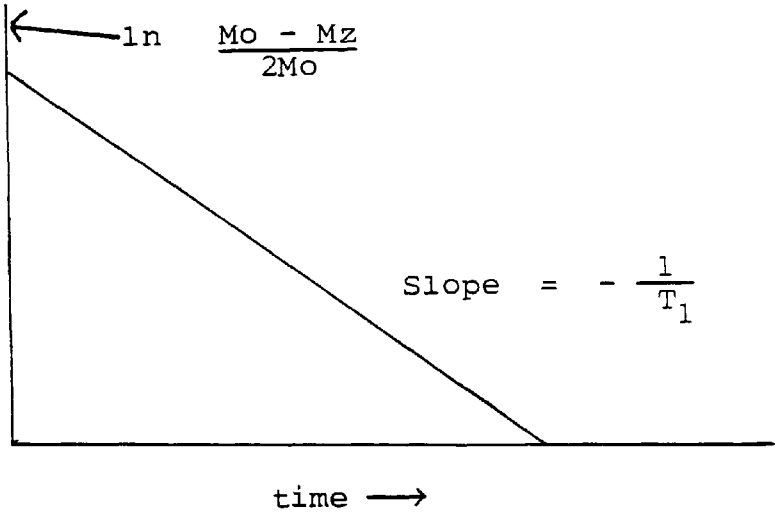

From the plot it can be seen that the T_1 value may be calculated fairly easily and such plots may be incorporated in the PG 200 pulse generator via program tapes or similar computer programs may be constructed for usage on microcomputers in order to analyse the results.

Information such as the values of t and peak intensities (α Mo - Mz) is given by the FX60Q print out.

The format of the obtained spectra for all the experiments will appear very similar. The outputted spectra will consist of a number (usually 10) of condensed spectra representing the position or status of Mz after a given time interval. It was established earlier that peak height was a function of the extent of relaxation and hence these spectra will have varying peak heights representing the extent of relaxation undergone by that particular nucleus for the varying of time.

The FID information stored at each acquisition point is stored on cassette tape. This allows the results to be processed via Fourier Transformation and outputted as peak height data at a more convenient time. For the Inversion-Recovery method the FID information could be analysed with the aid of tapes containing a preconstructed program containing the relevant equations and graphs. Thus the experiment

could be carried out and the results immediately processed by the spectrometer's Central Processing Unit (CPU) and the T_1 values printed out and the semi-logarithmic plots displayed on the spectrometer display screen.

Inversion-Recovery Fourier Transform (IRFT) Method

Here a pulse delay of the order of 40 to 120 seconds would be required. The high concentration of the samples reduces the number of scans required in order to obtain useful accumulated spectra for Fourier Transformation.

The recommended range of T values for IRFT are $0.3 \longrightarrow 1.5$ T.

Principle of Method

The basic version of IRFT rests on the sequence [18,19,20]

$$(\pi - T - \frac{\pi}{2} - A_t - D)_n$$

with all symbols having their normal meaning and D is the delay before the next π (180^o) pulse and the stipulation of the experiment is that:

$$A_t + D = \text{Pulse Delay} > 5\ T_1$$

where T_1 is the longest in the molecule. The problem with this sequence was, that if the T_1's are comparable to the line broadening $\frac{1}{T_2}$ *, then errors will occur as the initial pulse will produce transverse magnetisation which will persist and interfere with the 90^o pulse. Thus the sequence has now been modified HSOP's between the 180^o and 90^o pulses to eliminate this transverse magnetisation.

The modified sequence is the sequence used for these experiments and the representation is:

$$(\pi - (HSP) - T - \frac{\pi}{2} - A_t - D)_n$$

(Note: HSP is the Homogeneity Spoiling Pulse).

Equations for any T_1 derivation, determined via pulsed experimentation, make the important assumption that the magnetisation is purely longitudinal at the time of the sampling pulse, but in some experiments this may be invalid. This requirement can be circumvented by introducing a momentary degradation of the magnet homogeneity since the spins are expected to dephase rapidly in a homogenous B_0 field. A HSP is capable of destroying the residual transverse magnetisation before the next sampling pulse. The HSP is produced by applying a large voltage for a very short time to one of the magnet shim coils.

The action is then to invert initially the equilibrium magnetisation by a 180^{o} (π rads) pulse which is then subjected to a HSP before being allowed to recover during a period T. The value of the longitudinal magnetisation M_{zT} is then measured by acquiring the signal which follows a 90^{o} ($\frac{\pi}{2}$ rads) pulse, as shown in the following diagrams. It is important that the Mz magnetisation vector is allowed sufficient time between the $\frac{\pi}{2}$ and the next pulse in order to reattain its equilibrium value, otherwise errors will be computed after each new pulse.

Figure 28

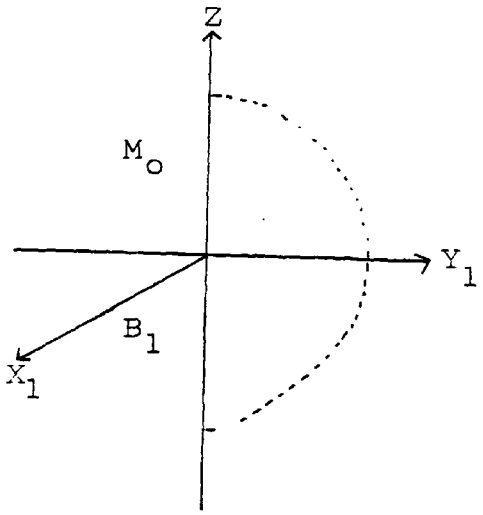

Pulse inverts equilibrium magnetisation vector

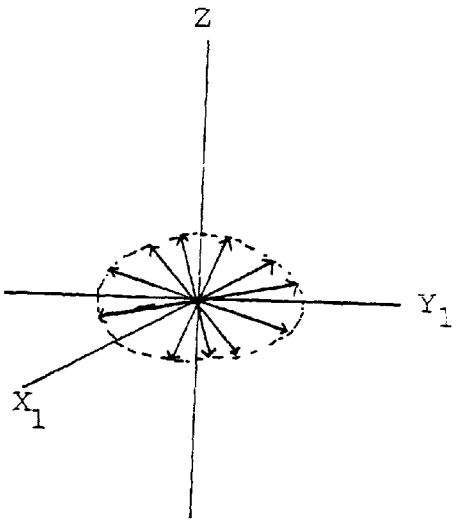

HSP eliminates transverse magnetisation

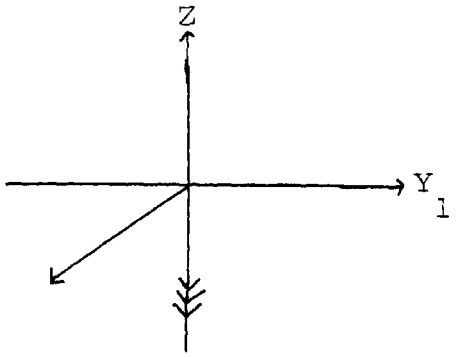

T pulse interval

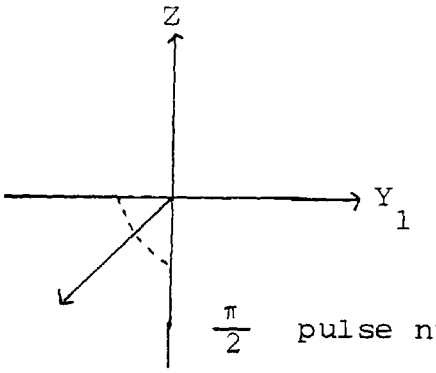

Magnetisation, M_zT through 90° and the FID is sampled

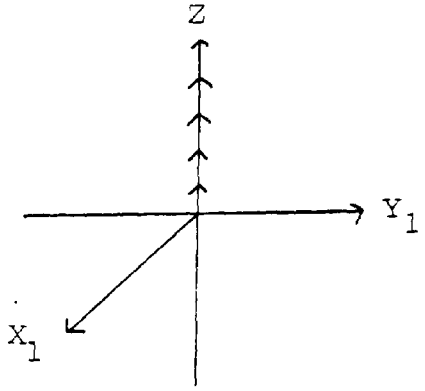

Delay D allows recovery of magnetisation to M_0 value

From the above figures it is clear that for short values of T the longitudinal magnetisation is still negative and the inverted signal is observed in the FT spectrum. For longer T values the signal becomes increasingly positive. The intensity I which corresponds to the equilibrium magnetisation Mo is obtained for $T > 5\ T_1$.

After Fourier Transformation, signals are observed which relax individually as a function of between -Mo(-I) and (+Mo + I). Integration of the equation:

$$\frac{dMz}{dt} = \frac{-Mz - Mo}{T_1} \qquad \text{Eqn (29)}$$

for the initial condition Mz (T=0) = -Mo leads to the variation law:

$$I_T = I\infty \left[1 - 2 \exp\ (-\frac{\pi}{T_1})\right] \qquad \text{Eqn (30)}$$

This equation may be rearranged to give:

$$I_T = I\infty - 2I \exp\ -\ (\frac{\pi}{T_1})$$

therefore $I\infty - I_T = 2I\infty \exp\ -\ (\frac{T}{T_1})$

therefore $\frac{I\infty - I_T}{2I\infty} = \exp\ -\ (\frac{T}{T_1})$

Taking natural logs

$$\ln \left[\frac{I\infty - I_T}{2I\infty}\right] = \frac{-T}{T_1} \qquad \text{Eqn (31)}$$

A plot of

$$\ln \frac{I\infty - I_T}{2I\infty} \text{ versus } T$$

will yield a straight line with gradient equal to $\frac{-1}{T_1}$.

Some preliminary experiments were carried out using the IRFT method to determine the order of the shorter T_1 values using a pulse delay of 60 seconds. The test helped to choose the right orders of pulse delays and T values to obtain meaningful results. The T_1 values are calculated using a departmental taped program and the results are printed out of the spectrometer. The semi-logarithmic plot obtained was displayed on the spectrometer monitor screen.

The Freeman-Hill Modification of the Inversion Recovery Method

In contrast to the IRFT method the department did not have available a taped program for the PG200 pulse generator to conduct the Freeman-Hill modification of the IRFT experiment. As the general principle was similar to the IRFT experiment but the pulse sequence was not, the PG200 had to be programmed manually for the operation. To generate a pulse sequence a program must be written into the PG200 RAM (Random Access Memory) and this is facilitated by use of the light pen and appropriate patterns on the monitor screen. The program is constructed by entering commands into each memory address. A variety of commands are available, each denoting a specific step in each scan and setting the states of the different gates by using time parameters. Some commands allow for variable parameters to be inputted during the running of the program, e.g. pulse delay, pulse widths, pulse intervals, etc. By referring to the required pulse sequence, the conditions of the observation, irradiation and decoupling gates may be specified. A coding sheet used for this experiment is shown along with a sample spectrum which illustrates the commands required to produce a Freeman-Hill pulse sequence[21], see page 180 and page 181. The crucial aspect of the programming is given in Jeol manuals. These were slightly

adjusted in constructing the programs to carry out the required pulse sequence and then subjecting the sequence to vigorous tests in order to ascertain whether the program was actually doing its job. The department had no analysing tapes to treat the results and calculate T_1 values, therefore a MIMI microcomputer program was written similar in construction to that written for the IRFT experiment.

Principle of Method

The initial problem to construct the PG200 program to suit the required pulse sequence[20]

$$(\tfrac{\pi}{2} - At - D - \pi - T - \tfrac{\pi}{2} - At - D)_n$$

(+) (-)

On studying the original sequence detailed above, it was decided to incorporate HSP's into the sequence, and so the modified version was

$$(\tfrac{\pi}{2} - \overset{I_\infty}{At} - HSP - D - \pi - T - \tfrac{\pi}{2} - \overset{I_T}{At} - HSP - D)_n$$

(+) (-)

The above sequence is very similar to the standard IRFT, except an initial 90^o ($\frac{\pi}{2}$ rads) pulse is added.

The sequence is to pulse the equilibrium magnetisation with a 90^o sample pulse, and to acquire the FID - wait for a delay D, which ideally should be 5 T. The system is then pulsed by 180^o as in the IRFT method, allowed to recover over varying T intervals, and sampled with a 90^o pulse and the FID acquired. Notice that the FID attained after T time is collected by the receiver coil at exactly 180^o out of phase. Now in IRFT experiments, it was seen that for short T values

the observed peaks were inverted (by the 180^{o} pulse), and as T increased, the peaks became more positive. In FHIRFT the magnetisation M_{zT} is sampled at 180° out of phase and so will appear positive. Hence, for short T values the collected peak will appear positive and large, exactly opposite to the IRFT experiment. As T increases the peaks will decrease in size, but they will not appear negative at very long T values. This is because the accumulation sequence will subtract the inverted peaks from the equilibrium peak for each accumulation thus as T gets larger, the value I_{∞} (Mo) - IT(MzT) will tend to zero and so will not invert.

It may be seen that the FHIRFT experiment will measure the equilibrium magnetisation, I_{∞} (Mo) for each new accumulation, and the recovery magnetisation value IT (MzT) is the IRFT method where I is measured only once during an entire experiment; whereas I is measured as many times as there are T values in FHIRFT. As there will be drifting of resolution, temperature and other effects during every experiment, it is intuitive that the FHIRFT experiment will compensate for these drifts by obtaining peak subtractions run under the same conditions for each T value. It is envisaged that the FHIRFT method will be an inherently more accurate experiment than standard IRFT which subtracts all I_{T} values from the single I obtained. However, as two pulse accumulation sequences are invalid in FHIRFT experiments for each accumulation which require a total delay of PD > 5 T, for each, then the method will be far more consuming than the standard IRFT method.

Practical Details

With a requirement of PD > 5 T, occurring twice in the sequence, the time considerations for testing and then running the experiments would be enormous. However, the testing of the sequence was carried out

using the proton FT analogue. Fortunately, no modification of the probe was required for the switch over, but obviously an irradiation frequency of 60 MHz would be required of the spectrometer. The advantage of using Proton FT nmr is that the T_1 values obtained are considerably shorter.

Further work was investigated using a ^{13}C experiment using the FHIRFT pulse sequence with a PD of 40 seconds. The experiment runs for about two hours.

It should be noted that the presence of a rotating methyl group in the molecule increases the effect of the spin rotational relaxation mechanism, $\frac{1}{T_1 SR}$, which is an inefficient relaxation process.

Also the high concentration of the sample increases H dipolar molecular interactions - although this may be thought to increase dipolar relaxation frequency it may also be that molecular motions are suppressed.

It can be noted from the sample spectra that 'dummy' pulses were incorporated into the sequence. This is when the system is pulsed according to the set sequence but the resultant FID is not sampled.

The inclusion of dummy pulses in the FHIRFT is not crucial but merely aids the setting up of the spin system. Dummy pulses can sometimes be very important in methods which require a steady state spin system before acquisition of the FID.

2 RESULTS AND DISCUSSIONS

2.1 Investigation of the change in chemical shift with concentration

2.2 Investigation of the change in chemical shift with temperature

2.3 Investigation of the effect of lanthanide shift reagents on chemical shift

2.4(1) Investigation of carbon-13 and proton relaxation times

2.4(2) Nuclear Overhauser effect versus position of carbon in compound and comparison of carbon T_1's

2.5 T_1 estimation by Freeman-Hill method

2.6 Comparison of inversion recovery and Freeman-Hill T_1 results

2.7 Proton T_1 and T_2 results

2.8 Determination of the conformation of molecules

2 RESULTS AND DISCUSSIONS

The main applications of the technique of NMR beside the determination of structure of organic molecules using proton and carbon 13 spectra are:

1. Investigation of the change in chemical shift with concentration.
2. Investigation of the change of chemical shift with temperature.
3. Investigation of the effect of lanthanide shift reagents on chemical shift.
4. Investigation of carbon 13 and proton relaxation times.
5. Determination of the conformation of molecules.

2.1 Investigation of the change in chemical shift with concentration

The molecules studied were cyclohexanol, cyclohexylamine, trans-2-aminocyclohexanol, 1-amino-1-hydroxymethylcyclopentane, 1-methylcyclohexanol, cis and trans-2-methylcyclohexanol, cis and trans-3-methylcyclohexanol, cis and trans-4-methylcyclohexanol.

In most cases the work was carried out with the solute dissolved in $CDCl_3$ or CCl_4 at a probe temperature of around 300 K.

Trans-2-aminocyclohexanol did not dissolve in CCl_4.

Cyclohexanol

It has been shown by Eliel [22] and many others that there is a much more open approach of reagents to the equatorial position relative to the axial position. Hence in the context of intermolecular hydrogen bonding, this would occur to a greater extent if the hydroxyl groups were in equatorial positions as opposed to axial positions.

The limiting chemical slope is a measure of the amount of intermolecular hydrogen bonding present in the system (in the low concentration range this would be mainly dimer —> monomer) i.e. as dilution is carried out it is effectively breaking down the intermolecular hydrogen bonding.

At first sight, this would appear to be quite straightforward, but in fact it is quite a complicated system with respect to the mode of the intermolecular hydrogen bonding. For cyclohexanol intermolecular hydrogen bonding can take place via three modes, e.g.

Figure 2(1)

A diagram to show the three possible ways in which hydrogen bonding can take place in cyclohexanol.

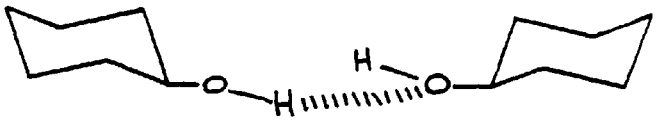

equatorial - equatorial

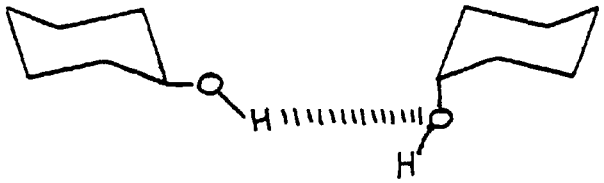

equatorial - axial

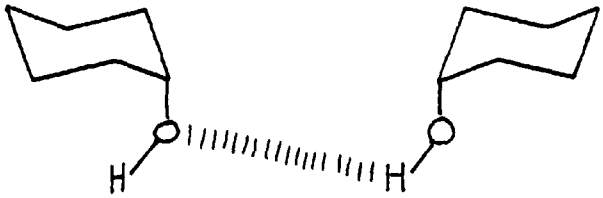

axial - axial

The limiting chemical slope will be an average of all these forms. It should be noted that the equatorial position is more open to approach for intermolecular hydrogen bonding.

The value for limiting chemical shift for cyclohexanol will be a standard value in the absence of intramolecular hydrogen bonding.

TABLE 2.1

Concentration versus chemical shift for cyclohexanol in deuterated chloroform $CDCl_3$ at different temperatures

		Chemical shift in Hz at different temperatures					
Mass in g	Concn.	30°C	35°C	38°C	42°C	46°C	51°C
0.0035	0.035	90.234	89.063	88.336	87.744	86.426	85.107
0.00758	0.0758	89.502	88.470	87.598	86.426	85.254	84.086
0.01344	0.1344	91.699	90.527	88.916	87.744	86.426	85.107
0.02611	0.2611	96.680	95.361	93.164	91.846	90.234	88.336
0.0350	0.350	101.367	99.316	97.114	95.801	93.604	91.699
0.04203	0.4203	107.227	104.590	101.593	100.195	98.291	95.564

The results were plotted on a British Micro using a graph plotting program (see page 63). For each temperature a limiting chemical shift and limiting slope can be found from the graph.

TABLE 2.2

A Table showing limiting chemical shifts and slopes at different temperatures for cyclohexanol

Temperature °C	Limiting Chemical Shift Hz	Limiting Chemical Slope Hz $mol^{-1}.dm^3$
30	86.688	44.321
35	85.919	40.585
38	85.234	35.781
42	84.457	33.696
46	83.357	31.406
51	82.358	28.069

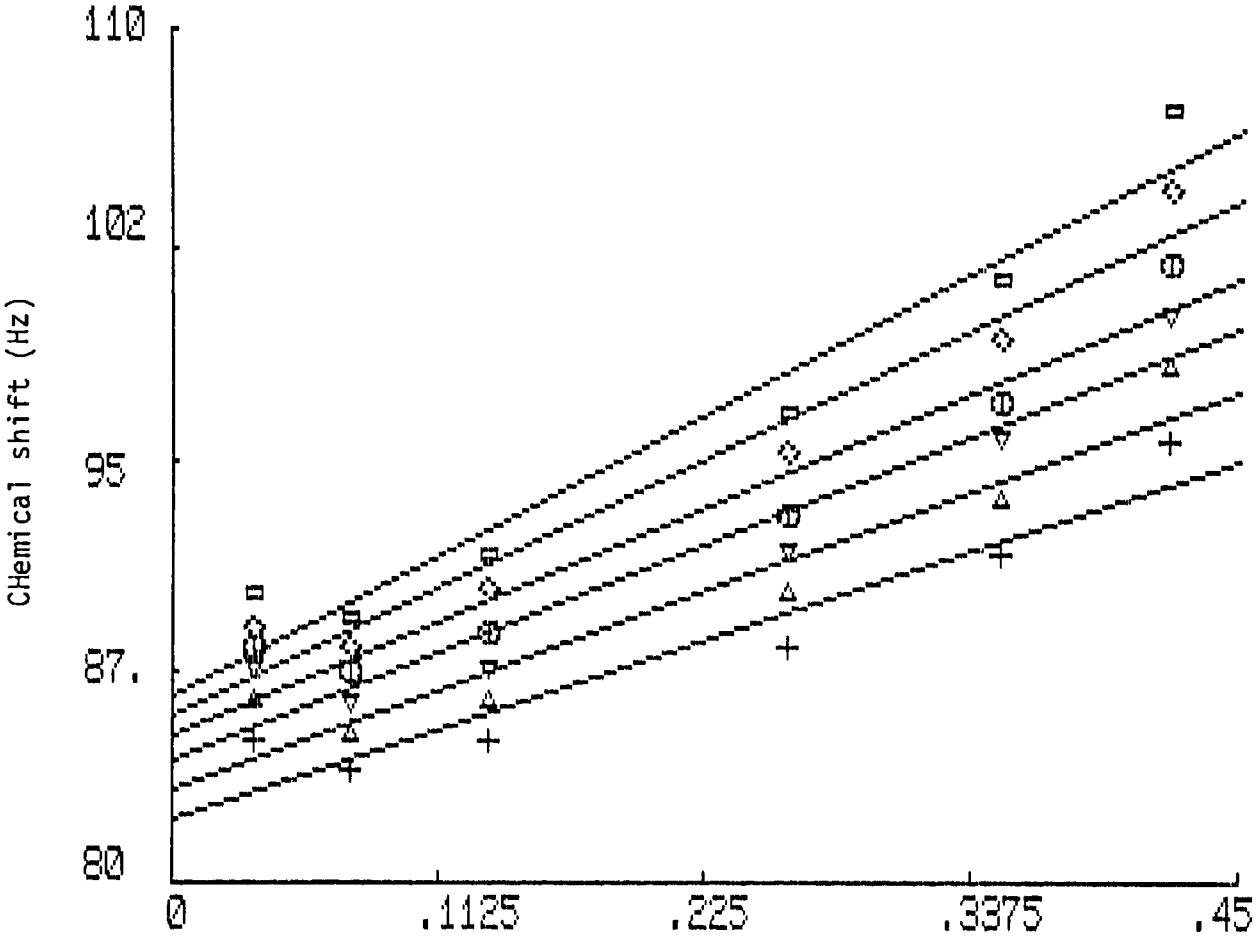
110
102
95
87.
80
CHemical shift (Hz)
0
.1125
.225
.3375
.45
Concentration (mol.dm⁻³)
Cyclohexanol

Cyclohexylamine

Cyclohexylamine and cyclohexanol have only the possibility of intermolecular hydrogen bonding, therefore as the solutions become more dilute, the chemical shift should fall.

The value for the limiting chemical shift for cyclohexylamine is a measure of the monomeric amino proton at infinite dilution and is a standard value set for the absence of intermolecular hydrogen bonding. See Table 2.3 on page 65.

A comparison of the graphs obtained with cyclohexylamine with those of cyclohexanol show a very interesting difference. With cyclohexylamine there is an increase in the value of chemical shift on dilution !

In general the reason for the pronounced downfield shift of a hydrogen bonded proton has not been completely explained. However, it seems clear that it is not merely a result of decreased electron density around the proton, for overall the proton is probably in a region of higher electron density in the hydrogen bond X - H ..... Y than it is in the X - H alone. Nevertheless, the electron distribution in the X - H covalent bond is evidently obtained by the electric field from Y in such a way that the proton is deshielded. In cyclohexylamine the amino proton may experience a neighbouring anisotropy effect from Y, this would result in a small upfield shift similar to when a proton is hydrogen bonded approximately to the centre of the π electron cloud.

TABLE 2.3

Concentration versus chemical shift for cyclohexylamine at different temperatures

Measurements were done in $CDCl_3$

		Chemical shift in Hz at different temperatures				
Mass in g	Concn.	28°C	33°C	38°C	43°C	48°C
0.0227	0.0225	86.719	84.521	84.521	82.837	81.079
0.00802	0.081	80.713	81.519	80.200	78.662	77.197
0.01388	0.140	80.347	79.980	77.637	77.344	76.758
0.02637	0.266	75.586	75.819	74.121	73.589	72.729
0.03930	0.3962	75.293	75.586	73.755	73.242	72.363

N.B. The graph slopes in the opposite way to cyclohexanol. For each temperature a value of limiting chemical shift and limiting slope can be found.

TABLE 2.4

A Table showing limiting chemical shifts and slopes at different temperatures for cyclohexylamine

Temperature °C	Limiting Chemical Shift Hz	Limiting Chemical Slope Hz $mol^{-1}.dm^3$
28	84.863	-28.457
33	83.841	-24.049
38	83.064	-27.826
43	81.555	-24.399
48	80.069	-22.322

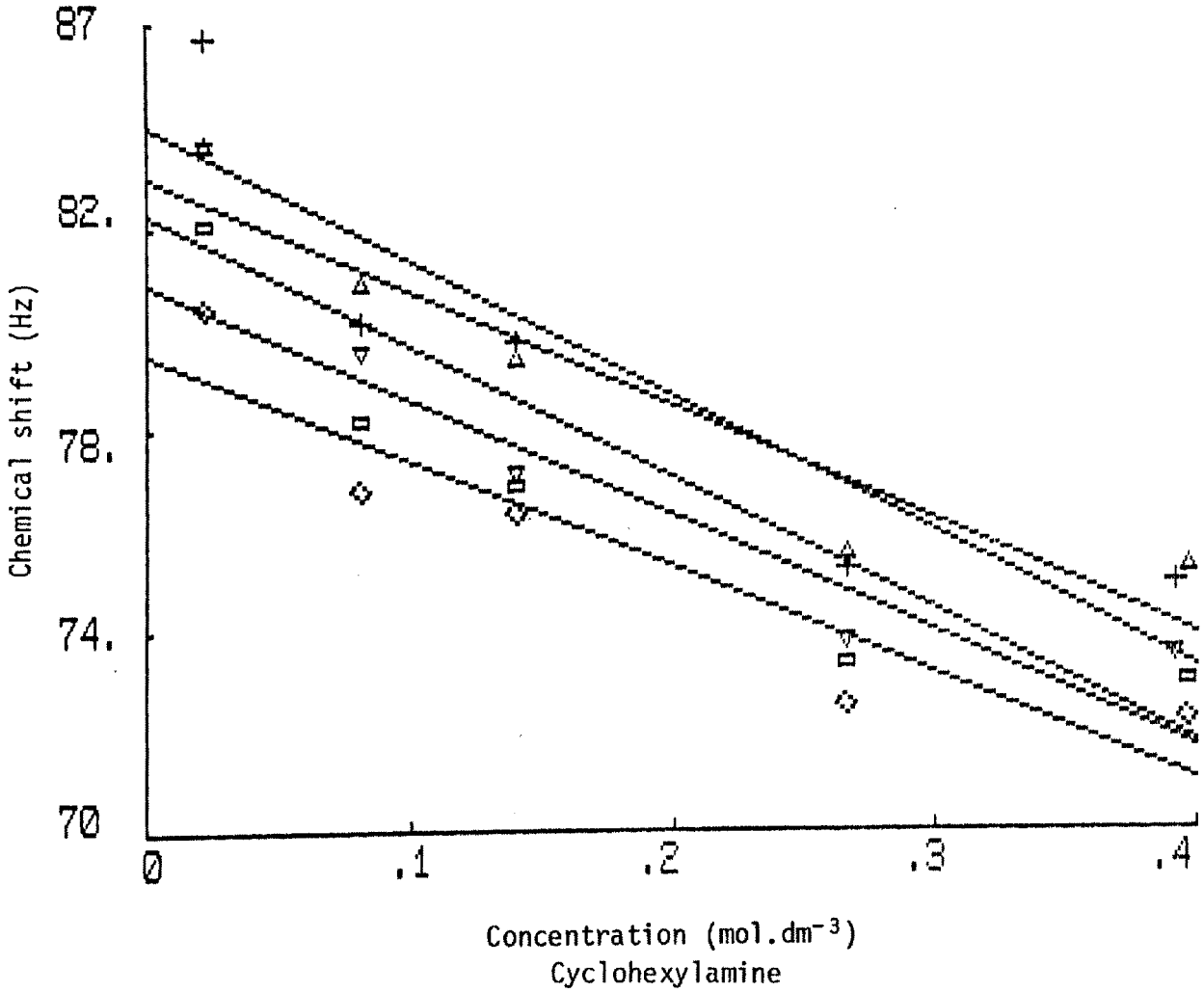
87
82.
78.
74.
70
Chemical shift (Hz)
0
.1
.2
.3
.4
Concentration (mol.dm⁻³)
Cyclohexylamine

1-Amino-1-hydroxymethylcyclopentane

When a second functional group, e.g. NH_2 is introduced into a ring structure there is the possibility of intramolecular hydrogen bonding as well as intermolecular hydrogen bonding. Dilution has a greater effect on intermolecular hydrogen bonding than on intramolecular hydrogen bonding. Hence, when intramolecular hydrogen bonding is present in a compound the hydroxyl or amino limiting chemical shift would be expected to be much larger, i.e. further downfield from TMS than the shift of a free hydroxyl or amino proton.

In order to test this assumption the concentration versus chemical shift plots of 1-amino-1-hydroxymethylcyclopentane were determined in $CDCl_3$ between 307 - 334 K.

This compound should have intramolecular hydrogen bonding as well as intermolecular hydrogen bonding.

See results in Table 2.4 and Table 2.5 and the graph (page 69).

From the results it can be seen that the limiting chemical shift is further downfield from TMS than either cyclohexanol or cyclohexylamine. Also the value of the limiting chemical slope is greater than either that of cyclohexanol or cyclohexylamine.

Hence it may be assumed that 1-amino-1-hydroxymethylcyclopentane contains both intermolecular and intramolecular hydrogen bonding.

TABLE 2.5

Concentration versus chemical shift for 1-amino-1-hydroxymethylcyclopentane at different temperatures

Measurements were done in $CDCl_3$

		Chemical shift in ppm at different temperatures					
Mass in g	Concn.	34°C	41°C	46°C	51°C	56°C	61°C
0.04043	0.351	2.3175	2.26	2.195	2.045	2.05	1.96
0.03214	0.279	2.25	2.15	2.103	2.01	1.978	1.928
0.02580	0.224	2.168	2.06	2.005	1.935	1.903	1.86
0.01610	0.140	1.98	1.918	1.880	1.82	1.795	1.76
0.0100	0.0868	1.85	1.802	1.776	1.725	1.7025	1.68
0.00617	0.0536	1.76	1.735	1.710	1.665	1.6625	1.633

From the graph on page 69 values of limiting chemical shifts and limiting slopes can be found.

TABLE 2.6

A Table showing limiting chemical shift and slope variation at different temperatures for 1-amino-1-hydroxymethylcyclopentane

Temperature °C	Limiting Chemical Shift		Limiting Slope	
	ppm	Hz	ppm $mol.^{-1}dm^3$	Hz $mol.^{-1}dm^3$
34	1.689	101.39	1.9266	115.59
41	1.676	100.56	1.977	118.62
46	1.654	99.24	1.7657	105.94
51	1.636	98.16	1.6345	98.07
56	1.623	97.38	1.114	66.84
61	1.587	95.22	1.144	68.64

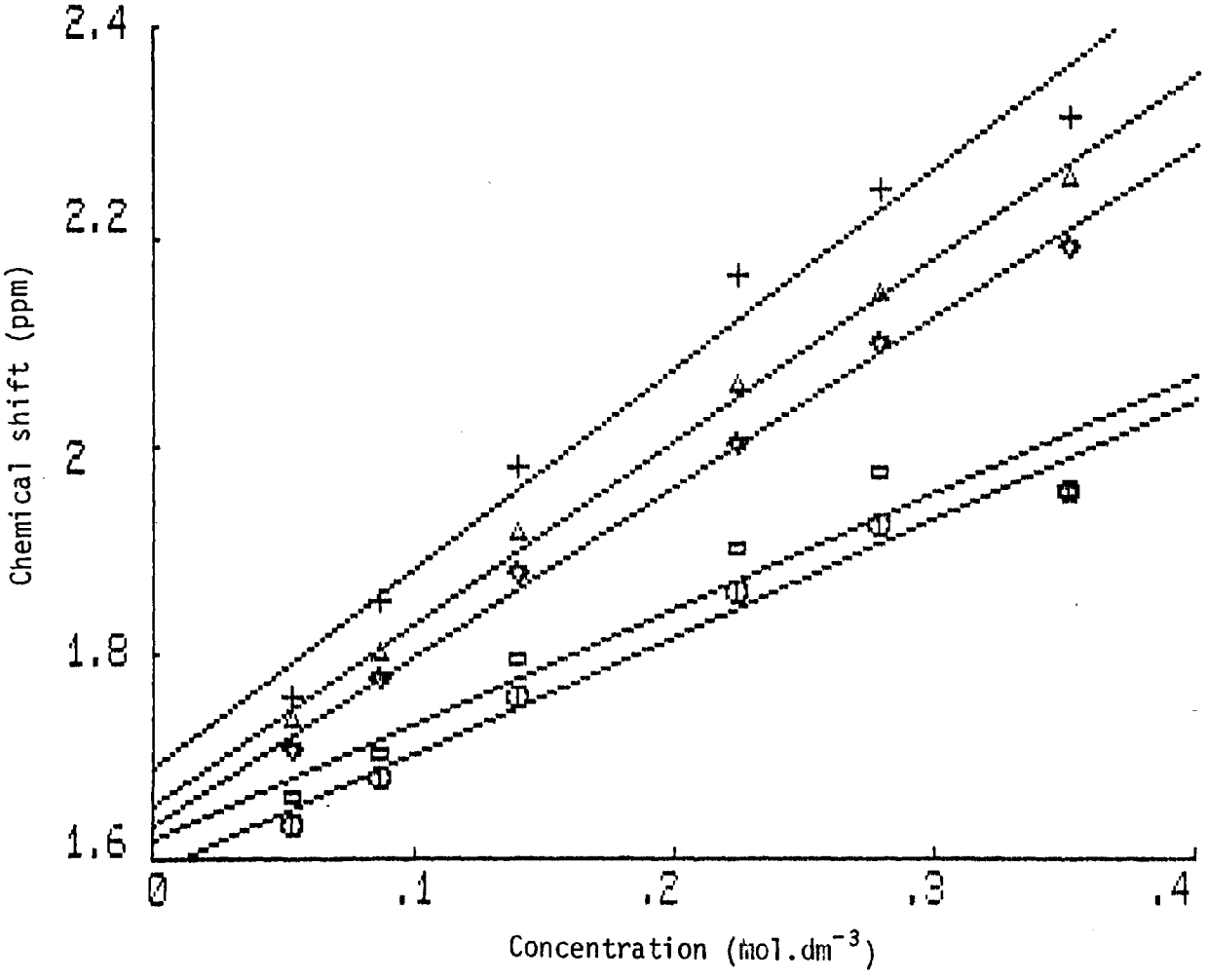

1-amino-1-hydroxymethylcyclopentane

trans-2-Aminocyclohexanol

In this molecule an amino group has been introduced into a cyclohexanol ring. There is now the possibility inter and intramolecular hydrogen bonding. See results in Tables 2.6 and 2.7, and the graph (page 72).

The value for the limiting chemical shift was further downfield from TMS than either cyclohexanol or cyclohexylamine. Also, the value of the limiting chemical slope was greater than that of cyclohexanol or cyclohexylamine.

Hence it may be assumed that trans-2-aminocyclohexanol contains inter and intramolecular hydrogen bonding.

Consider the possible conformations of this isomer.

Figure 2(2)

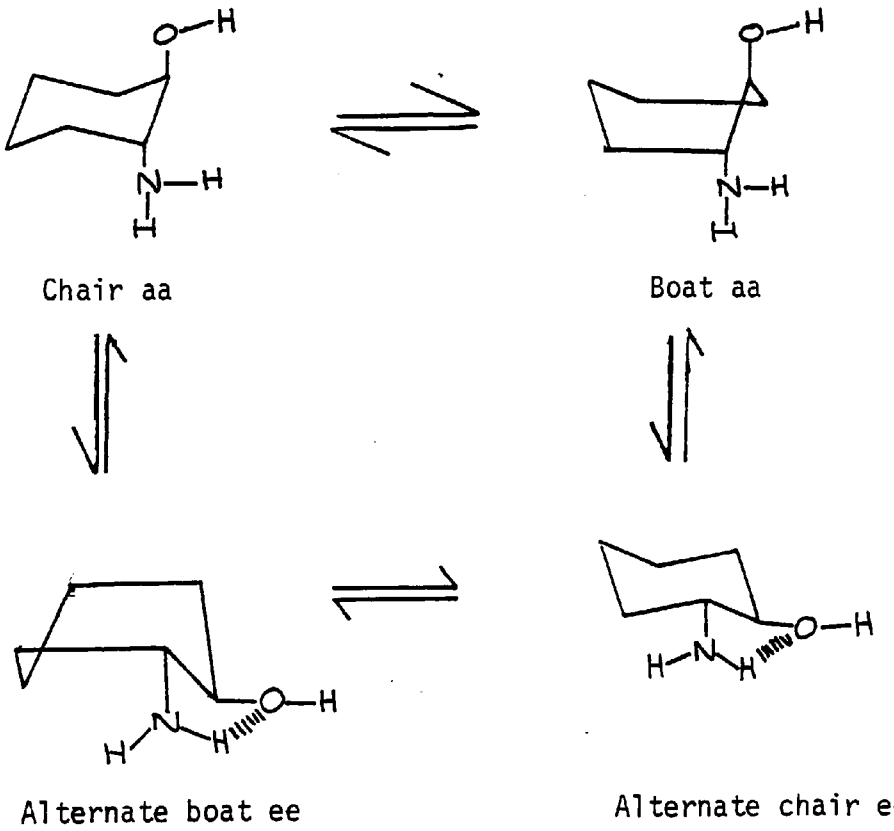

From Figure 2(2) it can be seen that in the chair conformer the hydroxyl and amino groups are diaxial which is energetically unfavoured whereas in the alternate chair the hydroxyl and amino groups are diequatorial which is energetically favoured.

The results show that the trans isomer forms an intramolecular hydrogen bond and that the compound is likely to show a conformational preference of being in the alternate chair with both amino and hydroxyl groups in the equatorial position.

TABLE 2.7

Concentration versus chemical shift for trans-2-aminocyclohexanol at different temperatures

Measurements were done in $CDCl_3$

		Chemical shift in ppm at different temperatures				
Mass in g	Concn.	32°C	40°C	46°C	50°C	60°C
0.03136	0.270	2.888	2.170	2.105	2.073	1.975
0.02321	0.202	2.1875	2.065	2.050	2.00	1.8875
0.01892	0.165	2.0625	1.993	1.945	1.90	1.8175
0.01484	0.129	1.995	1.950	1.905	1.875	1.8125

From the graph on page 72 values of limiting chemical shift and limiting chemical slope can be found.

TABLE 2.8

A Table showing limiting chemical shift and slope variations at different temperatures for trans-2-aminocyclohexanol

Temperature °C	Limiting Chemical Shift		Limiting Slope	
	ppm	Hz	ppm $mol.^{-1}dm^3$	Hz $mol.^{-1}dm^3$
32	1.724	103.44	2.135	128.1
40	1.739	104.34	1.5934	95.60
46	1.7512	105.07	1.3685	82.11
50	1.677	100.62	1.488	89.28
60	1.637	98.22	1.235	74.1

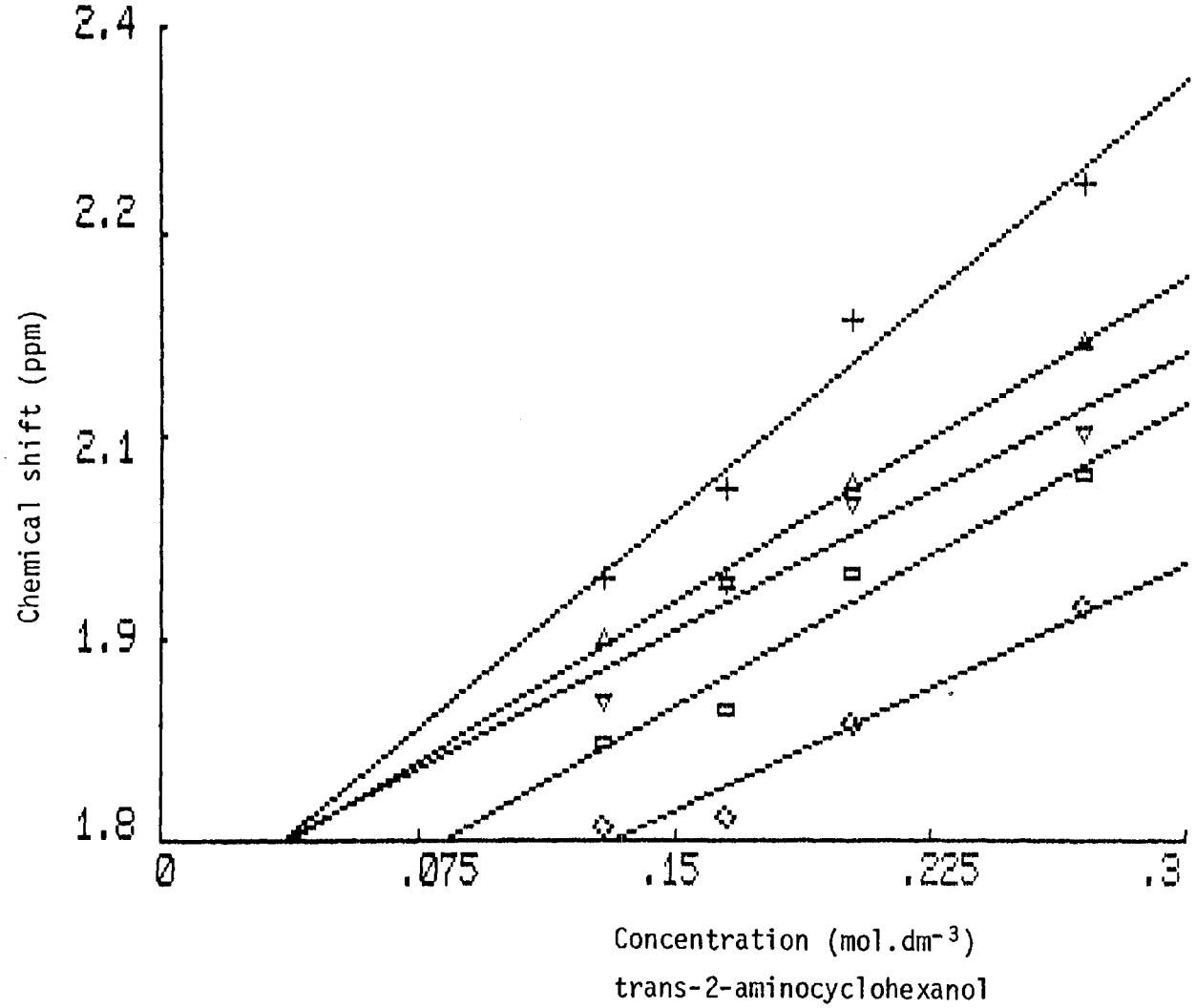
2.4
2.2
2.1
1.9
1.8
Chemical shift (ppm)
0
.075
.15
.225
.3
Concentration (mol.dm⁻³)
trans-2-aminocyclohexanol

Butylamine

In carrying out chemical shift versus concentration studies on cyclohexylamine, it was found that there was an increase in the value of chemical shift on dilution. The amino proton chemical shift was studied in a different environment using butylamine in deuterated trichloromethane at 300 K.

From Table 2.9 it can again be seen that on dilution the chemical shift increases, this may again be due to an anisotropic effect. It would have been expected that the chemical shift decreases in value on dilution. The anisotropic effect must be greater and in an opposite direction.

TABLE 2.9

Concentration versus chemical shift for butylamine at different temperatures

Mass in g.	Concn.	Chemical Shift at 300 K in Hz
0.05298	0.362	107.45
0.08831	0.6037	102.17
0.009592	0.0655	128.32
0.031628	0.2162	110.74
0.00522	0.03567	139.53

Limiting chemical slope = 132.956 Hz

Gradient = - 59.676 H $mol.^{-1}dm^3$

The graph was, however, more like a curve than a straight line.

Various techniques were used to separate the aminocyclohexanols but no satisfactory method was found for clean separation.

It was then decided to study the methylcyclohexanol isomers.

It was decided to use the concentration versus chemical shift method in order to try to differentiate between axial and equatorial hydroxyl groups.

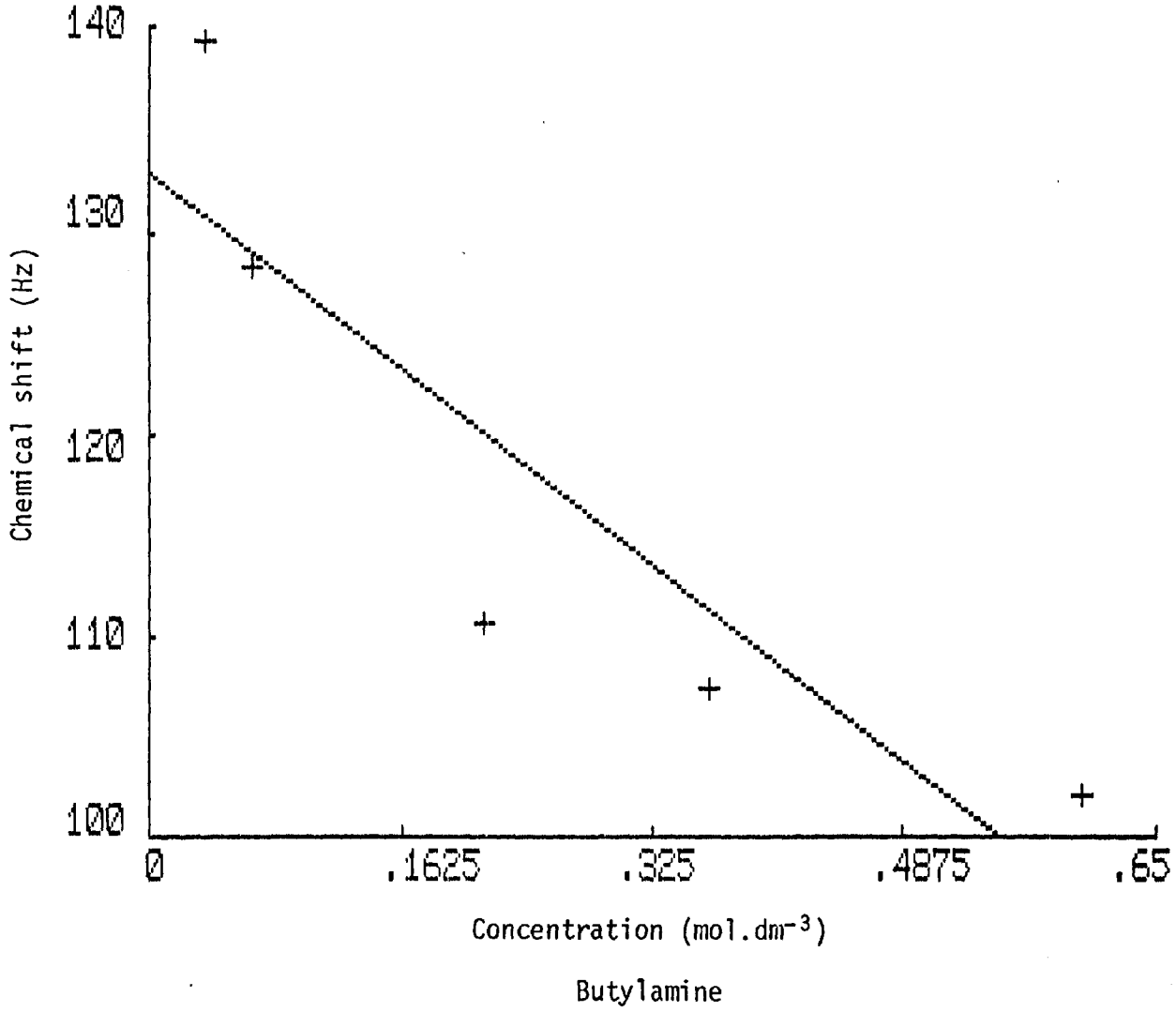
140
130
120
110
100
Chemical shift (Hz)
0
.1625
.325
.4875
.65
Concentration (mol.dm⁻³)
Butylamine

Methylcyclohexanol isomers

In order to demonstrate between axial and equatorial hydroxyl groups a study of cis and trans-4-tert-butylcyclohexanols was carried out. The tert-butyl group will ensure conformational homogeneity in the cyclohexane system because the size of the group ensures that it will be entirely in the equatorial position. It should be noted that the term cis and trans refers to the hydroxyl groups with respect to the tert-butyl group.

Also it is assumed that the tert-butyl group in the 4 position with respect to the hydroxyl group has no effect on the chemical shift associated with the hydroxyl group.

The study was carried out using cyclohexanol, cis-4-tert-butyl-cyclohexanol and trans-4-tert-butylcyclohexanol in tetrachloromethane using a probe temperature of 40°C.

TABLE 2.10

Cyclohexanol

Mass of Alcohol mg	Mass of CCl_4 g	Mole Fraction	Chemical Shift Hz
5.40	1.5805	0.005247	55.5
6.70	1.6802	0.006124	57.4
12.35	2.1736	0.008726	64.5
14.20	2.1131	0.010320	68.3
18.35	1.9679	0.014320	78.8

Limiting slope = 2575 Hz

Limiting chemical slope = 41.8 Hz

TABLE 2.11

cis-4-tert-Butylcyclohexanol

Mass of Alcohol mg	Mass of CCl_4 g	Mole Fraction	Chemical Shift Hz
6.70	1.5865	0.004157	35.3
10.35	1.7229	0.005913	39.4
18.20	1.3671	0.013104	52.1
21.70	1.2679	0.016820	60.0

Limiting slope = 1910 Hz

Limiting chemical shift = 27.6 Hz

TABLE 2.12

trans-4-tert-Butylcyclohexanol

Mass of Alcohol mg	Mass of CCl_4 g	Mole Fraction	Chemical Shift Hz
5.90	1.6424	0.003536	55.5
8.65	1.4399	0.005913	62.3
14.10	1.5538	0.008932	71.0
17.60	1.4644	0.011830	78.0

Limiting slope = 2725 Hz

Limiting chemical shift = 46.05 Hz

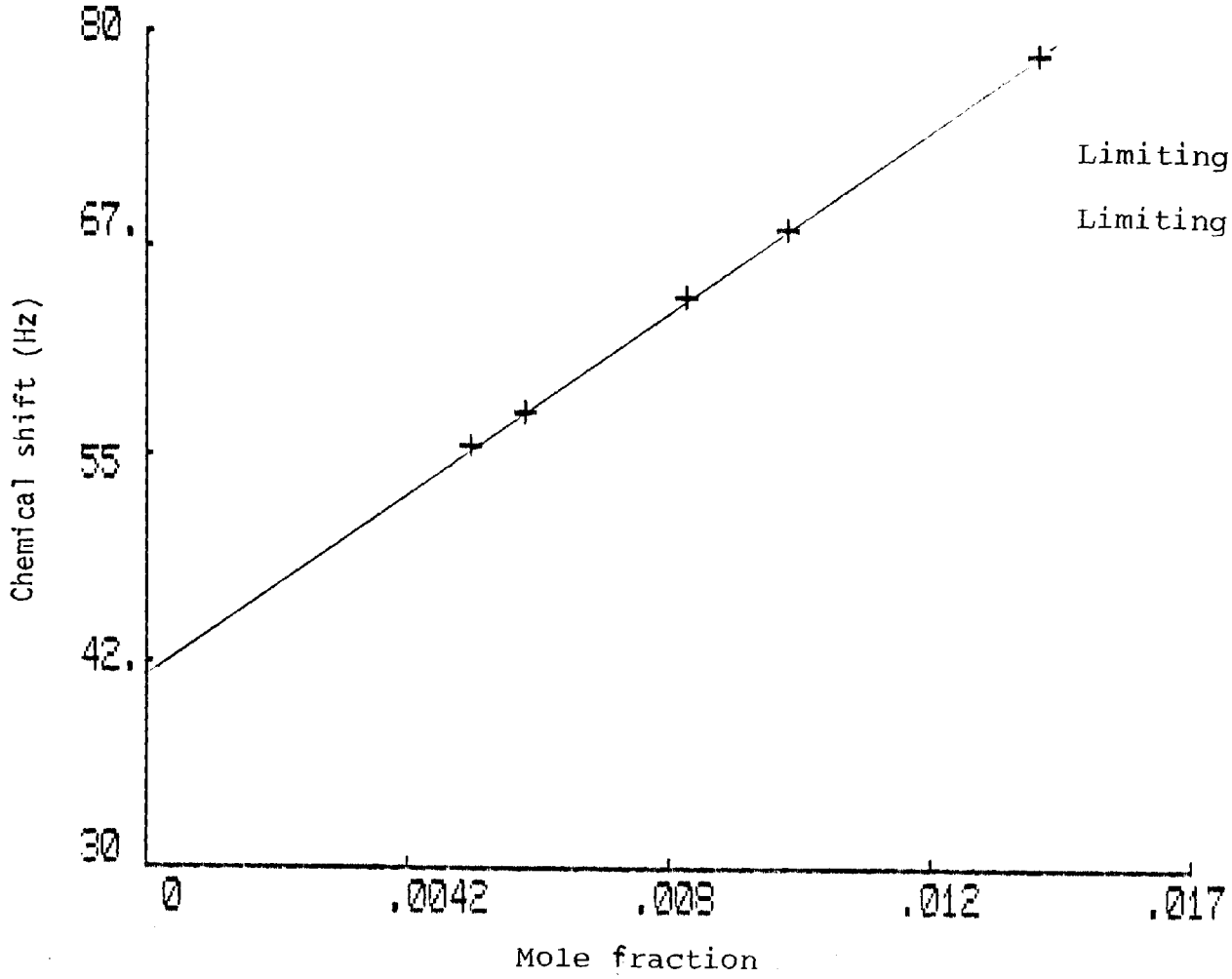

Limiting slope : 2575 Hz

Limiting chemical shift : 41.8 Hz

Chemical shift versus mole fraction for cyclohexanol in CCl_4 at $40^{o}C$

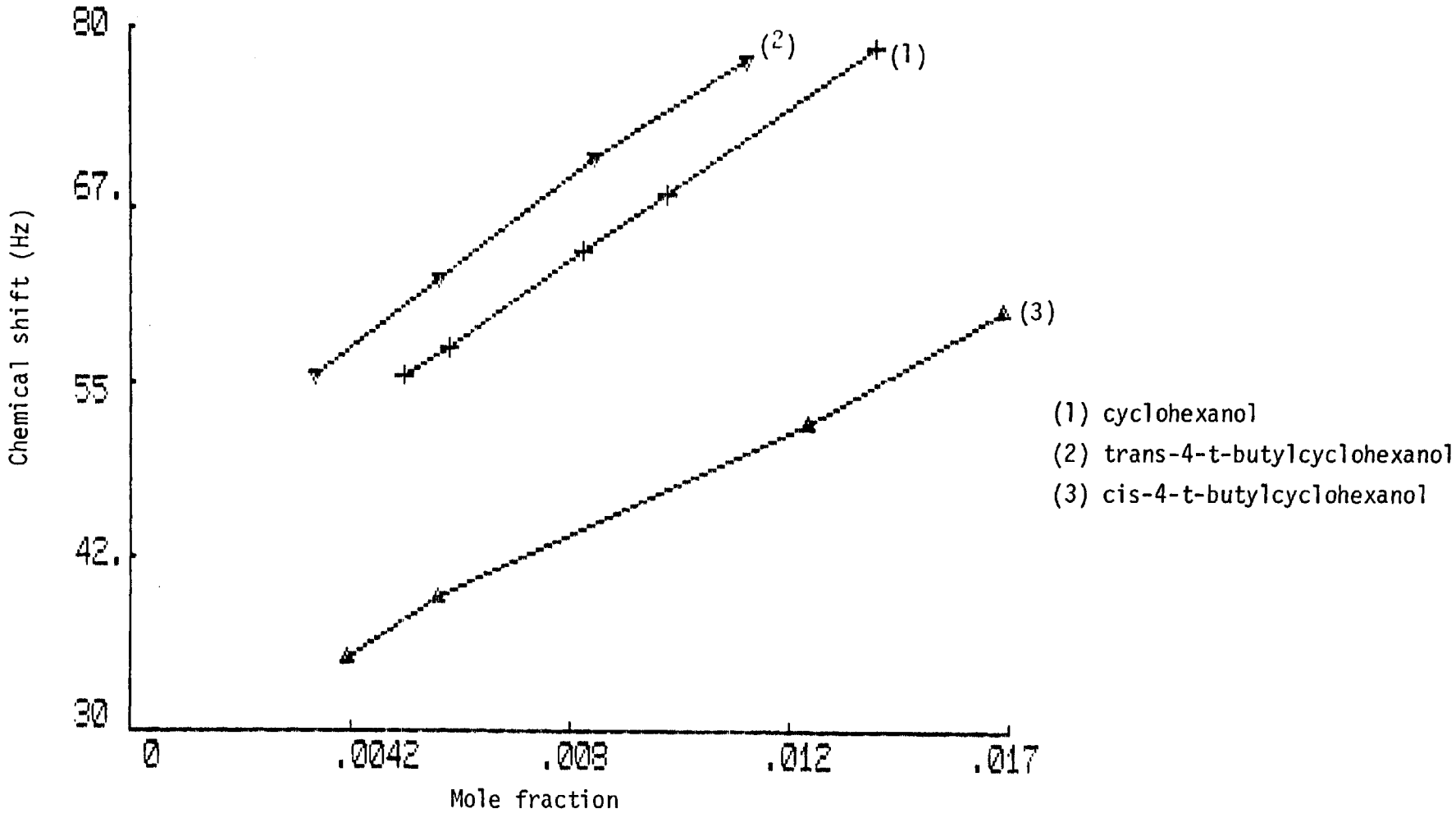

Chemical shift versus mole fraction for
(1) cyclohexanol
(2) trans-4-t-butylcyclohexanol
(3) cis-4-t-butylcyclohexanol
in CCl_4 at $40^{o}C$

The equilibrium involved with cyclohexanol is:

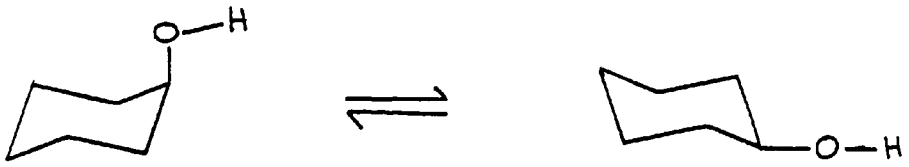

Eqn 2(1)

It can be seen from equilibrium 2(1) that the value of the chemical shift of 41.8 Hz at infinite dilution for cyclohexanol is an average of the pertinent hydroxyl groups in the two conformations. This average position gives rise to a chemical shift (i.e. 41.8 Hz) which will be given by the equation:

$$\delta = N_e\ \delta e + N_a\ \delta a \qquad \text{Eqn 2(2)}$$

where N_e is the mole fraction of cyclohexanol molecules with the hydroxyl group in the equatorial position and N_a the mole fraction with the hydroxyl group in the axial position. δe and δa are the chemical shifts for the hydroxyl groups in the pure equatorial and pure axial conformations.

Now:

$$N_a + N_e = 1 \quad \text{and} \quad \frac{N_e}{N_a} = K$$

therefore:

$$\delta = \frac{\delta a + K\delta e}{K + 1} \qquad \text{Eqn 2(3)}$$

hence:

$$K = \frac{\delta a - \delta}{\delta - \delta e}$$

where K is the equilibrium constant for equation 2(1).

Hence from the results obtained:

$$K = \frac{27.6 - 41.8}{41.8 - 46.0}, \quad \text{i.e.} \quad K = 3.38$$

and

$$-\Delta G_{OH} = RT \ln K$$

Hence:

$$-\Delta G_{OH} = 8.314 \times 313.5 \ln 3.38$$

$$= 3.17 \text{ kJ mol}^{-1}$$

Therefore, in cyclohexanol the preferred conformation of the hydroxyl group is in the equatorial position.

In cyclohexanol only one hydroxyl group is present and hence only one intermolecular hydrogen bond can occur. The slope of the graphs for cis and trans-4-t-butylcyclohexanol is interesting. For the trans compound the bonding chemical slope is 2725 HzN^{-1}, and for the cis 1910 HzN^{-1}. A hydrogen bond seems more likely to be formed when the hydroxyl group is in the equatorial position cis in trans-4-t-butyl-cyclohexanol.

TABLE 2.13

1-Methylcyclohexanol

Mass of Alcohol / mg	Mass of CCl_4 / g	Mole Fraction	Chemical Shift / Hz
21.45	2.2044	0.013110	72.75
10.65	1.5275	0.009392	68.25
6.90	1.6344	0.005687	63.20
6.25	2.0409	0.004125	60.75

Limiting slope = 1300 Hz

Limiting chemical shift = 56.0 Hz

The limiting chemical slope is 1300 Hz, which seems to indicate the OH group is in a preferred axial conformation with the larger methyl group in the equatorial position.

Figure 2(3)

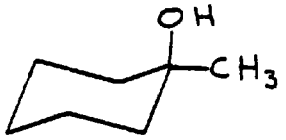

1-Methylcyclohexanol

The limiting chemical shift of the hydroxyl group in 1-methylcyclohexanol resonates at a position downfield from the hydroxyl group in trans-t-butylcyclohexanol. Possible steric interactions between the methyl and hydroxyl groups may lead to van der Waals deshielding which will be greatest for 1-methylcyclohexanol because of the closer proximity thus causing resonance at a lower field.

In cyclohexanol, purely from a steric point of view, it would be expected that the hydroxyl group in the axial position would have a greater steric interaction than the equatorial hydroxyl group and hence resonate further downfield.

Figure 2(4)

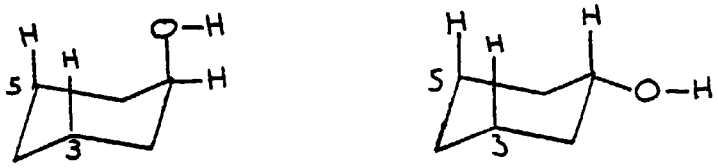

axial equatorial

Cyclohexanol

However, the opposite is actually found. The explanation given by Pople, Schneider and Bernstein [23] attributes this to the ring current effect. These workers drew a parallel between the cyclohexane system and the benzene ring where ring currents are known to be set up.

Figure 2(5)

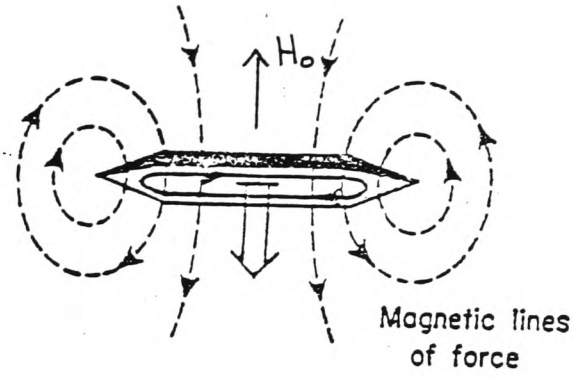

Current and magnetic lines of force induced in benzene by a primary field Bo

The secondary magnetic fields at the positions of the aromatic protons at the side of the ring will reinforce the primary field Bo and will, therefore, give a negative contribution to the screening constant. Hence the aromatic protons will resonate at lower field than others.

Although there is no direct magnetic evidence on the magnitude of the saturated ring currents, this could well be an explanation as to why the equatorial groups in the cyclohexane system appear at a lower field than axial groups (although only of the order of 1 ppm). The equatorial protons are considered to be in positions analogous to the ring protons in benzene. It must also be appreciated that this ring current effect must be greater than the effect of the van der Waal's deshielding.

TABLE 2.14

cis-2-Methylcyclohexanol

Mass of Alcohol mg	Mass of CCl_4 g	Mole Fraction	Chemical Shift Hz
11.80	1.6517	0.009624	56.25
7.85	1.6144	0.00655	53.65
22.80	1.9940	0.01540	61.50
4.55	1.7988	0.003407	51.75

Limiting slope = 840 Hz

Limiting chemical shift = 48.4 Hz

The limiting slope is 840 Hz which seems to indicate that the OH group is in a preferred axial conformation.

Figure 2(5)

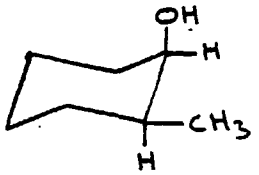

cis-2-Methylcyclohexanol

The limiting chemical shift of the hydroxyl group in cis-2-methylcyclohexanol resonates at a position downfield from the hydroxyl group in trans-t-butylcyclohexanol, but not as far downfield as in 1-methylcyclohexanol. This implies some steric interaction between the methyl and hydroxyl groups.

TABLE 2.15

trans-2-Methylcyclohexanol

Mass of Alcohol mg	Mass of CCl_4 g	Mole Fraction	Chemical Shift Hz
7.21	1.4805	0.00487	59.3
10.98	1.5844	0.00693	61.8
15.63	1.3930	0.01122	68.7
20.55	1.3023	0.01578	73.4

Limiting slope = 1206 Hz

Limiting chemical slope = 53.4 Hz

The limiting chemical shift for the hydroxyl group resonates at a position downfield from the hydroxyl group in trans-t-butylcyclohexanol but not as far downfield as in 1-methylcyclohexanol. This implies steric interaction between the methyl and hydroxyl groups.

The value of the limiting chemical slope is a measure of the amount of intermolecular hydrogen bonding present in the system, mainly dimer to monomer at low concentration. As dilution is carried out it is effectively breaking down the intermolecular hydrogen bonding.

As previously stated, the mode of intermolecular hydrogen bonding is quite complicated, taking place over at least three modes: equatorial-equatorial, equatorial-axial or axial-axial. However, since there is a much more open approach for reagents to the equatorial position, it would be expected that in the trans-2-methylcyclohexanol the hydroxyl group is in an equatorial position, as shown below:

Figure 2(6)

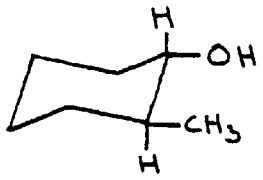

trans-2-Methylcyclohexanol

TABLE 2.16

cis-3-Methylcyclohexanol

Mass of Alcohol mg	Mass of CCl_4 g	Mole Fraction	Chemical Shift Hz
14.75	1.8540	0.01072	69.75
11.35	1.7086	0.008948	65.6
10.45	2.1372	0.006587	60.75
5.35	1.5424	0.004672	57.0
3.10	2.1879	0.001907	51.0
Limiting slope		= 2060 Hz	
Limiting chemical shift		= 47.4 Hz	

The limiting chemical shift for cis-3-methylcyclohexanol resonates at a position slightly downfield from trans-t-butylcyclohexanol. The limiting slope of 2060 Hz is quite near that of trans-t-butyl-cyclohexanol. This implies that the hydroxyl group is probably in an equatorial position. As the hydroxyl group and the methyl groups are quite far apart in the cis-3-methylcyclohexanol, intermolecular hydrogen bonding will be relatively easier than with the cis and trans 1 and 2 methylcyclohexanols. It would be expected that the hydroxyl group in cis-3-methylcyclohexanol exists in the equatorial position as shown below:

Figure 2(7)

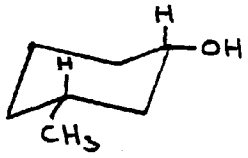

cis-3-Methylcyclohexanol

TABLE 2.17

trans-3-Methylcyclohexanol

Mass of Alcohol mg	Mass of CCl_4 g	Mole Fraction	Chemical Shift Hz
20.35	1.94750	0.01408	70.88
14.35	1.63620	0.01181	66.38
6.10	1.3177	0.006236	57.38
5.85	1.8813	0.004189	54.38

Limiting slope = 1630 Hz

Limiting chemical slope = 47.7 Hz

A comparison of these results with cis-3-methylcyclohexanol shows a difference in the limiting slope. Since the value of the limiting slope is a measure of the intermolecular hydrogen bonding in the system, it seems that in trans-3-methylcyclohexanol there is less intermolecular hydrogen bonding present, implying that the hydroxyl group exists in an axial position, as shown below:

Figure 2(8)

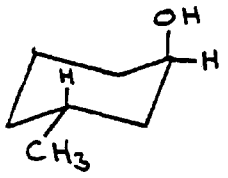

trans-3-Methylcyclohexanol

TABLE 2.18

cis-4-Methylcyclohexanol

Mass of Alcohol mg	Mass of CCl_4 g	Mole Fraction	Chemical Shift Hz
20.95	1.9840	0.014220	68.60
15.20	1.8647	0.01098	63.00
8.00	1.7358	0.006208	55.10
6.75	2.0767	0.004378	51.95
3.20	1.9727	0.002168	49.10

Limiting slope = 1660 Hz

Limiting chemical shift = 44.8 Hz

In cis and trans 4-methylcyclohexanols, the possible steric interactions between the methyl and hydroxyl groups will be at a minimum.

The limiting slope in cis-4-methylcyclohexanol implies that the hydroxyl group is in an axial conformation, as shown overleaf.

Figure 2(9)

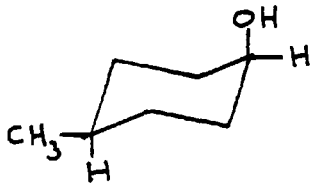

cis-4-Methylcyclohexanol

TABLE 2.19

trans-4-Methylcylohexanol

Mass of Alcohol mg	Mass of CCl_4 g	Mole Fraction	Chemical Shift Hz
25.45	2.2055	0.015540	87.40
19.60	2.1454	0.012310	78.20
10.55	1.7776	0.007995	67.10
6.00	1.5413	0.005244	61.50

Limiting slope = 2420 Hz

Limiting chemical shift = 48.2 Hz

The limiting slope and limiting chemical shift of trans-4-methylcyclohexanol are near to that of trans-4-t-butylcyclohexanol. The limiting slope of trans-4-methylcyclohexanol is also the nearest in the methylcyclohexanol series to the limiting slope of cyclohexanol.

In trans-4-methylcyclohexanol steric interactions between hydroxyl and methyl groups are at a minimum and it would be expected that the hydroxyl group is in an equatorial conformation, as shown below.

Figure 2(10)

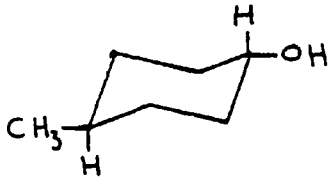

trans-4-Methylcyclohexanol

Summary of Results for Change in Chemical Shift with Concentration

Generally, as the solutions become more dilute, the value of the chemical shift falls. The change in chemical shift is due to altering the degree of hydrogen bonding in the solution. Interestingly, as solutions of cyclohexylamine and butylamine became more dilute, the value of the chemical shift was seen to increase.

The results given for the limiting chemical shift of cyclohexanol, cyclohexylamine, butylamine, the methylcyclohexanols, and the t-butylcyclohexanols are a measure of the monomeric hydroxyl proton at infinite dilution as well as a standard set for the absence of intramolecular hydrogen bonding.

Dilution has a great effect on intermolecular hydrogen bonding but not on intramolecular hydrogen bonding. Both trans-2-aminocyclohexanol and 1-amino-hydroxymethylcyclopentane have intramolecular hydrogen bonding as well as intermolecular hydrogen bonding, and their hydroxyl resonance position (limiting chemical slope) was much larger (further downfield from TMS), than that of a free hydroxyl proton.

The slopes of the graphs of concentration versus chemical shift varied from compound to compound, even when these were run in the same solvent and at the same constant temperature. This was due to the variation in the amount of intermolecular hydrogen bonding present. The concentration versus chemical shift graph makes it possible to distinguish between axial and equatorial hydroxyl groups in the methylcyclohexanol series.

TABLE 2.20

Compound	Hydroxyl Group	Methyl Group
1-methylcyclohexanol	axial	equatorial
cis-2-methylcyclohexanol	axial	equatorial
trans-2-methylcyclohexanol	equatorial	equatorial
cis-3-methylcyclohexanol	equatorial	equatorial
trans-3-methylcyclohexanol	axial	equatorial
cis-4-methylcyclohexanol	axial	equatorial
trans-4-methylcyclohexanol	equatorial	equatorial

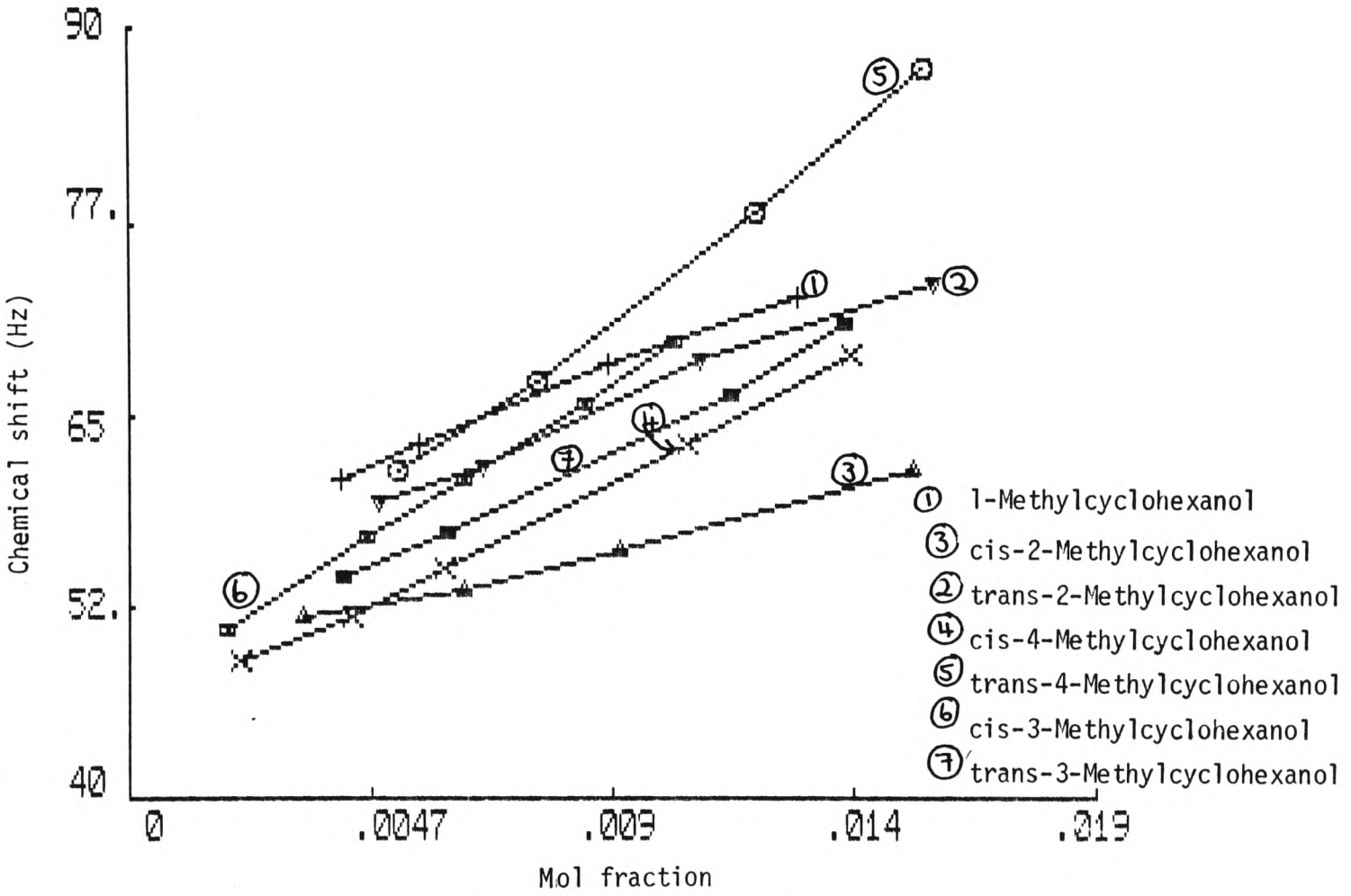

Isomers of Methyl-substituted cyclohexanols
in CCl_4 at $40^{o}C$

2.2 Investigation of the change in chemical shift with temperature

An increase in the temperature of a system containing intermolecular and intramolecular hydrogen bonding should bring about a decrease in both types of bonding, although it would be expected that intermolecular hydrogen bonding should decrease at a greater rate. In this investigation the intercept at 273 K ($0^{o}C$) and the slope were noted. The compounds studied were cyclohexanol, cyclohexylamine, trans-2-aminocyclohexanol.

The work was carried out with the solute dissolved in $CDCl_3$ at a probe temperature between 300 to 325 K.

Cyclohexanol

See Table 2.1 on page 62.

A graph was plotted of chemical shift versus temperature for solutions of cyclohexanol in $CDCl_3$.

From the graph of chemical shift versus temperature the following table was produced:

TABLE 2.21

Concn. cyclohexanol $mol.dm^{-3}$	Intercept at 273 K in Hz	Slope $Hz^{o}C^{-1}$
0.035	98.0	-0.245
0.0758	97.6	-0.307
0.1344	99.7	-0.261
0.2611	106.8	-0.357
0.350	113.15	-0.415
0.4203	117.6	-0.416

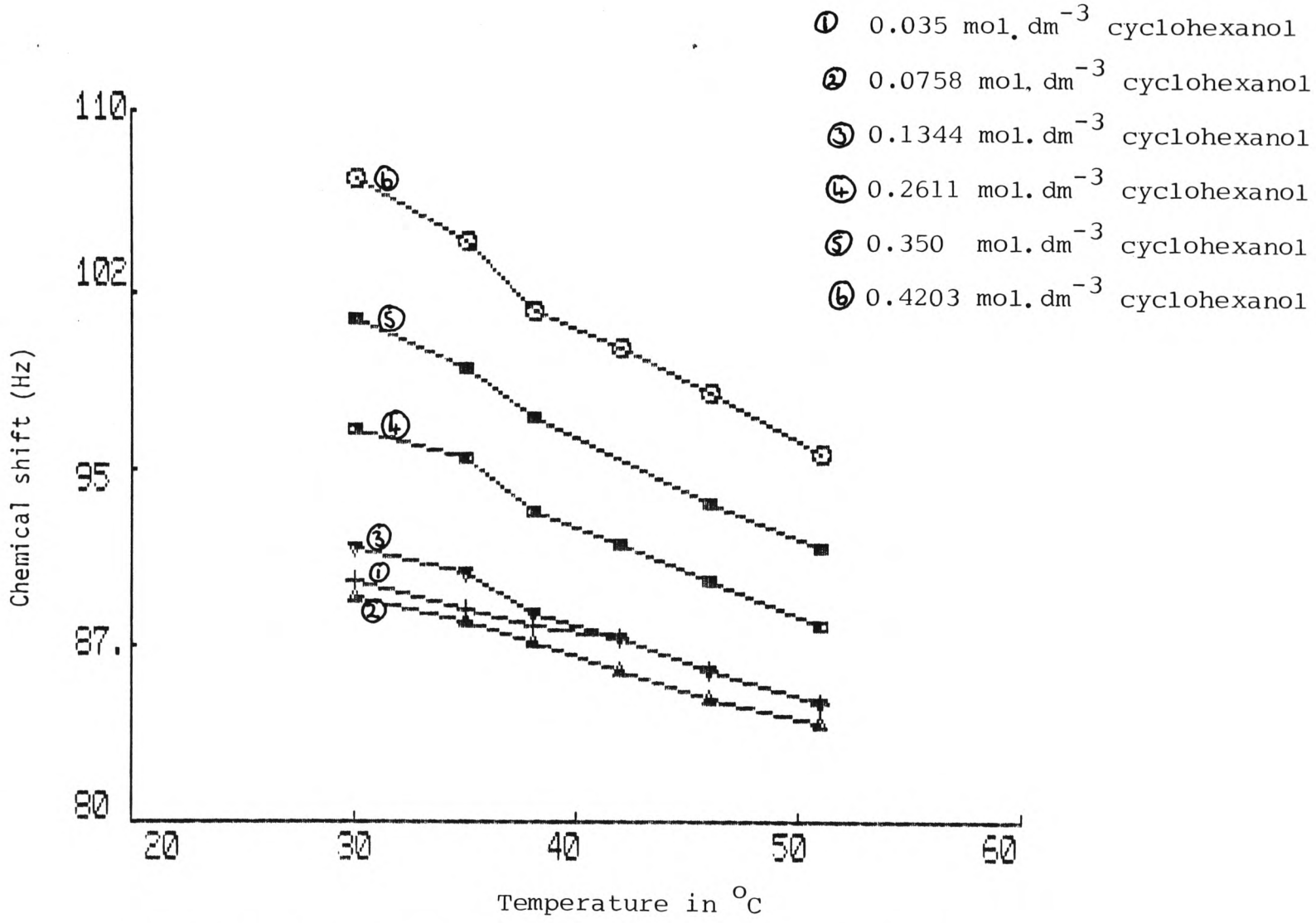

Chemical shift versus temperature for solutions of cyclohexanol in $CDCl_3$ at different concentrations of cyclohexanol

As previously stated, there are three main criteria which will affect hydrogen bonding, namely:

I. Solvent

II. Concentration

III. Temperature

In order to carry out experimental work on hydrogen bonding, it is necessary to keep two of the factors constant while varying the third. In this work the solvent and concentration were kept constant while varying the temperature.

Cyclohexanol molecules can be considered as a network in which the molecules are linked to one or more molecules by hydrogen bonds. The network of molecules will be continuously being built up and broken down with single molecules being added on or broken off randomly. There must also be free unbonded cyclohexanol molecules present. Solute solvent hydrogen bonding will also be present.

It would be expected that as the temperature increases, the amount of intermolecular hydrogen bonding will fall. The slope of the graph will give some indication of the intermolecular hydrogen bonding. At higher concentrations the negative slope increases as the temperature is lowered showing that more intermolecular hydrogen bonding is taking place, or conversely, more intermolecular hydrogen bonding breaks down on increasing the temperature.

Also for cyclohexanol it should be noted that the limiting chemical shift decreases with temperature, showing less hydrogen bonding is present at higher temperatures. Also the slope falls with increase in temperature, see graph on page 92, showing again less intermolecular hydrogen bonding as the temperature is increased.

Cyclohexylamine

See Table 2.3 page 65.

A graph was plotted of chemical shift versus temperature for solutions of cyclohexylamine in $CDCl_3$.

From the graph of chemical shift versus temperature the following table was produced:

TABLE 2.22

Concn. cyclohexylamine mol.dm^{-3}	Intercept at 273 K in Hz	Slope Hz $^{o}C^{-1}$
0.0225	92.6	-0.233
0.081	91.45	-0.304
0.140	89.35	-0.283
0.266	80.04	-0.150
0.392	78.8	-0.136

As the temperature is increased it is anticipated that the amount of intermolecular hydrogen bonding will fall. The slope of the graph will give an indication of the intermolecular hydrogen bonding.

An opposite trend is observed with cyclohexylamine compared to cyclohexanol in that as the concentration of the solution increases, the value of the negative slope decreases. However, the limiting chemical shift decreases as the temperature rises (see Table 2.4) as does that for cyclohexanol (see Table 2.2) but the value of the intercept at $0^{o}C$ for cyclohexylamine decreases with concentration, while cyclohexanol shows an increase.

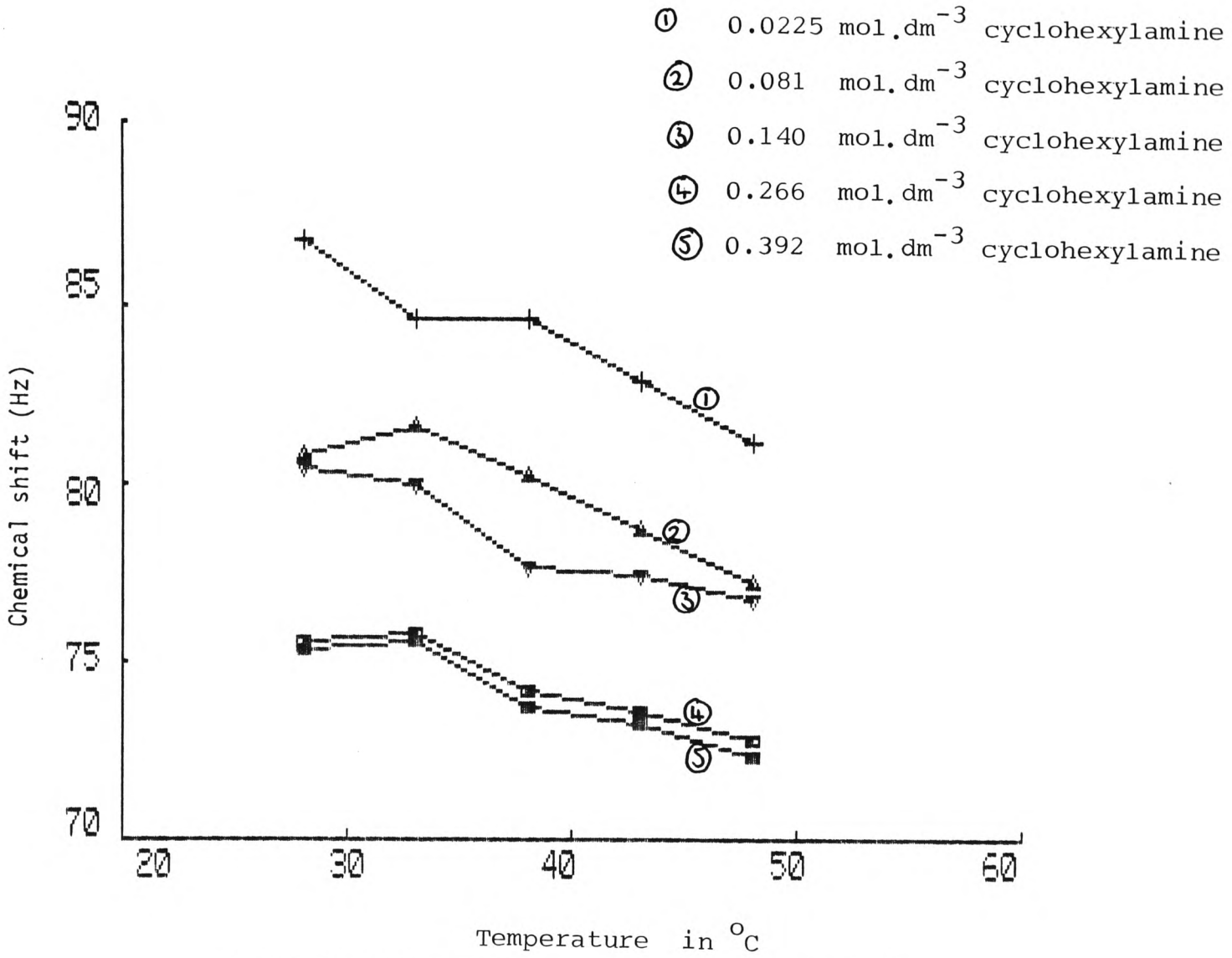

Chemical shift versus temperature for solutions of cyclohexylamine in $CDCl_3$

1-Amino-hydroxymethylcyclopentane

See Table 2.5.

In this compound the amino and hydroxyl groups are in close proximity. There exists the possibility of intermolecular and intramolecular hydrogen bonding.

Figure 2(11)

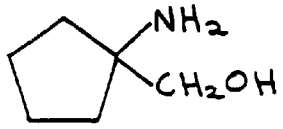

1-Amino-1-hydroxymethylcyclopentane

On increasing the temperature both the intermolecular hydrogen bonds and the intramolecular hydrogen bonds will be broken, as well as hydrogen bonding to the solvent.

The graph of chemical shift versus temperature for 1-amino-1-hydroxymethylcyclopentane gives the following results:

TABLE 2.23

Concentration 1-amino-1-hydroxymethylcyclopentane mol.dm^{-3}	Intercept at 273 K in Hz	Slope Hz $^{o}C^{-1}$
0.351	163.8	-0.762
0.279	161.4	-0.777
0.224	154.2	-0.72
0.140	135	-0.49
0.0868	126	-0.44
0.0536	113.4	-0.345

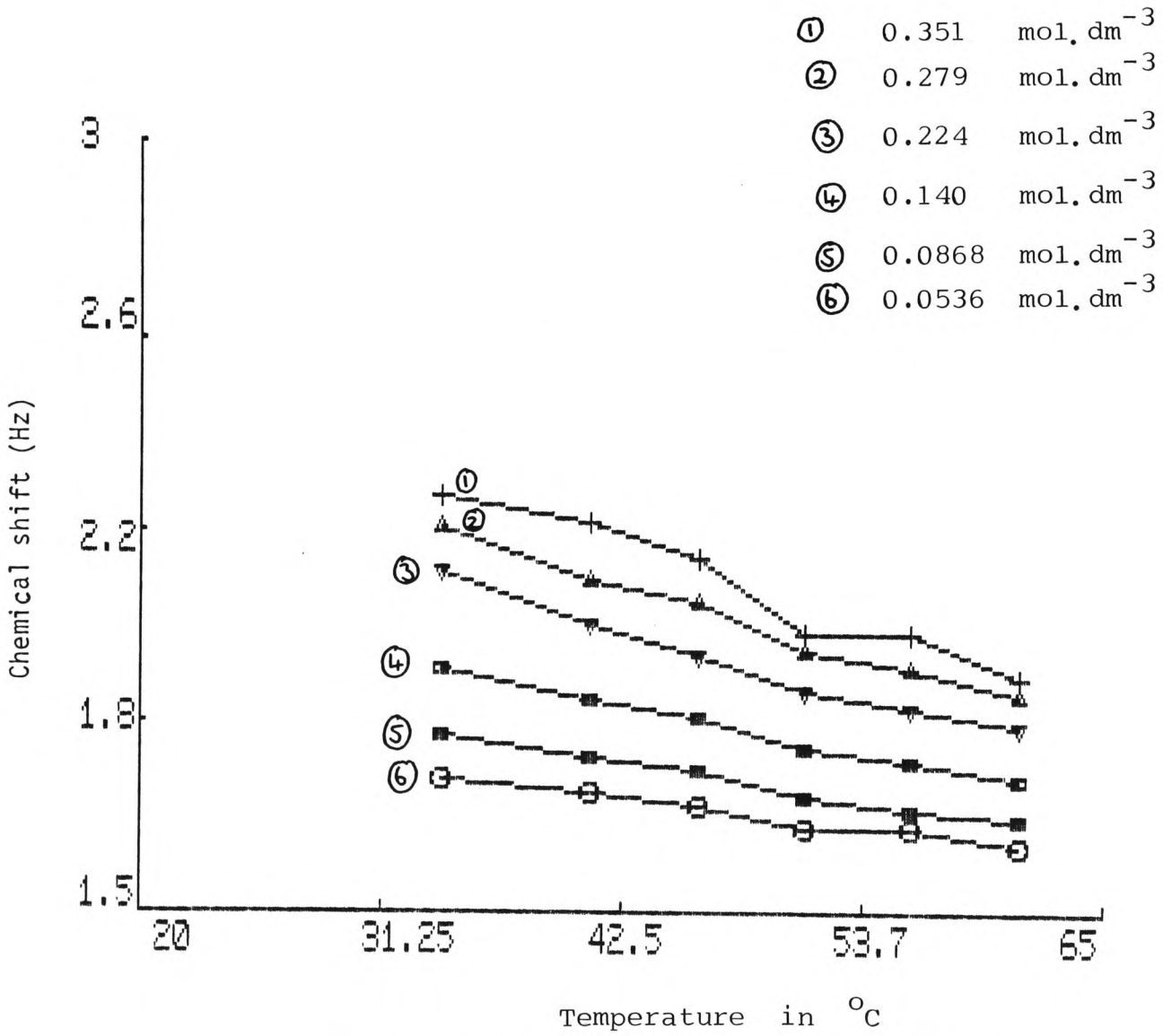

Chemical shift versus temperature for solutions of 1-amino-1-hydroxymethylcyclopentane in $CDCl_3$

The increase in negative slope with concentration indicates that as the concentration increases, the amount of hydrogen bonding increases. As the negative slope is greater for 1-amino-1-hydroxymethylcyclopentane than for either cyclohexanol or cyclohexylamine, this has given some indication that, on increasing the temperature, more hydrogen bonding is being broken down, i.e. both intermolecular and intramolecular.

Consider a comparison of the chemical slope versus temperature graph which can be obtained by plotting the chemical slope versus temperature for cyclohexanol, 1-amino-1-hydroxymethylcyclopentane and trans-2-aminocyclohexanol, which were obtained from Tables 2.2, 2.6 and 2.8 on pages

TABLE 2.24

Compound	Intercept at 273 K in Hz	Slope Hz $^{o}C^{-1}$
Cyclohexanol	59.1	-0.606
1-amino-1-hydroxymethylcyclopentane	194	-2.0
Trans-2-aminocyclohexanol	174.5	-1.8

The increase of negative slope with temperature for 1-amino-1-hydroxymethylcyclopentane and trans-2-aminocyclohexanol implies that as the temperature is increased, more hydrogen bonds are being broken than with cyclohexanol. As the temperature is decreased, more hydrogen bonds are being formed in the two compounds compared to cyclohexanol.

The value of the intercept at $0^{o}C$ also seems to be a good indicator of whether or not intramolecular hydrogen bonding is present.

N.B. Cyclohexylamine was not plotted as this graph slopes in the opposite direction to the three other compounds.

A graph was also plotted showing the variation of limiting chemical shift with temperature for cyclohexanol, cyclohexylamine, 1-amino-1-hydroxymethylcyclopentane and trans-2-aminocyclohexanol. The points were plotted from Tables 2.2, 2.4, 2.6 and 2.8 on pages 62,64,68 and 71.

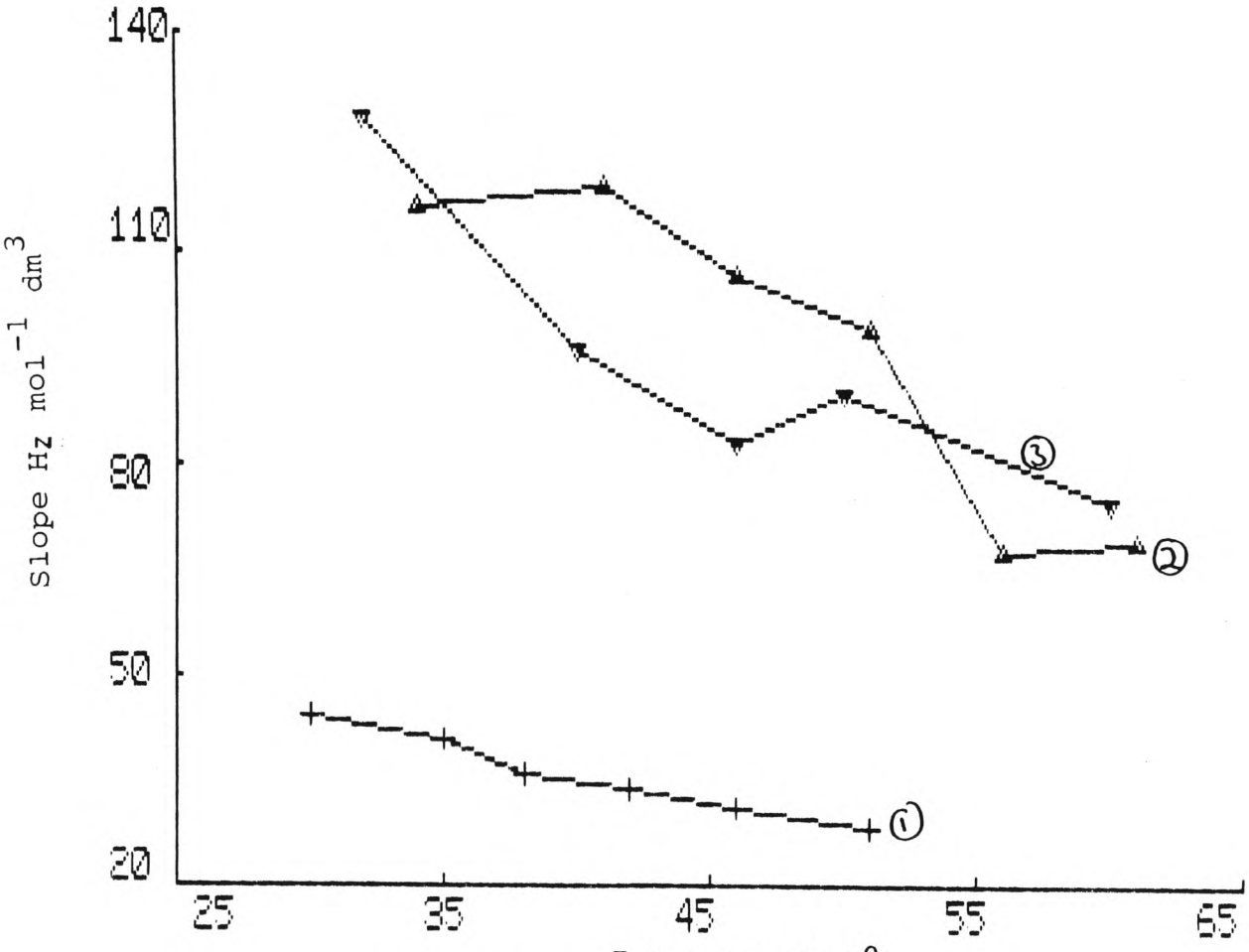

Chemical slope versus temperature for solutions of
(1) cyclohexanol
(2) 1-amino-1-hydroxymethylcyclopentane
(3) trans-2-aminocyclohexanol

in $CDCl_3$

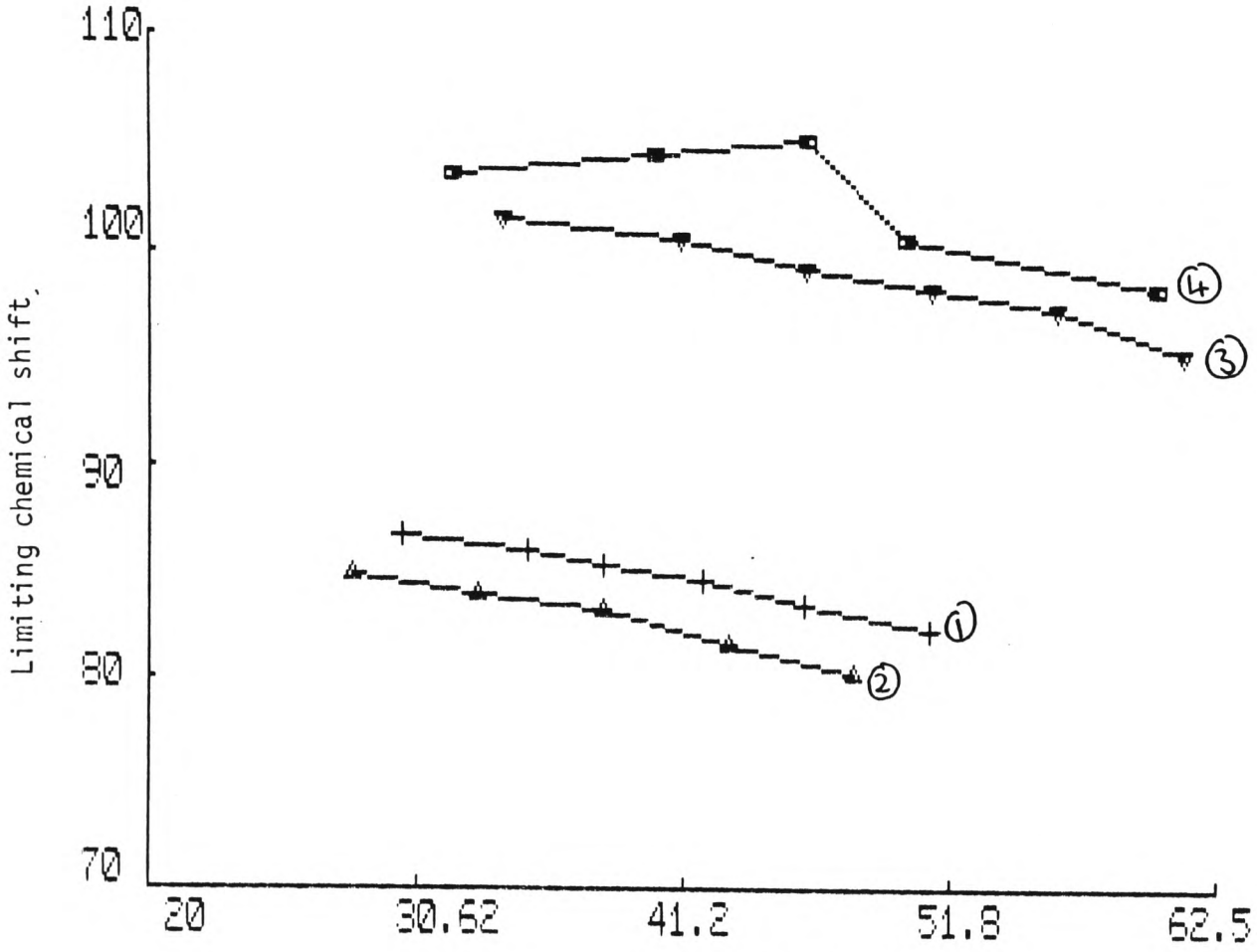

Variation of limiting chemical shift with temperature for
(1) cyclohexanol (3) 1-amino-1-hydroxymethylcyclopentane
(2) cyclohexylamine (4) trans-2-aminocyclohexanol in $CDCl_3$

Limiting chemical shift versus temperature

TABLE 2.25

Compound	Intercept at 273 K in Hz	Slope Hz $^{o}C^{-1}$
Cyclohexanol	92.2	-0.192
Cyclohexylamine	90.5	-0.192
1-amino-1-hydroxymethylcyclopentane	105.8	-0.145
Trans-2-aminocyclohexanol	106.9	-0.067

As previously stated, increase or decrease in temperature should have a greater effect on intermolecular hydrogen bonding than intramolecular hydrogen bonding.

Therefore, the limiting chemical shift should be greater, further downfield from TMS, for compounds which have an intramolecular hydrogen bond as well as an intermolecular hydrogen bond. It would be expected that 1-amino-1-hydroxymethylcyclopentane and trans-2-aminocyclohexanol would have an intramolecular hydrogen bond.

The intercept at $0^{o}C$ also gives an indication of whether or not intramolecular hydrogen bonding is present in the compounds.

trans-2-Aminocyclohexanol

See Table 2.7 on page 71.

In this compound the amino and hydroxyl groups are in close proximity, so there is the possibility of intramolecular hydrogen bonding as well as intermolecular hydrogen bonding.

The compound should show similar results to 1-amino-1-hydroxymethylcyclopentane when the temperature is varied.

After plotting a graph of chemical shift versus temperature for trans-2-aminocyclohexanol the following results were obtained:

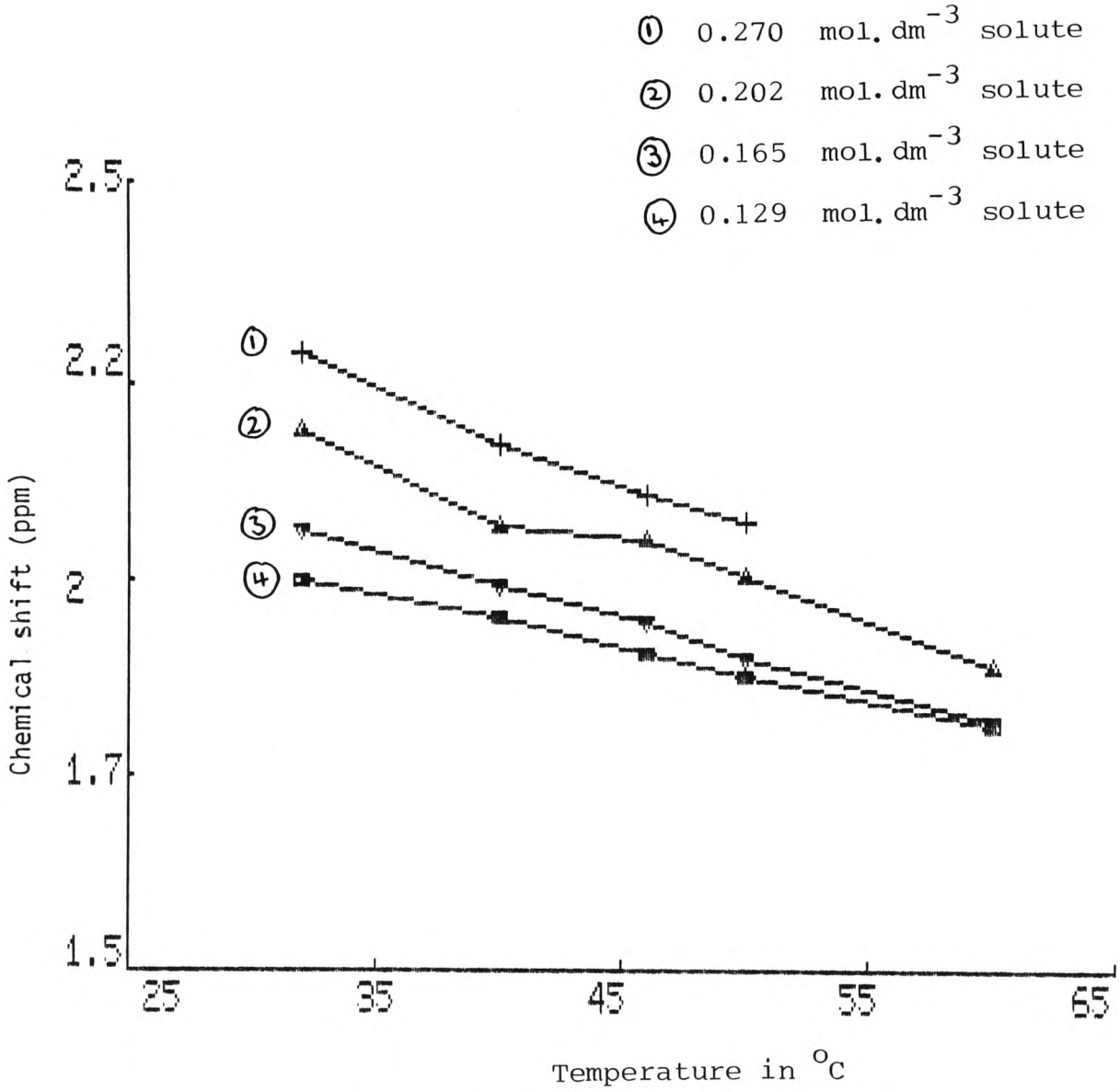

Chemical shift versus temperature for solutions of trans-2-aminocyclohexanol in $CDCl_3$

TABLE 2.26

Concn. trans-2-aminocyclohexanol mol.dm^{-3}	Intercept at 273 K in Hz	Slope Hz $^{o}C^{-1}$
0.270	155.4	-0.621
0.202	140.4	-0416
0.165	133.2	-0.343
0.129	128.4	-0.295

From the previous Tables 2.24, 2.23 and 2.22, it would be expected that trans-2-aminocyclohexanol contains an inter and an intramolecular hydrogen bond. The more concentrated the solution the quicker the hydrogen bonds are broken as the temperature increases, as shown by the slope.

The intramolecular hydrogen bond is more stable to temperature increase than the intermolecular hydrogen bond at the intercept at $0^{o}C$ is much further downfield (further away from TMS) than either cyclohexanol or cyclohexylamine.

As previously discussed, the preferred conformation for trans-2-aminocyclohexanol seems to be the alternate chair, as shown by the following.

Consider the possible conformations of trans-2-aminocyclohexanol.

Figure 2(12)

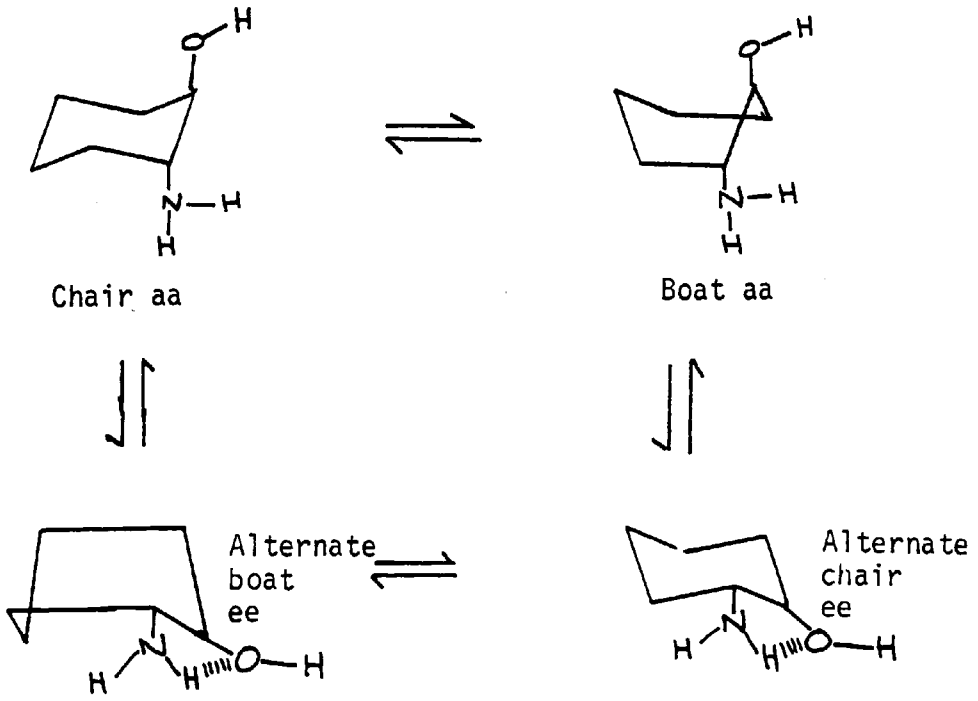

Intramolecular hydrogen bonding can take place in two conformations: (i) the alternate chair conformation and (ii) the alternate boat conformation. In (i) the two groups are equatorial which is energetically favoured, while in (ii) both groups are again equatorial.

The alternate chair is the most likely conformation for trans-2-aminocyclohexanol as the alternate boat would be energetically less favoured than the chair and probably only a very small amount would be present.

Summary of Results for Investigation of Chemical Shift Versus Temperature

As the temperature increases, the value of chemical shift falls. The change in chemical shift is due to altering the degree of hydrogen bonding in solution. Less hydrogen bonding is present at higher temperatures.

Interestingly, solutions of cyclohexylamine showed a difference in that, as the concentration increases, the value of the negative slope decreases.

An indication of intramolecular hydrogen bonding is given by the intercept in Hz at $0^{o}C$ and the negative slope. See Tables 2.24 and 2.25 on pages 98 and 101.

2.3 Investigation of the effect of lanthanide shift reagents on the chemical shift

The effects of paramagnetic species are commonly used to simplify spectra of organic compounds. A lanthanide shift reagent is an octahedral complex of lanthanide element (Eu, Dy, Pr, or Yb) with a ligand chosen to make the complex soluble in organic solvents, and this is dissolved in a solution of the compound. The lanthanides are capable of assuming higher co-ordination numbers than six, so that if the organic molecule possesses a suitable co-ordination site like O or N, it can interact with the complex. This produces on average pseudo-contact shift of the protons in the organic molecule which can be very large.

The effect on the resonance positions of the different protons in cyclohexanol upon addition of increasing amounts of Eu $(fod)_3$ is shown in the results. In the absence of Eu $(fod)_3$ only H_1 and OH protons are readily assignable. Increasing the amounts of Eu $(fod)_3$ demonstrates the linearity.

The shift of all cyclohexanol protons was in the same direction, i.e. to lower field values.

Approximate deuteriotrichloromethane resonance protons for the various protons of cyclohexanol can be obtained by extrapolation of the concentration lines to their origin. Accordingly, if the resulting $CDCl_3$ values for different protons are subtracted from corresponding values obtained by extrapolating in the opposite direction to a point where the molar concentration of complex to solute is one, a paramagnetic induced shift for different solute protons was determined.

A distinct advantage of this method, is that it allows the estimation of chemical shift values for protons where resonances are not evident in the normal spectrum of the compound.

It appears that the nearer the proton is to the metal ion the greater the deshielding effect.

It is realised from the results that the saturation point, solute: Eu $(fod)_3$, has not been achieved. To reach this point would require the addition of more Eu $(fod)_3$ to the solution, which is not possible for solubility reasons, or reduction in the amount of solute present. Experimentally it was found that there was very poor signal to noise levels at low concentration of the solute making measurements generally unfeasible.

The lanthanide chemical shift reagents that are used to simplify ^1H NMR spectra of compounds can also be used in ^{13}CMR studies. Since ^{13}C resonances enjoy a far greater freedom from overlap than proton resonances, chemical shift reagents do not yield the same benefits as in proton NMR.

TABLE 2.27

Chemical shift (ppm) when Eu $(fod)_3$ is added in increasing quantities to cyclohexanol (PMR)

7.35×10^{-5} mole of cyclohexanol used in 1.5 cm^3 $CDCl_3$ at 19°C

Mass Eu $(fod)_3$	Moles Eu $(fod)_3$	OH	$H_{(1)}$	$H_{(2+6)}$	$H_{(3+5)}$	$H_{(4)}$
0.02836	0.273×10^{-4}	6.01	4.53			
0.03798	0.366×10^{-4}	7.46	4.902	2.55		
0.05345	0.515×10^{-4}	10.03	5.51	2.91	2.35	
0.09809	0.945×10^{-4}	16.43	7.014	3.83	2.67	2.11
0.18150	1.749×10^{-4}	27.275	9.65	5.55	3.39	2.71

A graph was plotted of chemical shift ppm versus moles Eu $(fod)_3 \times 10^{-5}$.

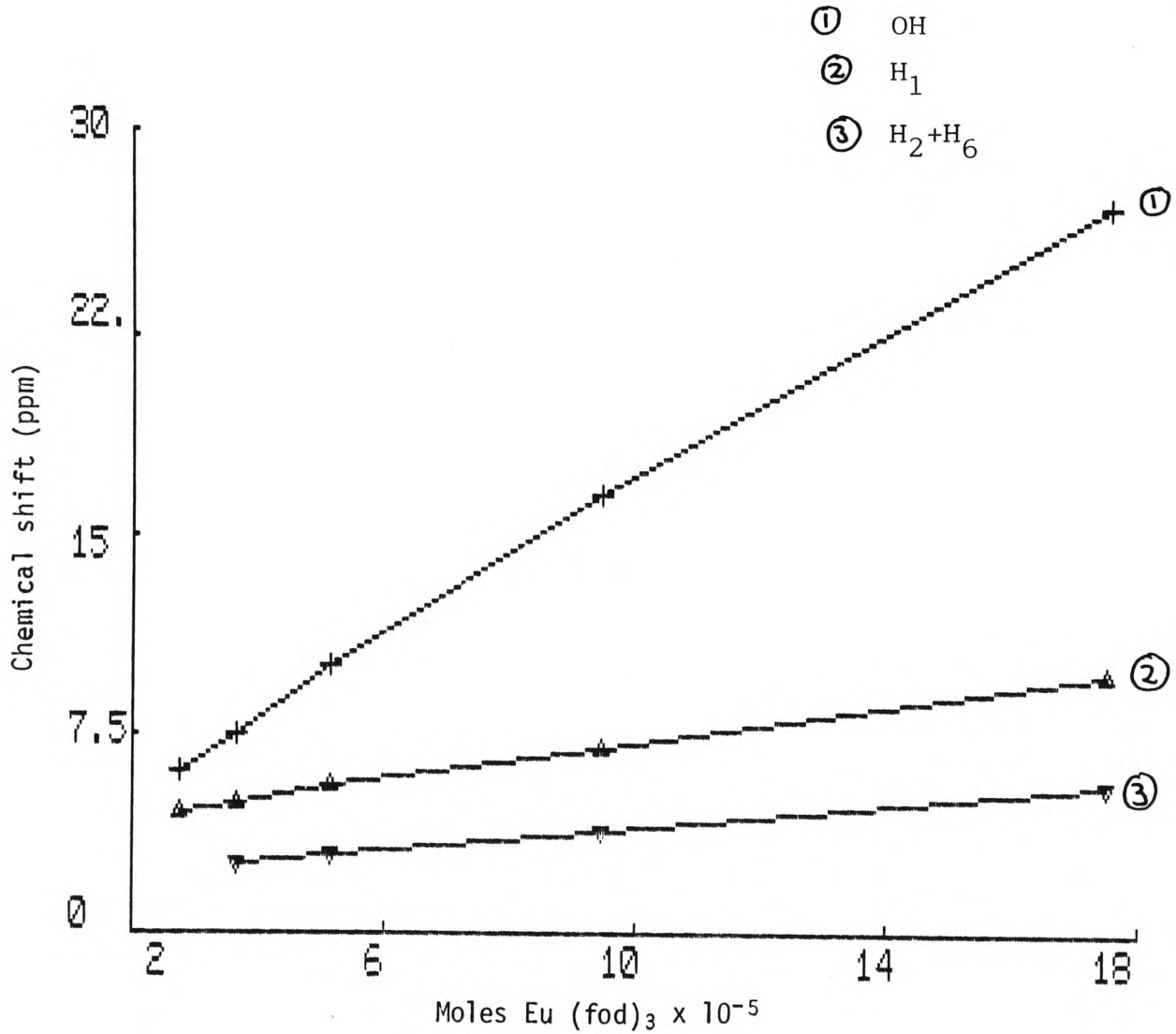

Proton chemical shift (ppm) when Eu $(fod)_3$ is added in increasing quantities to cyclohexanol

Values at 1:1 cyclohexanol : Eu $(fod)_3$ were found from the graph by extrapolation.

A table to show the difference in resonance position for a given solute proton when dissolved in inert $CDCl_3$ from that when an equimolar amount of Eu $(fod)_3$ is present in the same solvent.

TABLE 2.28

Chemical shift in ppm

Cyclohexanol	OH	$H_{(1)}$	$H_{(2+6)}$	$H_{(3+5)}$	$H_{(4)}$
	-97.48	-54.06	-29.79	-20.77	-16.02

TABLE 2.29

Proton chemical shift when Eu $(fod)_3$ is added in increased quantities to a fixed amount of cyclohexylamine

Cyclohexylamine = 3.61×10^{-4} mole

^1H - NMR was carried out in deuteriotrichloromethane at 19°C

Mass Eu $(fod)_3$	Moles Eu $(fod)_3$	N-H	H (1)	H (2 + 6)	H (3 + 5)	H (4)
0.00316	3.19×10^{-5}	8.79	5.59	3.43	2.55	-
0.09929	9.57×10^{-5}	22.39	8.11	6.55	5.59	-
0.18245	1.758×10^{-4}	34.15	11.27	9.11	8.07	-
0.24106	1.32×10^{-4}	36.67	11.91	9.63	8.47	-

A graph was plotted of chemical shift ppm versus moles Eu $(fod)_3$.

Values at 1:1 cyclohexylamine : Eu $(fod)_3$ were found from the graph by extrapolation.

A table to show the difference in resonance position for a given solute proton when dissolved in inert $CDCl_3$ from that when an equimolar amount of Eu $(fod)_3$ is present in the same solvent.

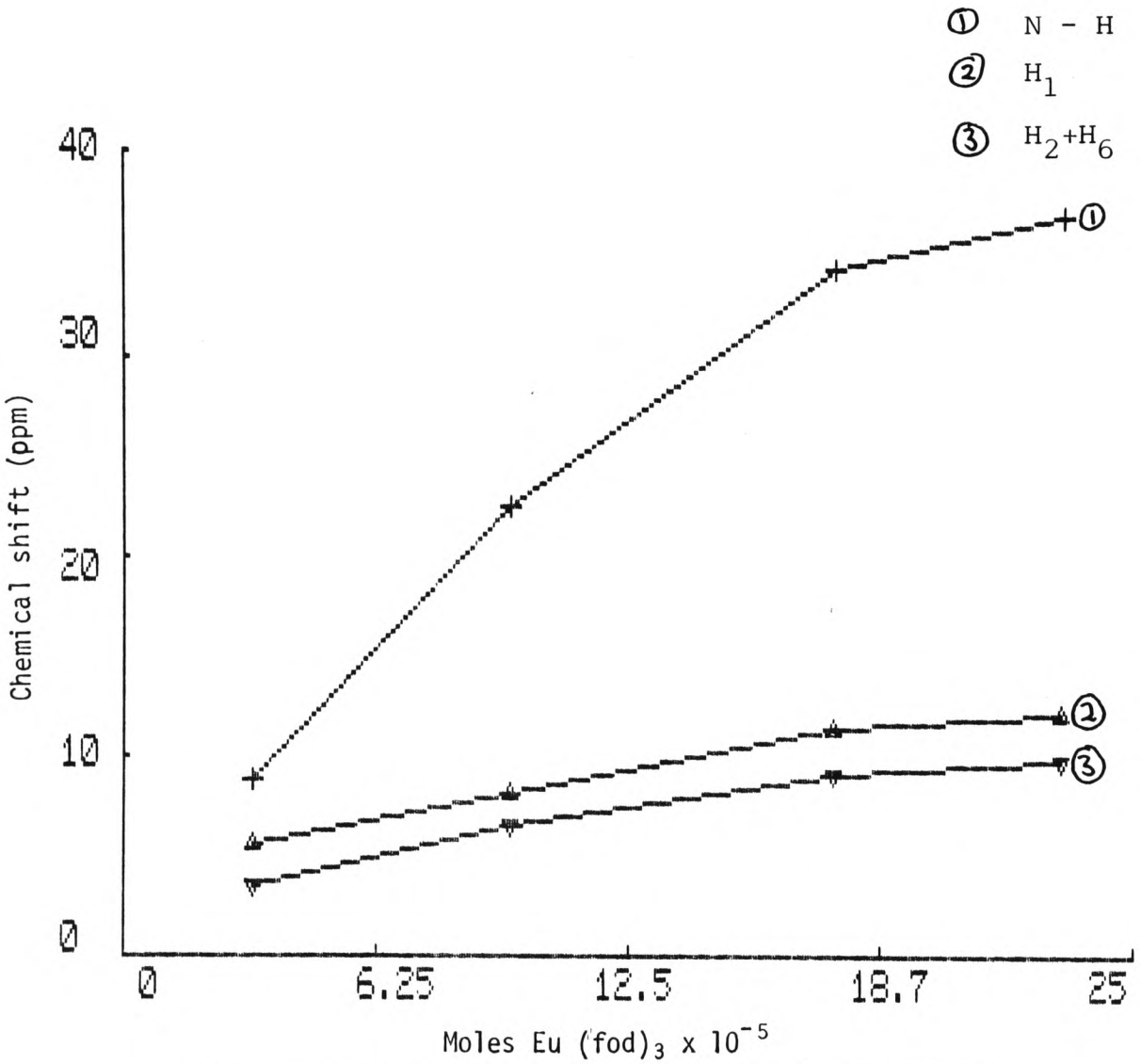

Proton chemical shift (ppm) when Eu $(fod)_3$ is added in increasing quantities of cyclohexylamine

TABLE 2.30

Chemical shift in ppm

Cyclohexylamine	N-H	$H_{(1)}$	$H_{(2+6)}$	$H_{(3+5)}$
	63.18	20.06	15.88	14.26

TABLE 2.31

Chemical shift when Eu $(fod)_3$ is added in increased quantities to a fixed amount of cyclohexylamine

Cyclohexylamine = 3.61×10^{-4} mole

^{13}C spectra in deuteriotrichloromethane at room temperature 19 °C

Moles Eu $(fod)_3$	$C_{(1)}$	$C_{(2+6)}$	$C_{(3+5)}$	$C_{(4)}$
3.19×10^{-5}	56.535	36.990	26.656	25.901
1.758×10^{-4}	74.914	36.238	28.812	27.521
2.32×10^{-4}	78.981	36.282	28.947	27.953
9.57×10^{-5}	67.14	36.429	27.899	26.730

A graph was plotted of chemical shift H_2 versus moles Eu $(fod)_3$.

Values for equimolar cyclohexylamine : Eu $(fod)_3$ were found from the graph by extrapolation.

A table to show the difference in resonance position for a given solute proton when dissolved in inert $CDCl_3$ from that when an equimolar amount of Eu $(fod)_3$ is present in the same solvent.

TABLE 2.32

Cyclohexylamine	C-N	$C_{(2+6)}$	$C_{(3+5)}$	$C_{(4)}$
Chemical shift in Hz	122.26	52.56	42.16	40.72
Chemical shift in ppm	2.04	0.88	0.70	0.68

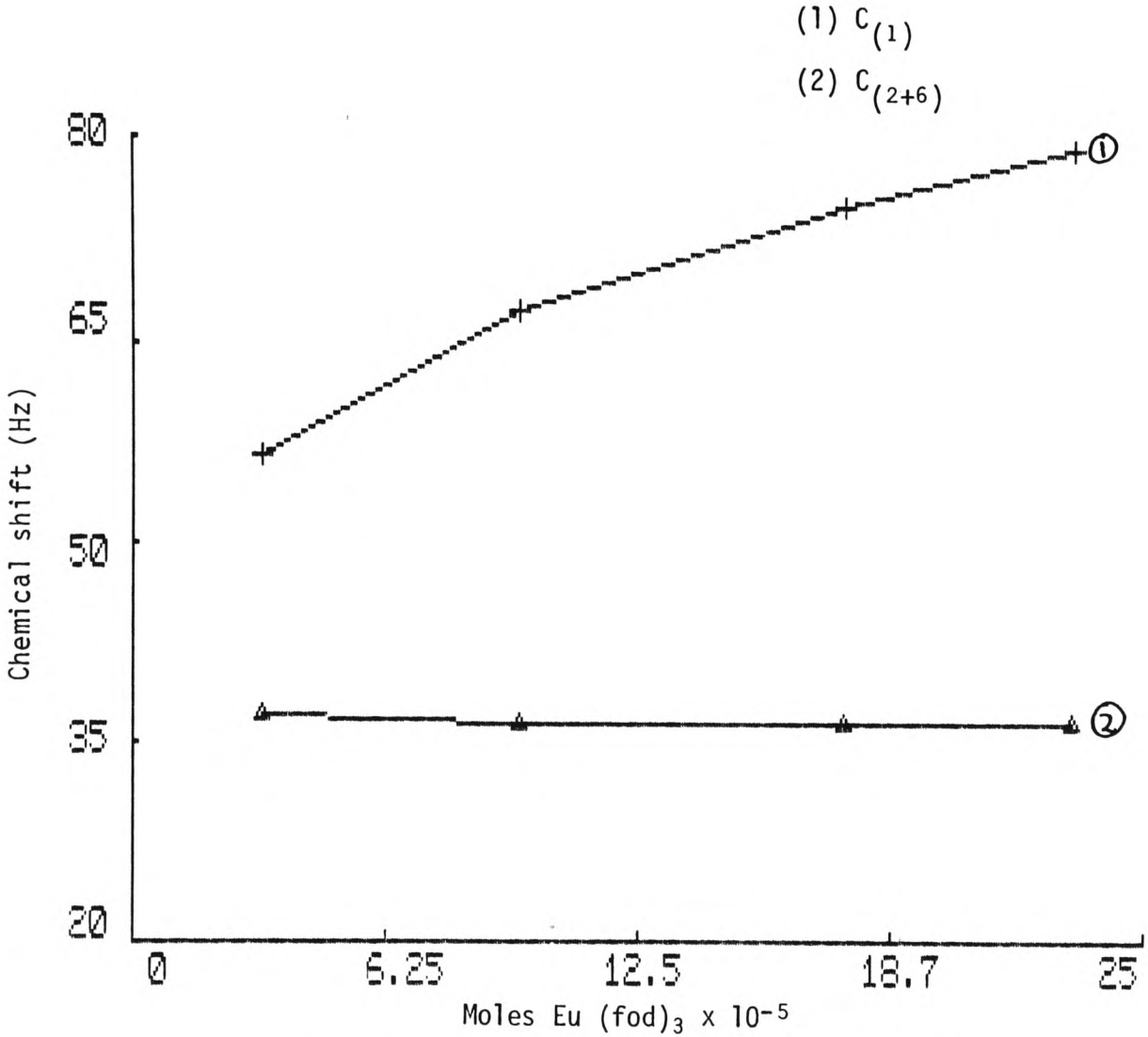

^{13}C chemical shift when EU $(fod)_3$ is added in increasing quantities to a fixed amount of cyclohexylamine

TABLE 2.33

Chemical shift when Eu $(fod)_3$ is added in increased quantities to a fixed amount of cyclohexanol

Cyclohexanol = 3.49×10^{-5} mole

^{13}C spectra in deuteriotrichloromethane at room temperature 19°C

Moles Eu $(fod)_3$	Values in Hz $C_{(1)}$	$C_{(2+6)}$	$C_{(3+5)}$	$C_{(4)}$
1.17×10^{-5}	401.63	240.95	138.93	102.01
2.333×10^{-5}	680.65	413.31	213.25	176.76
3.46×10^{-5}	882.03	561.93	266.9	229.08

Chemical shift at equivalent amounts of Eu $(fod)_3$ and cyclohexanol were found from the graph.

TABLE 2.34

$C_{(1)}$	=	876 Hz
$C_{(2+6)}$	=	556 Hz
$C_{(3+5)}$	=	268 Hz
$C_{(4)}$	=	228 Hz

These values were converted to ppm

Cyclohexanol	$C_{(1)}$	$C_{(2+6)}$	$C_{(3+5)}$	$C_{(4)}$
	14.6	9.27	4.47	3.8

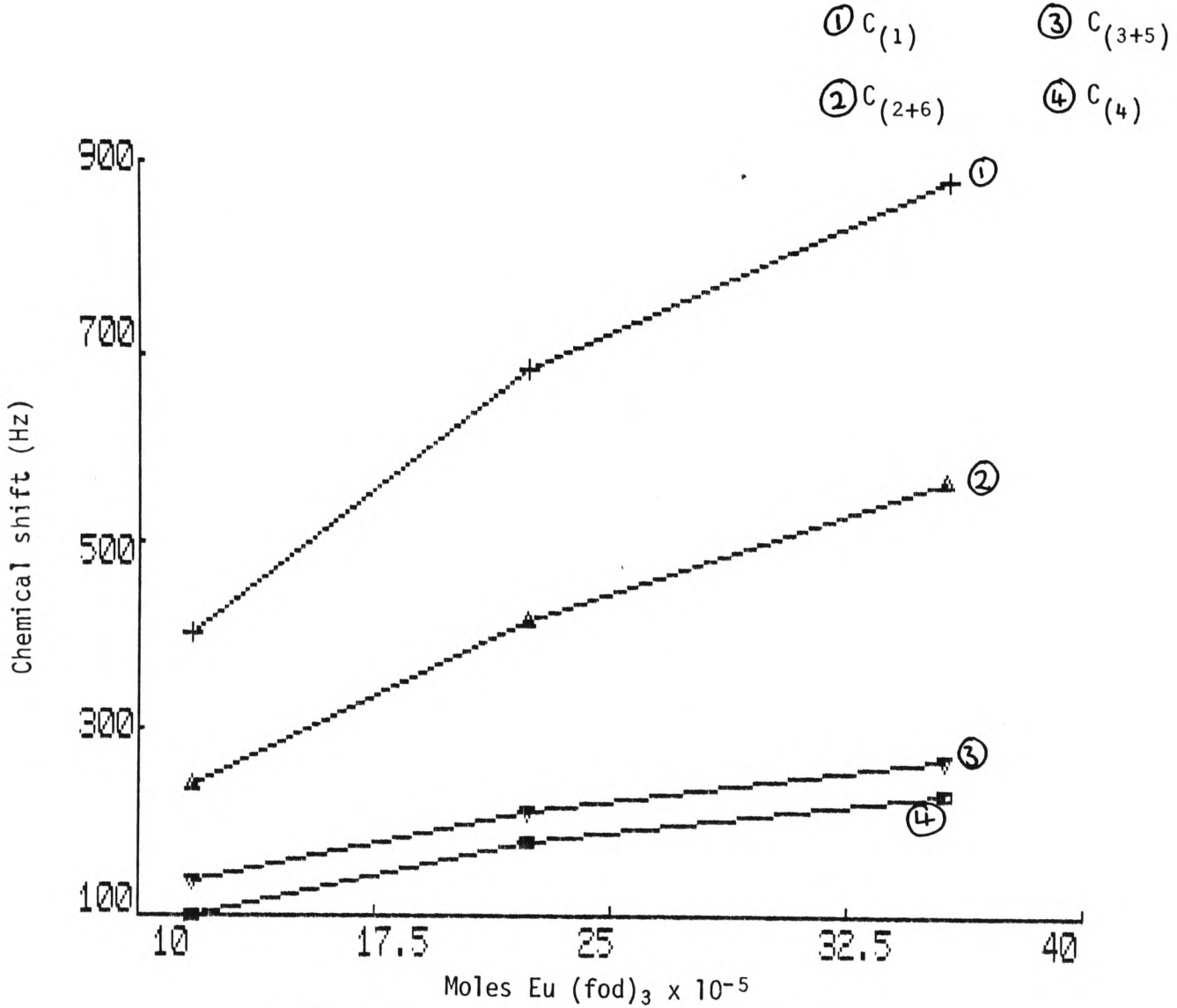

^{13}C chemical shift when Eu $(fod)_3$ is added in increasing quantities to a fixed amount of cyclohexanol

Summary of Results of the Effect of Lanthanide Shift Reagents on Chemical Shift

Eu $(fod)_3$ was used in PMR and ^{13}CMR as a chemical shift dispersion agent. The induced shifts, generally brought about by secondary internal fields originating from unpaired electron spins, resulted in greatly simplified spectra.

Eu $(fod)_3$ was found to induce downfield shifts and the shift values quoted are for 1:1 solute to shift reagent.

When the molecule contains a polar group like OH or NH_2 the progressive addition of shift reagent enables one to differentiate between hydrogen located in different sections of the molecule with PMR and also between different carbon atoms if ^{13}CMR was used.

2.4(1) Investigation of carbon-13 and proton relaxation times

Carbon-13 relaxation times

In a proton NMR experiment the protons are subjected to a powerful, uniform magnetic field. The protons may be considered to be aligned with the field and precessing about the axis of the applied magnetic field B_0.

Because of thermal disorder, only a small fraction of the total population of protons is properly aligned but this factor is sufficient. The radiofrequency electromagnetic energy is applied in such a way that the magnetic component B_1 is at right angles to the main magnetic field B_0 and is rotating with the precessing proton. This is accomplished by a coil with its axis at right angles to the axis of the main magnetic field B_0.

At this stage the absorbed energy is at a maximum and the precessing nuclei are tilted away from alignment with B_0 towards the horizontal plane. The magnetic component generated in that plane can be detected. Alternatively, the oscillator frequency is held constant, and B_0 is swept over a narrow range.

It is now important to discuss how the nucleus in the higher energy state returns to the ground state. In the absence of such a mechanism, all of the small excess population of nuclei in the lower energy state will be raised to the high energy state, and no more energy could be absorbed. Fortunately there exists a mechanism whereby the nucleus in the high energy state can loose energy to is environment and thus return to its lower energy state. The mechanism is called a spin-lattice or longitudinal relaxation process and involves the transfer of energy from the nucleus in its high energy state to the molecular-lattice. Its efficiency is described as the half life T_1, for the

transfer, an efficient relaxation process involving a short time T_1.

There is another effect called spin-spin or transverse relaxation described in terms of time T_2. This involves transfer of energy from one high energy nucleus to another. There is no net loss of energy but the spread of energy among the nuclei concerned results in line broadening.

Relaxation and nuclear Overhauser effect

There are two different methods of relaxation, spin-lattice T_1, and the spin-spin relaxation, T_2. The former term implies a process based upon an interaction between spins and their surroundings, commonly referred to as the lattice. If transitions are induced by application of a radiofrequency field at resonance, the equilibrium concentrations are perturbed in that spins are promoted to the higher energy level. In other words the net energy of the spin system has increased. In order to return to thermal equilibrium, the excess energy has to be dissipated. This is brought about by an energy exchange between the spin system and the lattice. The excited (hot) spins are cooled by the thermal broth in which they are immersed, i.e. the lattice. Since the spins are isolated from the lattice, the mutual interaction is small and consequently the time constant for the process leading to restoration of the equilibrium is long.

Another way of looking at this process involves the macroscopic spin magnetisation, i.e. the vector sum of orientated spins. In the absence of an external field there is no net magnetisation because the spins are randomly orientated. Only if placed in a static field will the spins eventually line up, some parallel with the field and some

anti-parallel, with a slight predominance of the former. The vector sum of individual magnetic moments or magnetisation consequently points along the field axis. However, the polarisation does not take place instantaneously when the sample is placed in the field, but with a certain time constant. In most cases this process is found to be first order, i.e. the magnetisation builds up exponentially with a time constant equal to the spin-lattice or longitudinal relaxation time T_1. Likewise, if the spin system has been subjected to a strong saturating radiofrequency field, the return towards thermal equilibrium takes place with a time constant T_1. The process is therefore a spin-lattice relaxation process. ^{13}C spin-lattice relaxation times of molecules in an isotropic liquid phase are found to be of the order of 10^{-2} to 10^{-3} seconds.

Spin-spin lattice relaxation, on the other hand results from interactions among the spins themselves. In the absence of an oscillating radiofrequency field, the spins precess about the external field axis with their phases at random.

There is consequently no net magnetisation perpendicular to the field (transverse magnetisation). Let us suppose a radiofrequency field is at resonance with the precessing spins, a net transverse magnetisation Mxy is generated. The individual magnetic moments are polarised along the axis of the rotating field. This transverse magnetisation however, does not persist indefinitely. It decays to zero because of transverse spin-spin relaxation. Even in an ideally homogeneous magnetic field there is a spread of Larmor frequencies across the sample. As a consequence of this the spins dephase with a time constant given by the transverse or spin-spin relaxation time T_2.

In a perfectly homogeneous field, the slow passage width of a resonance line is inversely proportioned to T_2, i.e.

$$\Delta\nu_{\frac{1}{2}} = \frac{1}{(\pi T_2)} \quad .$$

However, the magnetic field is never perfectly homogeneous, i.e. there are always transverse gradients across the sample, which means that the transverse magnetisation decays faster than that predicted by T_2.

For the effective transverse relaxation time T_2, the inequality $T_2 < T_1$ holds. The full equilibrium magnetisation along the magnetic axis can only build up after Mxy has decayed to zero. From this it follows $T_2 \triangleq T_1$. In ^{13}C NMR it is found that in the majority of cases $T_1 = T_2$.

Another phenomenon which plays an important part in ^{13}C NMR is the Nuclear Overhauser Effect (NOE).

It is well known that the relaxation of a ^{13}C nucleus in an organic molecule originates from a dipolar interaction with the magnetic moments of neighbouring protons. Since the majority of ^{13}C experiments are carried out under simultaneous proton decoupling, saturation of proton transitions takes place which leads to a redistribution of spin in the ^{13}C energy levels. If the ^{13}C dipolar relaxation mechanism dominates, it can be shown that the population difference between the ground and excited states of the nuclear Zeeman levels increases above that given at thermal equilibrium. This, however, is equivalent to an increased magnetisation and hence enhanced sensitivity.

Apart from very small molecules, proton bearing carbons are known to be predominantly relaxed via the dipolar mechanism. Under these conditions, the NOE is defined by the quotient $\frac{M_z}{M_0}$ where M_z represents

^{13}C magnetisation with and M_o without radiation of protons

$$NOE = \frac{M_z}{M_o}\frac{(^{13}C)}{(^{13}C)} = 1 + \frac{\gamma(^1H)}{2\gamma(^{13}C)} \simeq 3$$

where (^1H) and (^{13}C) are the magnetogyric ratios of the proton and ^{13}C respectively.

Apart from the increased signal to noise ratio brought about by the collapse of spin multiplets when protons are decoupled, the signals of most carbons experience an additional three-fold enhancement due to the NOE.

Under common recording techniques, ^{13}C NMR does not produce quantitative information because it is possible that not all carbons within the same molecule yield equal NOE. A second cause for the non-quantitative behaviour lies in differences of the spin-lattice relaxation times which become particularly severe if the spectra are obtained in pulsed mode.

It can be seen from the results that the carbon-13 relaxation time is roughly inversely proportional to the number of hydrogen atoms directly bonded to the carbon atom and allows, CH, CH_2 and CH_3 groups to be distinguished. This assumes that the relaxation mechanism is dipole-dipole in each case, a condition which can be verified by a Nuclear Overhauser measurement. Because relaxation is also determined by the rate of molecular motion, the T_1 values can also tell us a great deal about the way the molecule is moving in solution and even about differential motion within the same molecule.

The quaternary carbon in 1-methylcyclohexanol has a very long T_1. Also the CH carbons relax more efficiently but at different rates. This occurs because molecular reorientation is anisotropic.

The relaxation of the CH_3 methyl group is so fast that the spin rotation mechanism (see below) comes into play and the relaxation time is shortened instead of increased by this motion.

In the Inversion Recovery Experiment Eu $(fod)_3$ was added in increasing amounts to try to identify the peaks.

Each molecule has an axis of rotation around which it rotates. If the carbon atom is on the axis its T_1 is very long. It appears that in most of the molecules the CHOH carbon is near the axis.

Proton T_1 and T_2 measurements on the cyclohexanols indicate that the OH peak has the longest relaxation times and T_1 is greater than T_2.

Spin-lattice relaxation mechanisms

There are several common mechanisms that lead to spin relaxation for ^{13}C nuclei.

1. Dipole-dipole relaxation

Spin-lattice relaxation for ^{13}C nuclei can arise from fluctuating fields due to dipole-dipole interactions with neighbouring magnetic nuclei (or with unpaired electrons).

2. Spin-rotation relaxation

Small molecules and freely rotating CH_3 groups can be effectively relaxed by a mechanism involving quantum rotational states of the molecule or group. In these cases, spin rotation relaxation often competes with dipole-dipole relaxation for protonated carbons, whereas the spin-rotation interaction dominates the relaxation of non-protonated carbons.

3. Chemical shift anisotropy

Significant anisotropy (directionality) in the shielding of a nucleus can give rise to fluctuating magnetic fields when the molecule tumbles in solution (relative to the fixed laboratory magnetic field).

4. Scalar relaxation

A ^{13}C nucleus that is spin-spin (scalar) coupled to a nucleus X that is undergoing rapid spin-lattice relaxation, may itself be relaxed due to the fluctuating scalar interaction between the two nuclei. This mechanism is normally encountered when the X nucleus has a spin I, which is > $\frac{1}{2}$ (and X is relaxed by a mechanism known as quadrupolar relaxation), but a scalar relaxation of ^{13}C nuclei may also occur when X = ^{1}H. Scalar relaxation of ^{13}C nuclei is generally confined to spin-spin relaxation (spin-spin relaxation time is T_2).

In a few cases, spin-lattice relaxation of ^{13}C nuclei also occurs. When X is undergoing (quadrupolar) spin-lattice relaxation very rapidly and when the Larmor (resonance) frequency of X is close to the Larmor frequency for ^{13}C, scalar spin-lattice relaxation of ^{13}C nuclei is competitive with the other mechanisms.

In cases where scalar relaxation of ^{13}C nuclei is limited to spin-spin relaxation, line broadening is often evident in the CMR spectra, e.g. ^{13}C nucleus attached to ^{14}N frequently appears as very broad resonances.

^{13}C-^{1}H Dipole-dipole relaxation

In most organic molecules ^{13}C-^{1}H dipole-dipole relaxation is dominant for ^{13}C spin-lattice relaxation. This is particularly true for carbons that have directly attached protons (protonated carbons).

Two main factors determine the efficiency of dipole-dipole relaxation in individual cases; the magnetogyric ratio of the nucleus causing relaxation and the proximity of that nucleus to the nucleus being relaxed. In both ^{1}H and ^{13}C NMR protons usually dominate dipole-dipole relaxation because of their high magnetogyric ratio (dipole-dipole relaxation is proportional to γ^2). The distance dependence of

^{13}C-^{1}H dipole-dipole relaxation is extremely strong, proportional to $\frac{1}{r^6}$ where r is the internuclear distance.

It is for this reason that protonated carbons are most easily relaxed and that the dipole-dipole mechanism usually dominates the relaxation of these carbons. For ^{13}C nuclei that do not have directly attached protons (non-protonated carbons), other mechanisms may compete with or replace ^{13}C-^{1}H dipole-dipole relaxation.

The presence of unpaired spins can lead to very efficient dipole-dipole relaxation (replacing the ^{13}C-^{1}H dipole-dipole relaxation). Since the magnetic moment of the electron is much greater than that of the proton, both T_1 and T_2 can be effected by the presence of unpaired spins.

N.B. Dissolved oxygen contains unpaired spins and this is why it must be removed from the samples by degasing or paramagnetic O_2 gives rise to significant relaxation.

The methylcyclohexanols will have rapid molecular motion in solution, the relative orientation of ^{13}C and ^{1}H with respect to B_0 is constantly changing. The rapid internal reorientation of the two nuclei gives rise to rapid fluctuations of the localised (and therefore total) magnetic field as seen by each nucleus, these fluctuations effect relaxation of the nuclei. Intermolecular relaxation is generally insignificant for ^{13}C nuclei and therefore only rotational motions (e.g. tumbling of the molecules) need to be considered (N.B. If O_2 was present this would give rise to significant relaxation, and translational motions of the molecule would have to be considered).

Frequencies of motions for molecules in solution range from very slow to very fast. In the case of very small molecules most of the individual molecules will be rotating at rates of $> 10^{12}$ revolutions per

second while a few will be rotating much more slowly. Actually the movements of a molecule in solution are very complex, characteristic rotation rates cannot be dissected easily from overall tumbling motions.

Fortunately, it is generally not necessary to consider the separation of the various molecular motions. It is usually sufficient to describe an effective correlation time T_c, which represents the average time for a molecule to rotate through 1 radian (2π rad per second = 1 revolution per second). Dipole-dipole relaxation is best effected by rotational motions with frequencies comparable with the resonance frequency.

A graphical representation of the effect of T_c on T_1 and T_2 values is shown below:

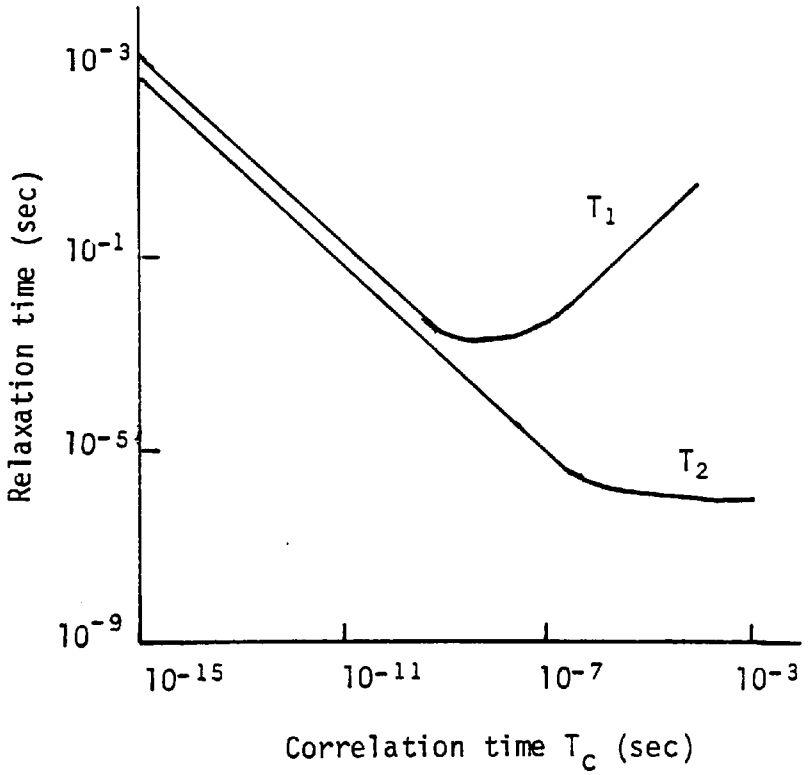

Relationship between T_1 and T_2 and molecular tumbling as represented by T_c

A correlation time of 7 x 10^{-9} seconds (the reciprocal of resonance frequency in rad/sec) leads to most efficient dipole-dipole spin-lattice relaxation of a ^{13}C nucleus.

It is clear from the above that the correlation time falls on the left-hand side of the graph. Typical T_c values for small molecules would be 10^{-12} to 10^{-13} seconds and for large molecules as long as 10^{-10} seconds.

It is also clear from the graph that generally any change that shortens T_c results in a lengthening of T_1 . For example, lowering solution viscosity and raising the temperature.

Investigation of T_1 values versus concentration for some methylcyclohexanol isomers

The isomers studied were 1-methylcyclohexanol, trans-2-methylcyclohexanol, cis-2-methylcyclohexanol and cis-3-methylcyclohexanol.

Using Table 2.39 on page131, a graph of T_1 versus concentration was plotted for each of the compounds. From the graph a table was produced of the intercept and slope of each carbon.

TABLE 2.35

1-Methylcyclohexanol

Peak Number	Intercept T_1 in seconds	Slope seconds $mol.^{-1}dm^3$
2 CH_2 (2+6)	5.20	-0.242
3 CH_3	5.23	-0.769
4 CH_2	4.12	very large, almost a straight line
5 CH_2 (3+5)	6.6	-1.09

The compound probably has an axial hydroxyl group. On dilution there is a small increase in T_1 except for Peak 4. This seems to imply that there is only a small amount of hydrogen bonding taking place in solution.

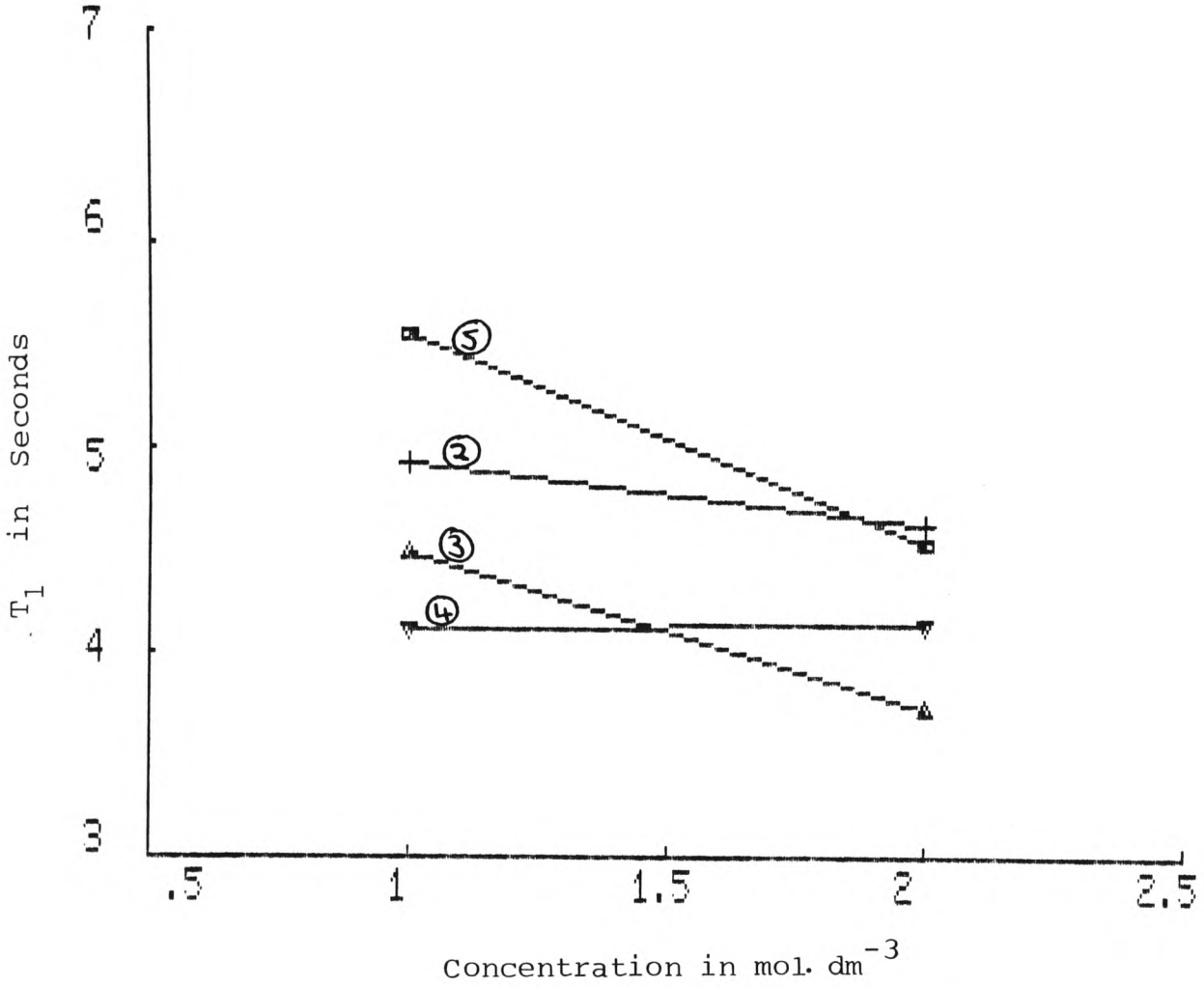

T_1 versus concentration for 1-methylcyclohexanol

TABLE 2.36

trans-2-Methylcyclohexanol

Peak Number	Intercept T_1 in seconds	Slope seconds $mol.^{-1}$ dm^3
1 CHOH	11.2	-1.88
2 CH_2 (2)	10.38	-1.7
3 CH	7.08	-1.44
4 CH_2 (4)	6.6	-1.09
5 CH_2 (3)	6.85	-1.79
6 CH_2 (5)	6.77	-1.28
7 CH_3	6.58	-1.45

The highest gradient is with the CHOH group. It would be expected that this compound would form a stronger hydrogen bond than the cis-2-compound as the hydroxyl group in the trans-2-compound is in the equatorial position. The results seem to confirm this as both the intercept and slope of the trans-2-compound are less than with the cis isomer.

Note: the smaller intercept T_1 value for the trans-2-compound indicates that this molecule has a relatively larger molecular weight in solution than the cis compound, implying greater intermolecular hydrogen bonding in the trans-2-compound.

TABLE 2.37

cis-2-Methylcyclohexanol

Peak Number	Intercept T_1 in seconds	Slope seconds $mol.^{-1}$ dm^3
1 CHOH	13.05	-3.3
2 CH_2 (2)	12.72	-2.78
3 CH	9.72	-2
4 CH_2 (4)	8.2	-1.8
5 CH_2 (3)	7.64	-2.37
6 CH_2 (5)	8.72	-1.28
7 CH_3	7.35	-1.18

T_1 versus concentration for trans-2-methylcyclohexanol

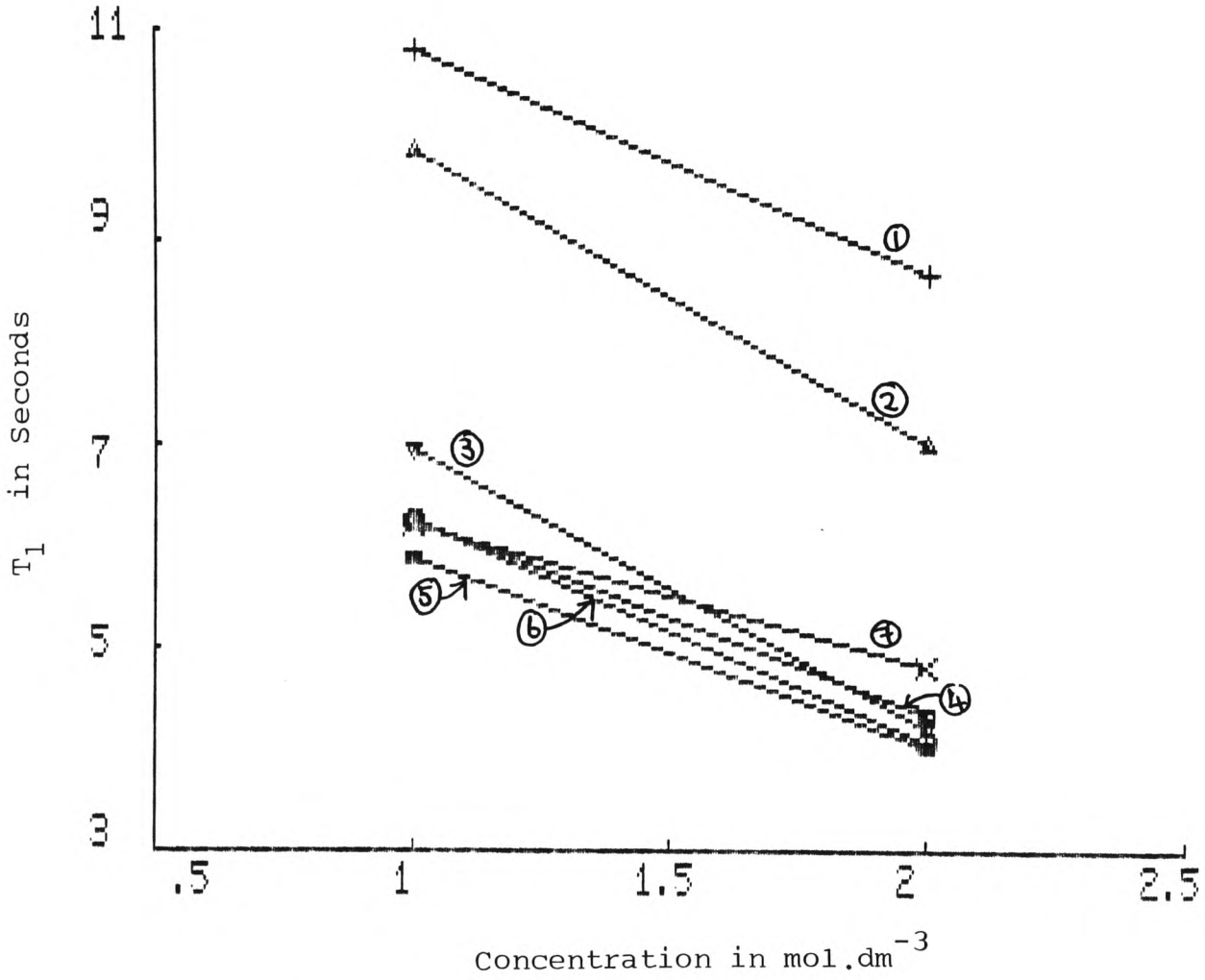

T_1 versus concentration for cis-2-methylcyclohexanol

The cis-2-methyl compound is likely to have an axial OH and it would seem unlikely to have a strong intermolecular hydrogen bond. It is probable that the intermolecular hydrogen bond between cis-2-methyl molecules breaks more easily on dilution than that in the trans-2-methyl compound.

Overall measurement of ^{13}C T_1 can give a view of the intermolecular solution effects such as hydrogen bonding, e.g. when the methylcyclohexanols are diluted with $CDCl_3$ the molecular weight aggregates begin to dissociate, i.e. dimer to monomer. This effect is observed in the ^{13}C T_1 values increasing as the molecular weight decreases.

TABLE 2.38

cis-3-Methylcyclohexanol

Peak Number	Intercept T_1 in seconds	Slope seconds $mol.^{-1}$ dm^3
1 CHOH	11.0	-2.67
2 CH_2 (2 or 6)	2.73	-1.89
3 CH_2 (2 or 6)	6.50	-1.63
4 CH_2 (5)	5.55	-1.72
5 CH_2	11.80	-2.67
6 CH_2 (4)	7.4	-2.09
7 CH_3	4.95	-1.03

In cis-3-methylcyclohexanol it is thought that the hydroxyl group is in an equatorial position. This position will encourage the formation of an intermolecular hydrogen bonded dimer to the axial hydrogen group.

Both trans-2-methylcyclohexanol and cis-3-methylcyclohexanol seem to form a relatively strong intermolecular hydrogen bond.

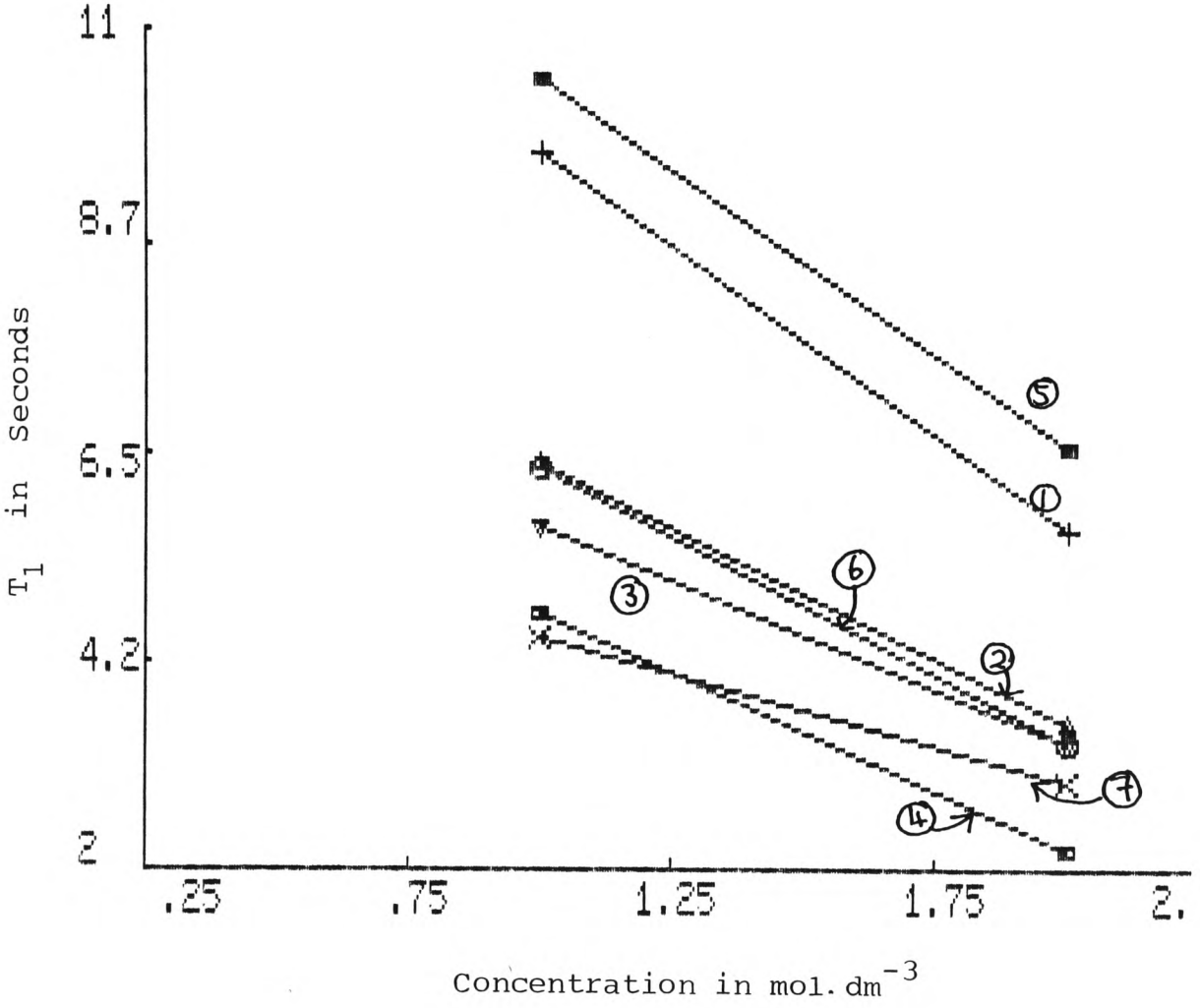

T_1 versus concentration for cis-3-methylcyclohexanol

TABLE 2.39

Sample: 1-Methylcyclohexanol

Concn.	Peak No.	T_1 Value		COM/NNE
2 M	2	4.63	Peak 1	1.4554/0.5163 = 2.819
		3.71		
		4.13	Peak 2	6.2136/1.7782 = 3.494
		4.52		
1 M	2	4.92 (0.29)	Peak 3	2.5217/0.8512 = 2.963
	3	4.48 (0.77)	Peak 4	2.6255/0.8272 = 3.174
	4	4.11 (-0.02)	Peak 5	5.8924/1.8819 = 3.131
	5	5.54 (1.02)		

Sample : trans-4-Methylcyclohexanol

2 M	1	5.70	Peak 1	6.9207/3.0588 = 2.263
	2	3.82	Peak 2	12.5420/4.5769 = 2.7403
	3	4.22	Peak 3	10.4311/4.6727 = 2.2323
	4	6.61	Peak 4	5.7812/2.4978 = 2.3145
	5	4.04	Peak 5	4.2076/2.3135 = 1.8187

Sample: cis-4-Methylcyclohexanol

2 M	1	7.19	Peak 1	3.1722/1.4523 = 2.1843
	2	4.20	Peak 2	6.4095/2.6416 = 2.4264
	3	6.11	Peak 3	3.1921/1.4774 = 2.1606
	4	4.33	Peak 4	6.7270/2.8413 = 2.3676
	5	4.27	Peak 5	3.0548/1.2088 = 2.5271

Sample: trans-2-Methylcyclohexanol

2 M	1	7.02	Peak 1	4.6460/1.8030 = 2.5768
	2	7.08	Peak 2	4.0991/1.6691 = 2.4559
	3	4.24	Peak 3	4.1233/1.6836 = 2.4491
	4	4.41	Peak 4	4.0713/1.6252 = 2.5051
	5	3.50	Peak 5	4.6367/1.6234 = 2.8562
	6	4.37	Peak 6	4.7323/1.6125 = 2.9348
	7	4.17	Peak 7	4.1726/1.4140 = 2.9509
1 M	1	8.94		
	2	8.70		
	3	5.63		
	4	5.30		
	5	4.83		
	6	5.17		
	7	4.83		

Concn.	Peak No.	T_1 Value	COM/NNE
0.66 M	1	10.25	
	2	9.36	
	3	5.88	
	4	6.06	
	5	5.92	
	6	6.00	
	7	5.79	

Sample: cis-2-Methylcyclohexanol

2 M	1	8.63	
	2	6.96	
	3	4.20	
	4	4.32	
	5	4.01	
	6	4.08	
	7	4.81	
1 M	1	10.83	2.15
	2	9.83	2.87
	3	6.94	2.74
	4	6.25	1.53
	5	5.85	1.84
	6	6.26	2.18
	7	6.17	1.36

Sample: cis-3-Methylcyclohexanol

2 M	1	5.66	Peak 1	2.9493/1.0957 = 2.6917
	2	3.54	Peak 2	2.7691/1.0195 = 2.7160
	3	3.36	Peak 3	2.7317/1.0296 = 2.6532
	4	2.27	Peak 4	2.8796/1.0065 = 2.8610
	5	6.51	Peak 5	2.7661/1.0488 = 2.6375
	6	3.37	Peak 6	3.08
	7	2.96	Peak 7	2.69

Sample: trans-3-Methylcyclohexanol

2 M	1	7.41	2.23
	2	4.62	2.44
	3	3.93	2.63
	4	4.00	1.95
	5	6.59	2.71
	6	4.36	2.35
	7	4.40	2.45

Sample: cis-3-Methylcyclohexanol

0.5 M	1	9.709
	2	6.344
	3	5.678
	4	4.76
	5	10.484
	6	6.329
	7	4.517

2.4 (2) Nuclear Overhauser effect versus position of carbon in the compound and a comparison of carbon T_1's

In cyclohexane all the carbon atoms will be strongly affected by molecular motions in the medium. Therefore the correlation time T_c is the same for all carbons. The C-C and C-H bond lengths are all the same in the molecule.

Carbon atom's dipole-dipole (DD) relaxation time depends upon the number of directly bonded hydrogen atoms. The T_1 values of CH and CH_2 carbon atoms in the same molecule should be in the ratio of 2:1 while quaternary carbon atoms with no directly attached hydrogen atoms should relax considerably more slowly.

Methyl carbon atoms have shorter correlation time than do CH or CH_2 because of their methyl group rotations which are usually faster than the overall molecular motions and their T_1 values are larger.

It should be noted that the above relationships are only valid when rotation of the molecule is isotropic, i.e. has no preferred axis of rotation.

If a molecule has a preferred axis of rotation it is said to be anisotropic.

If the molecular rotation passes through the molecular axis, when the molecule rotates the C-H does not alter its orientation with regard to the external magnetic field vector B_o. Fluctuating local fields at this carbon atom arise then, only by molecular rotations perpendicular to the preferred axis, but these less favoured rotations still have large enough frequency and therefore small enough correlation time to relax this carbon atom rapidly.

However, the preferred and thus the faster rotation alters the orientation of the other carbon-hydrogen groups in the ring with regard to B_o too rapidly for the other carbon atoms to relax completely by dipole-dipole mechanism.

It should be noted that steric interactions can hinder the methyl rotation and thus accelerate relaxation of the methyl carbon nucleus. Therefore T_1 values of methyl groups can serve as probes for steric interactions.

When a molecule contains a polar grouping like a hydroxyl group the formation of an intermolecular hydrogen bond can hinder the mobility of molecules and affected portions of molecules. Thus they raise the correlation times T_c of the ^{13}C-H nuclei and favour their dipole-dipole relaxation (DD).

If the ^{13}C relaxation proceeds exclusively by dipole-dipole relaxation, the Nuclear Overhauser effect factor η_c which measures the intensity loss of the ^{13}C signal is about equal to 3.

$$\frac{M_z}{M_o} = 1 + \frac{\gamma(^1H)}{2\gamma(^{13}C)} \triangleq 3$$

where (^1H) and (^{13}C) are gyromagnetic ratios of ^1H and ^{13}C.

The NOE factors η_c are measured by comparing the signal intensities of the proton coupled and proton decoupled ^{13}C spectra with the same base line noise amplitude.

NOE factors of $\eta_c \triangleq 3$ are therefore indicative of total DD mechanism.

If η_c is less than three other spin-lattice relaxation mechanisms are operating for the ^{13}C nuclei bonded to H.

The percentage contribution to the DD mechanism can be calculated from η_c using

$$\% \text{ DD} = \frac{\eta_c}{3}$$

The time constant, T_{1DD} for a DD mechanism can be determined:

$$T_{1DD} = T_1 \frac{3}{n_C}$$

If several relaxation times are operating in conjunction, the measured relaxation rate $\frac{1}{T_1}$ is the sum of the rate constants $\frac{1}{T_{1's}}$ for all participating mechanisms.

1-Methylcyclohexanol

This molecule contains a quaternary carbon atom which has a T_1 of 23.63 seconds in 2 mol.dm^{-3} concentration. From Table 2.39 the following table can be produced.

The contribution of ^{13}C-^{1}H dipole-dipole interaction can be determined directly from NOE:

TABLE 2.40

Carbon Position	NOE	% DD	% Other Relaxation Mechanisms
C-OH	2.819	93.97	6.03
CH_2 (2 or 6)	3.494	100	0
CH_3	2.963	98.77	1.23
CH_2 (4)	3.174	100	0
CH_2 (3 or 5)	3.131	100	0

Relaxation of all carbons in the molecule proceeds almost exclusively by the dipole-dipole mechanism.

Also from Table 2.39 the CH_2 group on position 4 exhibits a shorter T_1 than the other CH_2 carbons in 1-methylcyclohexanol. This may be because this carbon atom is on the axis of rotation of the molecules (i.e. it is aligned with main axis of reorientation). Hence the local field B_{LOC} produced by proton $^{13}C_4$-H is not modulated and cannot give rise to relaxation of this carbon.

T_1 for the methyl group is quite large and this may give a measure of the steric interactions which can hinder the rotation of the CH_3.

trans-2-Methylcyclohexanol

This molecule is expected to have an equatorial hydroxyl group as well as an equatorial methyl group. It is therefore more likely to form an intermolecular hydrogen bond than the cis-2-compound.

TABLE 2.41

Carbon Position	NOE	% DD	% Other Relaxation Mechanisms
CHOH	2.577	85.67	14.33
CH_2 (6)	2.46	82.0	18
CH	2.45	81.67	18.33
CH_2 (4)	2.51	83.67	16.33
CH_2 (3)	2.86	95.33	4.67
CH_2 (5)	2.93	97.66	2.33
CH_3	2.95	98.33	1.67

From Table 2.39 the CH_2 group on carbon 3 exhibits a shorter T_1 than the other CH_2 carbon atoms in the molecule and this may be because this carbon atom is on the axis of rotation of the molecule.

Figure 2(13)

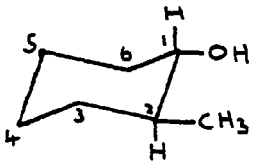

trans-2-Methylcyclohexanol

The carbon -T_1 for the methyl group is quite large and this may be because of steric interaction which hinders the relaxation of the methyl group (in the absence of any internal rotation the T_1 of CH_3 is one-third the T_1 of a CH, the maximum value when fast internal rotation is taking place is 3 x T_1 of a CH).

cis-2-Methylcyclohexanol

From Table 2.39 the carbon T_1 values of cis-2-methylcyclohexanol are higher than those of the trans isomer, especially as the solutions become more dilute. With increased concentration the diffusion of the molecules slows down as a consequence of increased friction among the solute molecules.

It appears that trans-2-methylcyclohexanol forms a stronger inter molecular hydrogen bond than does the cis-isomer.

TABLE 2.42

Carbon Position	NOE	% DD	% Other Relaxation Mechanism
CHOH	2.15	71.67	28.34
CH_2 (6)	2.87	95.67	4.33
CH	2.74	91.33	8.67
CH_2 (4)	1.93	64.33	35.67
CH_2 (3)	1.84	61.33	38.67
CH_2 (5)	2.18	72.66	27.34
CH_3	1.36	45.33	54.67

From Table 2.39 CH_2(3)has the lowest CH_2 T_1 giving an impression that the axis of rotation passes through CH_2(3).

Figure 2(14)

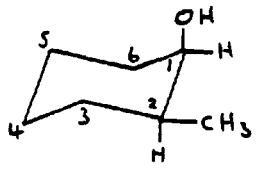

cis-2-Methylcyclohexanol

The T_1 value of the methyl group is quite large indicating internal rotation.

trans-3-Methylcyclohexanol

It would be expected from previous work on chemical shift versus concentration studies that this compound would not form as strong an intermolecular hydrogen bond as cis-3-methylcyclohexanol. It would be expected that the ^{13}C T_1 values of the trans-3-isomer would be greater than the cis-3-isomer.

TABLE 2.43

Carbon Position	NOE	% DD	% Other Relaxation Mechanisms
CHOH	2.23	74.3	25.7
CH_2 (2 or 6)	2.44	81.3	18.7
CH_2 (2 or 6)	2.63	87.67	12.33
CH_2 (5)	1.95	65	35
CH	2.71	83.67	16.33
CH_2 (4)	2.35	78.33	21.67
CH_3	2.45	81.67	18.33

The major relaxation mechanism of the ^{13}C atoms is DD.

From Table 2.39 all the ^{13}C T_1 of trans-3-methylcyclohexanol are larger than those of the cis isomer indicating that a stronger intermolecular hydrogen bond is formed with the cis-isomer. Also from this table CH_2 (2 or 6) has the lowest CH_2 T_1 indicating that the axis of rotation passes through either CH_2 (2 or 6).

Figure 2(15)

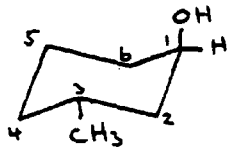

trans-3-Methylcyclohexanol

The methyl group rotation is high indicating some spin rotation.

cis-3-Methylcyclohexanol

As mentioned previously, this compound seems to form a stronger intermolecular hydrogen bond than the trans-3-isomer.

TABLE 2.44

Carbon Position	NOE	% DD	% Other Relaxation Mechanisms
CHOH	2.69	89.67	10.33
CH_2 (2 or 6)	2.71	90.33	9.67
CH_2 (2 or 6)	2.65	88.33	11.66
CH_2 (5)	2.86	95.33	4.67
CH	2.64	88.0	12
CH_2 (4)	3.08	100	0
CH_3	2.69	89.67	10.33

The major relaxation mechanism for the ^{13}C atoms is DD.

The smallest T_1 for CH_2 carbons is found on carbon CH_2 (5) indicating that the axis of rotation may travel through CH_2 (5).

Figure 2(16)

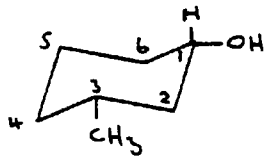

cis-3-Methylcyclohexanol

In the cis-3-isomer the axis of rotation is thought to pass through CH_2 (2 or 6). The difference in the axis of rotation between the two compounds may be due to the formation of intermolecular hydrogen bonds with the cis-isomer which tends to "anchor" the molecule in a different way compared to the trans-isomer.

Generally in cis-3-methylcyclohexanol T_1 CH:CH_2 is about 2:1.

The methyl group T_1 is relatively high indicating some spin rotation.

trans-4-Methylcyclohexanol

From previous chemical shift versus concentration studies it would be expected that this compound forms a stronger intermolecular hydrogen bond than the cis-4-isomer.

TABLE 2.45

Carbon Position	NOE	% DD	% Other Relaxation Mechanisms
CHOH	2.26	75.33	24.67
CH_2 (2 or 6)	2.74	91.33	8.67
CH_2 (3 or 5)	2.23	74.33	25.67
CH	2.31	77.0	23
CH_3	1.82	60.66	39.33

The major relaxation mechanism is DD.

From Table 2.39 the T_1 values of the trans-4-isomer are lower than the cis-4-isomer indicating a stronger intermolecular hydrogen bond with the trans-4-isomer.

CH_2 (2 or 6) has the lowest CH_2 T_1 indicating the axis of rotation may travel through CH_2 (2 or 6).

Figure 2(17)

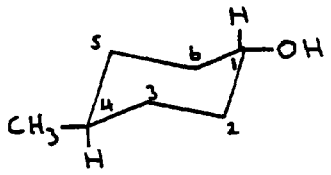

trans-4-Methylcyclohexanol

The methyl group T_1 is relatively high indicating some spin rotation.

cis-4-Methycyclohexanol

This molecule does not form as strong an intermolecular hydrogen bond as the trans-4-isomer.

TABLE 2.46

Carbon Position	NOE	% DD	% Other Relaxation Mechanisms
CHOH	2.18	72.67	27.33
CH_2 (2 or 6)	2.43	81.0	19.0
CH_2 (3 or 5)	2.16	72.0	28.0
CH	2.37	79.0	21.0
CH_3	2.53	84.33	15.67

The major relaxation mechanism is DD.

The axis of rotation is through CH_2 (2 or 6).

Figure 2(18)

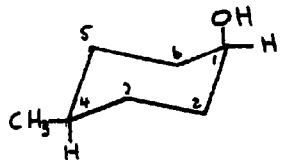

cis-4-Methylcyclohexanol

The methyl group T_1 is relatively high indicating spin rotation.

2.5 T_1 Estimation by the Freeman-Hill Modification of Inversion Recovery

The previous T_1 values were found by the Inversion Recovery method. This method utilises a (180^o-t-90^o) pulse sequence. The 180^o pulse inverts the two ^{13}C energy level populations, instantaneously producing a Boltzmann excess of nuclei in the higher energy level. Following the 180^o pulse the nuclei begin to relax to re-establish the normal Boltzmann distribution (excess nuclei in lower energy state). The 90^o pulse is applied after a waiting period t, which is varied with successive experiments. A free induction decay results from the 90^o pulse and is recorded or digitised and stored. If t is very long relative to the longest T_1 for any nucleus being observed, then the FID yields a fully relaxed spectrum, indistinguishable from the spectrum resulting from a single pulse experiment. If, on the other hand, t is comparable to T_1 for one or more nuclei, then the FID resulting from the 90^o pulse will yield no data (after Fourier Transformation).

Consider four cases:

1. $t << T_1$. The signal for this nucleus appears inverted indicating that little relaxation occurred following the 180^o pulse.
2. $t \sim (T_1 (\ln 2) = 0.69\ T_1$. The signal is nearly nulled.
3. $t \sim T_1$. The signal is small and positive.
4. $t >> T_1$. The signal is positive and is full intensity.

Figure 2(19)

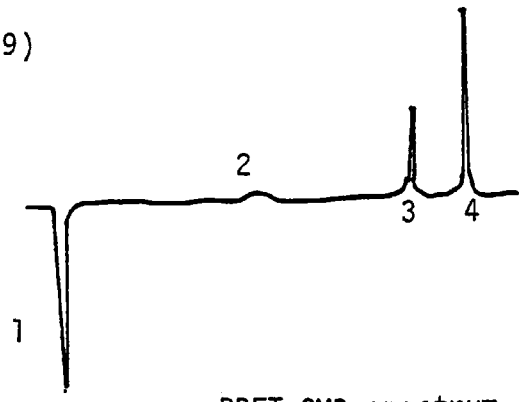

PRFT CMR spectrum

A spectrum such as the previous one is called a partially relaxed Fourier transform spectrum or PRFT spectrum. A set of these spectra with variation of t allows calculation of the T_1 values for all the different nuclei in a molecule.

In practice it is necessary to accumulate many FIDs to achieve usable signal to noise ratios. In most relaxation studies a pulse sequence such as $(T\text{-}180^{o}\text{-}t\text{-}90^{o})_x$ is used. Here, the new waiting time T allows the sample to recover completely from the previous pulse sequence, thereby stimulating an isolated (180^{o}-t-90^{o}) pulse sequence. In practice it is necessary to wait three to four times longer than the longest T_1 value to be determined in the experiment.

Freeman and Hill introduced a variation of the $(T\text{-}180^{o}\text{-}t\text{-}90o)_x$ pulse sequence which represents all PRFT spectral lines in the same sense. The pulse sequence is $(T\text{-}90^{o}\infty\text{-}T\text{-}180^{o}\text{-}t\text{-}90^{o}{}_t)_x$ where T and t have the meaning above. The $90^{o}\infty$ pulse results in an FID of a completely relaxed system while the FID resulting rom the $90^{o}{}_t$ pulse contains PRFT information. In the Freeman-Hill modification the computer alternately collects and adds the FID data from the 90^{o} pulse and subtracts the FID resulting from $90^{o}{}_t$ pulse. These PRFT spectra plot (S-St) where and St are the signals obtained after Fourier transformation of the free induction decays resulting from the 90^{o} and $90^{o}{}_t$ pulses, respectively. If $t >> T_1$ then (S∞-St) approaches (S∞-S∞) or zero peak height. If $t \ll T_1$ St is the same size as S∞but is negative; (S∞-St) is thus equivalent to (S∞-(-S∞)) or 2 S∞. All intermediate values of t result in positive but lower intensity (S∞-St) plots.

A series of these PRFT spectra as a function of t results in excellent spectral representations.

In order to achieve accurate t=0 values, the intensities are plotted as a function of t to obtain a straight line from which T_1 may be determined.

2.6 Comparison of T_1 Values by Inversion Recovery and Freeman-Hill Methods

TABLE 2.47

Peak	Inversion Recovery Method	Freeman-Hill Method	Difference
	cis-2-methylcyclohexanol (2 mol.dm^{-3})		
	(All values in seconds)		
1	8.63	9.39	0.76
2	6.96	6.83	-0.13
3	4.20	3.85	-0.35
4	4.32	4.20	-0.12
5	4.01	4.33	0.32
6	4.08	4.08	0.0
7	4.81	4.51	-0.30
	trans-2-methylcyclohexanol (2 mol.dm^{-3})		
	(All values in seconds)		
1	7.02	6.53	-0.49
2	7.08	6.41	-0.67
3	4.24	3.83	-0.41
4	4.41	4.08	-0.33
5	3.50	2.77	-0.73
6	4.37	3.37	-1.0
7	4.17	3.59	-0.58
	cis-3-methylcyclohexanol (2 mol.dm^{-3})		
	(All values in seconds)		
1	5.66	5.37	-0.29
2	3.54	3.17	-0.37
3	3.36	3.09	-0.27
4	2.27	2.32	0.05
5	6.51	5.87	-0.64
6	3.37	3.20	-0.17
7	2.96	2.64	-0.32
	trans-3-methylcyclohexanol (2 mol.dm^{-3})		
	(All values in seconds)		
1	7.41	6.71	-0.70
2	4.62	3.38	-1.24
3	3.93	3.01	-0.92
4	4.00	3.02	-0.98
5	6.59	5.50	-1.09
6	4.36	3.52	-0.84
7	4.40	3.42	-0.97

Peak	Inversion Recovery Method	Freeman-Hill Method	Difference
	cis-4-methylcyclohexanol (2 mol.dm^{-3})		
	(All values in seconds)		
1	7.19	6.98	-0.21
2	4.20	3.94	-0.26
3	6.11	5.33	-0.78
4	4.33	4.09	-0.24
5	4.27	4.26	-0.01
	trans-4-methylcyclohexanol (2 mol.dm^{-3})		
	(All values in seconds)		
1	5.70	5.75	0.05
2	3.82	3.92	0.10
3	4.22	3.73	-0.49
4	6.61	6.04	-0.57
5	4.04	3.36	-0.68

Generally both methods give a similar order of result. The Freeman-Hill method generally gives lower T_1 values than the Inversion Recovery method.

In the IR method the intensity, I, is measured only once during an entire experiment, whereas I is measured as many times as there are T values in the F-H method.

As there will be drifting of resolution, temperature and other effects during every experiment the F-H method will compensate for these drifts by obtaining peak subtractions run under the same conditions for each T value.

In summary, the F-H method is a more accurate method but is more time consuming than IR.

2.7 Proton T_1 and T_2 Results on some methycyclohexanols

When a sample is placed in a magnetic field its moment changes from zero to Mo, the equilibrium value. The approach to thermal equilibrium is known as relaxation and T_1 and T_2 are relaxation times. The decay of the longitudinal component Mz may differ from the decay of the transverse components Mx and My because the energy of the spin system depends on Mz. Any change in Mz is accompanied by an energy flow between the nuclear spin system and the other degrees of freedom of the system known as the "lattice." The relaxation time T_1 which describes this flow is sometimes known as the spin-lattice relaxation time or longitudinal relaxation time, emphasising the relationship of Mz and the applied field. T_2 is known as the transverse relaxation time or the spin-spin relaxation time. The latter name arises because direct interactions between the spins of different nuclei can cause relaxation of Mz and My without energy transfer to the lattice. In high resolution nuclear resonance of fluids T_1 and T_2 both arise from energy exchange between the spin system and the lattice.

T_1 was measured by free induction decay. A 90^o pulse first turns the equilibrium magnetisation Mo from the z axis to the xy plane. The height of the free induction signal immediately after turning off the pulse is proportional to Mo. The signal decays with a time constant T_2. However concurrently with this decay the magnetisation along the z axis is being re-established by spin-lattice relaxation. If a second 90^o pulse is now applied at time t after the first pulse, the height of the free induction signal immediately after the pulse will in general be smaller than Mo if the equilibrium magnetisation along the z axis has not been achieved. By measuring the initial height at various values of t between the two pulses, one can determine T_1 with high accuracy over a wide range of values.

Free induction decay cannot generally be used to measure T_2, since the lifetime of the decay is often dominated by the effect of magnetic field inhomogeneity. This problem of homogeneity is circumvented by an ingenious type of experiment called the spin-echo technique [23,24]. In this technique the magnetisation initially lies along the z axis parallel to B_0. A pulse is applied which begins to tip M towards the y axis in the rotating co-ordinate system. At the time t_w the pulse has achieved a 90^o rotation of M and is turned off. Since t_w has been selected to be much smaller than T_2, no loss of phase coherence has yet occurred. Because of magnetic field inhomogeneity, nuclei in different parts of the sample have different Larmor frequencies. We can think of a number of macroscopic magnetisations M_i arising from different portions of the sample. After the pulse these M_i begin to "fan out" in the rotating xy plane since they rotate at rates different from that of the co-ordinate system. The resultant free induction signal decays with time constant T_2.

After a time t a pulse of 2 t_w is applied. This is a 180^o pulse and rotates each magnetisation vector M_i through 180^o. Since each M_i continues to precess in the same direction as before, the resultant motion causes the vector to draw together, rather than to continue to fan out. At the time 2 t the vectors coalesce leading to a strong resultant magnetisation in the negative y direction. This magnetisation induces in the receiver coil an observable signal, the "echo." This echo is less intense than the original initial free induction, since spin-spin relaxation has occurred during the interval. Thus, while all M_i are brought into phase at 2 t each M_i is less intense because the nuclei contributing to it have lost phase coherence. Following the echo, the vectors again fan out leading to another free induction decay.

In principle, T_2 can be obtained from a 90^0 - 180^0 spin-echo experiment by measuring the height of the echo as a function of T. Actually, the experiment as described, does not lead directly to measurement of T_2 because of the effect of molecular diffusion.

The effects of diffusion can be removed by a modification of this experiment in which 180^0 pulses are applied at T, 3 T, 5 T, and so on, and echoes are observed at 2 T, 4 T and 6 T .

Therefore T_1 and T_2 are closely related because both modes of relaxation depend on the same interactions between the spins and their surrounds.

TABLE 2.48

All values at 300 k

$CDCl_3$ solution T_1 and T_2 values in seconds

Compound	Concn.	Peak	T_1 Value	T_2 Value
1 methylcyclohexanol	2 mol.dm^{-3}	OH	3.74	1.07
		CH_2	3.74	
		CH_3	2.78	1.55
trans-2-methylcyclohexanol	2 mol.dm^{-3}	OH	2.69	1.06
		CH_3	2.18	0.94
cis-2-methylcyclohexanol	2 mol.dm^{-3}	OH	2.74	0.9868
		CHOH	2.904	
		CH_3	2.10	
trans-3-methylcyclohexanol	2 mol.dm^{-3}	OH	1.921	
		CH_3	1.84	
cis-3-methylcyclohexanol	2 mol.dm^{-3}	OH	1.77	
		CHOH	2.27	
		CH_2	1.68	
		CH_3	1.65	
trans-4-methylcyclohexanol	2 mol.dm^{-3}	OH	1.89	0.71
		CH_3	1.48	0.46
cis-4-methylcyclohexanol	2 mol.dm^{-3}	CH_3	1.71	0.74

There is good agreement between ^{13}C T_1's and ^{1}H T_1's in that trans-2-methyl, cis-3-methyl and trans-4-methyl seem to form a stronger intermolecular hydrogen bond.

For the isomers studied, H^1 $T_1 > T_2$. Generally $T_1 \eqsim T_2$, the difference in values may be due to experimental error.

2.8 Determination of the Conformation of Molecules

^1H NMR can be used in the studies of fast chemical processes, as previously discussed.

At around 180 to 190 K chemical shifts of the axial and equatorial α proton were measured, also the position of resonance of this proton was measured at 300 K. Now the position of resonance at 300 K is an average position for the two conformers, e.g.

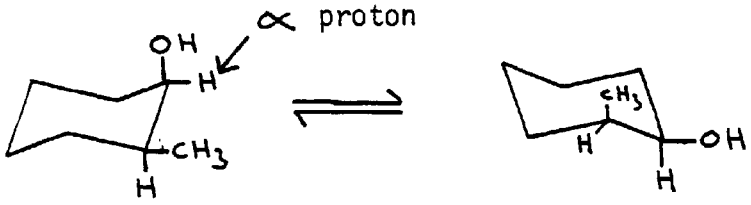

cis-2-Methylcyclohexanol

The proportions of these may be obtained by linear extrapolation between the axial and equatorial shifts which are known from low temperature measurements.

The solvent was a 1:1 mixture of carbon disulphide to deuterated chloroform (volume to volume). Deuterated chloroform was added to the carbon disulphide as it was found that the methylcyclohexanols started to come out of solution in CS_2 at around 200 to 220 K.

Some preliminary work was carried out with cyclohexanol, CS_2 was used as a solvent.

Results with cyclohexanol

At 190 K two resonances corresponding to equatorial α proton H_1 at approximately δ 3.85 and to the axial H_1 at approximately δ 3.28 were shown together with the "average" position of δ 3.52 at 300 K.

Electronic integration under the peaks gave a ratio of 3005:215 which in turn gives a value of K = 14.0 and hence a value of ΔG_{OH} = 4.17 kJ mol^{-1} at 190 K.

The value is quite high because the concentration used (2.5 $mol.dm^{-3}$) will give rise to quite considerable intermolecular hydrogen bonding at 190 K.

Therefore the hydroxyl group in cyclohexanol shows a marked preference for the equatorial position.

The position of resonance at 300 K is an averaged one for the time conformers. The proportions of these may be obtained by linear intrapolation between the equatorial and axial shifts which are known from the low temperature measurement.

Hence δ 3.28 corresponds to 100 % axial conformer

δ 3.85 corresponds to 0 % axial conformer (100 % equatorial)

$$\delta \text{ 3.52 corresponds to } \frac{3.52 - 3.28}{3.85 - 3.28} \times 100$$

= 23.8 % of axial conformer at 300 K.

$$\text{Hence } K = \frac{76.2}{23.8} = 3.20$$

$$\text{Thus } -\Delta G_{OH} = RT \ln K$$

$$= 8.314 \times 300 \ln 3.20$$

$$= 2.90 \text{ kJ mol}^{-1}$$

Results with methylcyclohexanols

cis-2-methylcyclohexanol

At 299 K α H_1 peak = 140.75

At 190 K 168.24 = 100 % axial

125.36 = 100 % equatorial

$$140.75 = \frac{140.75 - 125.36}{168.24 - 125.36}$$

= 35.89 % axial and

64.11 % equatorial

for the α hydrogen.

Therefore OH group is 64.11 % axial and 35.89 % equatorial.

trans-2-methylcyclohexanol

There was no observable splitting of the α hydrogen peak at 190 K. The compound prefers one conformation probably when both methyl and hydroxyl groups are in an equatorial position.

cis-3-methylcyclohexanol

1:78 ratio of splitting peaks at 185 K. The compound prefers one conformation probably when both methyl and hydroxyl groups are equatorial.

trans-3-methylcyclohexanol

1:11 slight splitting of peaks at 185 K, a somewhat surprising result since the hydroxyl group is probably in an axial configuration in the most stable conformer.

cis-4-methylcyclohexanol

3:1 split at 190 K.

trans-4-methylcyclohexanol

No observable splitting at 190 K. The compound prefers one conformation with both hydroxyl and methyl groups in the equatorial position.

Conclusion

The concentration versus chemical shift and chemical shift versus temperature techniques via NMR have given good results in the determination of the presence of intramolecular hydrogen bonding and the preferred conformation of trans-2-aminocyclohexanol, i.e. alternate chair equatorial OH and equatorial amino group.

The concentration versus chemical shift NMR technique has given some information on the preferred conformations of the methylcyclohexanols, e.g.

Compound	Hydroxyl Group	Methyl Group
1-methylcyclohexanol	axial	equatorial
cis-2-methylcyclohexanol	axial	equatorial
trans-2-methylcyclohexanol	equatorial	equatorial
cis-3-methylcyclohexanol	equatorial	equatorial
trans-3-methylcyclohexanol	axial	equatorial
cis-4-methylcyclohexanol	axial	equatorial
trans-4-methylcyclohexanol	equatorial	equatorial

The chemical shift of the amino group in cyclohexylamine and butylamine has produced some very interesting results.

T_1 studies seem to confirm the above conclusions regarding the methylcyclohexanols in that the trans-2-methyl, cis-3-methyl and trans-4-cyclohexanol molecules seem to form the stronger intermolecular hydrogen bonds in solution.

Inversion Recovery and Freeman-Hill methods produce similar reproducable T_1 values, the Freeman-Hill method gives generally shorter T_1 values.

3 SYNTHESIS OF ALICYCLIC COMPOUNDS

The aminocyclohexanols

As stated previously, the aminocyclohexanols with 1,2-, 1,3- and 1,4- configurations exist in cis and trans forms.

The trans-2-aminocyclohexanol was the only compound which was prepared directly and in a pure state; the remaining aminocyclohexanols were produced via the aromatic aminophenols by hydrogenation, followed by the separation of the cis and trans isomers.

Two methods of hydrogenation of the acetamidophenols were tried:

(i) low pressure hydrogenation method used by Freifelder[26] : the acetamidophenols (20 g in 75 cm^3 methanol) were placed in a high pressure bomb. Hydrogenation was carried out for 100 hours at a pressure of 35 pounds per square inch (241 K Nm^{-2}) at room temperature using a 5 % rhodium/alumina catalyst. The product was then filtered and a PMR spectrum obtained. It was found that very little hydrogenation took place using this method.

(ii) high pressure hydrogenation method recommended by Hartmann[27] : the acetamidophenol (20 g in 75 cm^3 methanol) was placed in a high pressure bomb (to which 3 g of Raney Nickel catalyst was added). Hydrogen gas was added to the mixture until the pressure reached 1000 pounds per square inch. The mixture was then heated to 180°C and maintained at that temperature for 1.75 hours, or until the absorption of hydrogen ceased. Hydrogenation started at 175°C. The product was then cooled, filtered, evaporated to dryness and a PMR spectrum obtained. Hydrogenation was more successful using the high pressure method.

trans-2-aminocyclohexanol

The amino alcohol was prepared according to Brunnel[28] by reaction of cyclohexene oxide (5.3 cm^3) in methanol (50 cm^3) with liquid ammonia (40 cm^3) in a sealed tube for 12 hours at room temperature or 2 hours at 80oC. The product was purified by sublimation at 45^o and 2 Torr. It was obtained as colourless needles Mp 67-69^{o}C in 60 % yield.

The trans-2-aminocyclohexanol was very hygroscopic. It was used for experiments immediately it was prepared. Its solubility in trichloromethane fell if it was kept for any length of time.

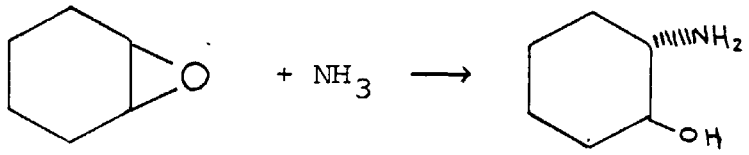

cis-2-aminocyclohexanol and trans-2-aminocyclohexanol

2-aminophenol (20.5 g) was added to distilled water (500 cm^3) and concentrated hydrochloric acid (18.3 cm^3) contained in a one litre beaker. The mixture was stirred vigorously until the solid passed into solution. Decolourising carbon (3.4 g) was added and the solution heated to about 50^{o}C for five minutes. It was then filtered at the pump.

To the resulting solution ethanoic anahydride (27.7 g, 25.6 cm^3) was added. The reaction mixture was stirred, and poured into a solution containing crystalline sodium ethanoate (33 g) in water (100 cm^3). The solid was filtered by suction, washed with a little water and drained. The substance was recrystallised from the minimum amount of boiling water.

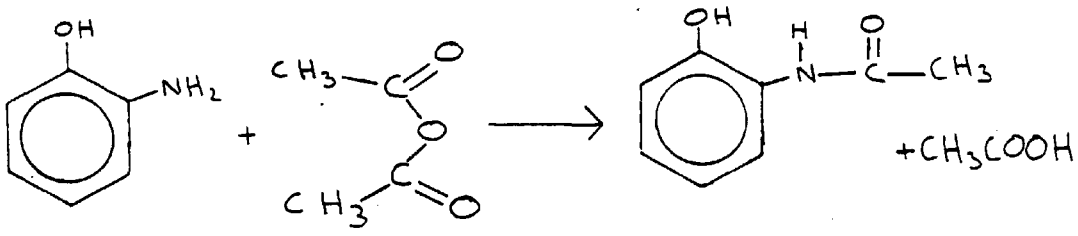

Protecting the amino group stops the formation of secondary amines at the high pressures involved in the reduction process.

The melting point of 2-acetamidophenol was 201°C, yield 75 %. A PMR spectrum of the product was obtained.

The 2-acetamidophenol (14.7 g) was then dissolved in methanol (60 cm^3), two or three measures of Raney Nickel catalyst were added and reduction was carried out at 180°C and 100 atmospheres pressure for four hours.

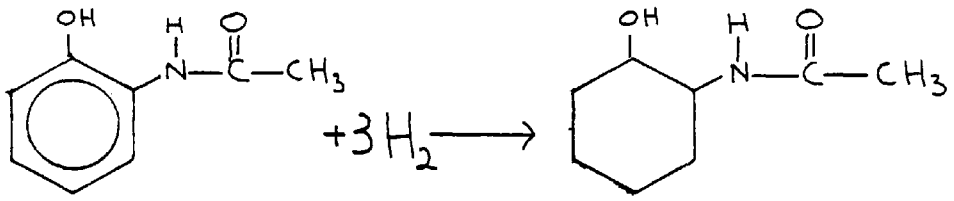

The product was checked for purity with PMR.

The product was refluxed with sodium hydroxide solution (30 cm^3 of 6 $mol.dm^{-3}$) for five days, ensuring that all the glass joints of the apparatus were well greased. This treatment liberated the free amino group of the cyclohexane ring.

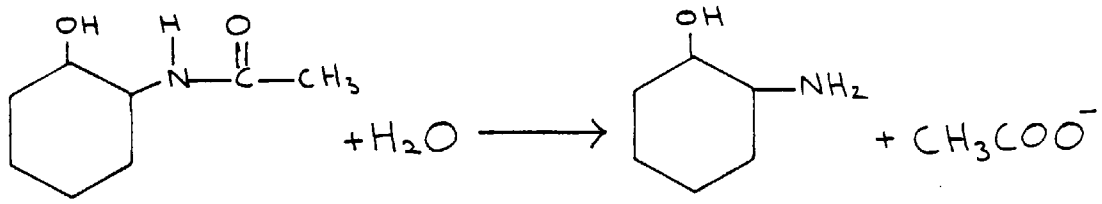

The 2-aminocyclohexanol (trans and cis) was then extracted into chloroform by continuous liquid/liquid extraction. The extracted sample was checked with NMR. It contained a mixture of cis- and trans-2-aminocyclohexanols.

Hartmann suggested that the isomers could be separated by re-crystallisation from acetone or ethyl acetate, the less soluble trans isomer separating first.

It proved impossible to separate the isomers by this method.

Paper, thin layer, column and gas liquid chromatography were used to try and separate the isomers but both isomers ran together using these methods under various conditions.

cis-2-aminocyclohexanol

Owing to the difficulty of producing cis-2-aminocyclohexanol by a hydrogenation method another technique was tried, viz: the conversion of trans-2-aminocyclohexanol to cis-2-aminocyclohexanol via oxazolines[29].

The trans-2-aminocyclohexanol (0.5 g) was acetylated with 4-nitro-benzoylchloride (3 g), and then treated with a four-fold excess of thionyl chloride for several hours at 25°C. The yellow solution was poured into dry ether at 0°C. The white precipitate was collected and washed successively with dry ether and water. The cold aqueous washings were neutralised with sodium hydroxide (dilute) which gave a white precipitate (0.52 g).

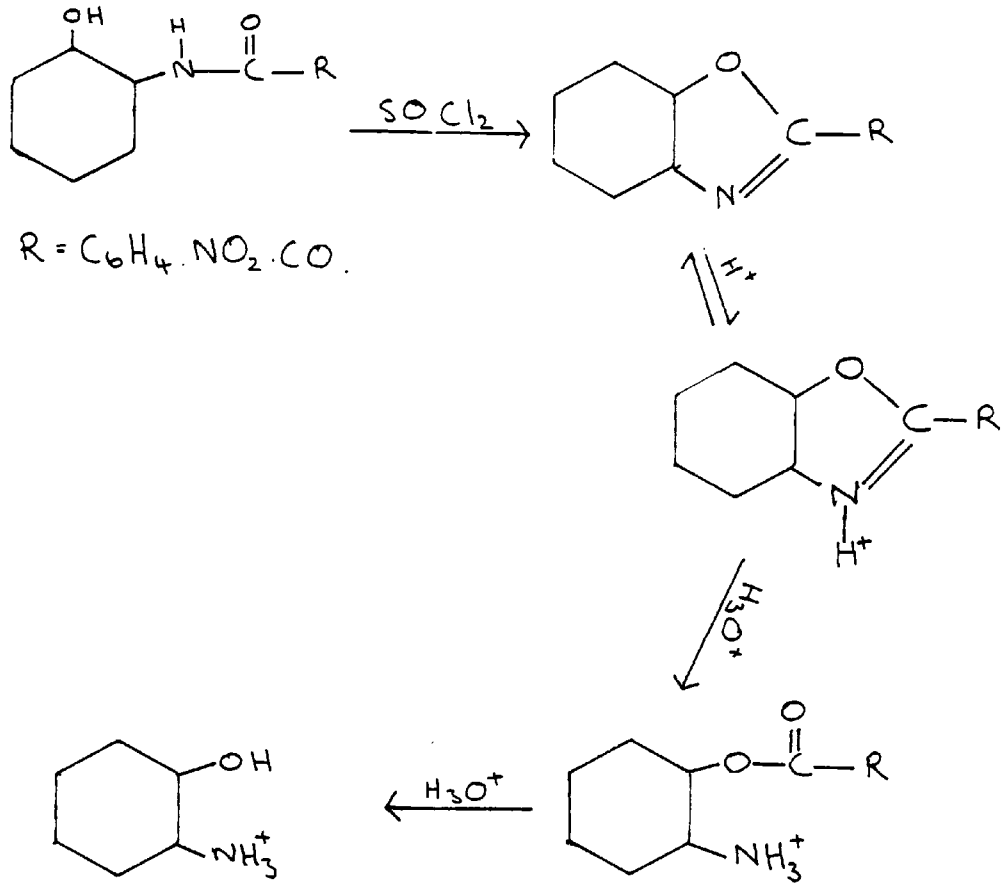

The oxazoline was recrystallised from absolute ethanol. The crystals were then heated to just boiling in hydrochloric acid (20 cm^3 of 5 %). The product cis-2-nitrobenzoxycyclohexylamine hydrochloride crystallised.

This was refluxed with sodium hydroxide (dilute) and extracted by chloroform. Very little yield was obtained (less than 2 %). A CMR spectrum was the same as the original trans-2-aminocyclohexanol.

cis and trans-3-aminocyclohexanol

These may be prepared either by the high pressure hydrogenation method of Hartmann or by a low pressure method used by Renwick and Williams[30].

3-acetamidophenol (20 g) in methanol (75 cm^3) was hydrogenated for 100 hours at a pressure of 35 pounds per square inch (241 K Nm^{-2}) at room temperature using a 5 % rhodium/alumina catalyst. The solution was filtered and evaporated to dryness. The 3-acetamidocyclohexanols were hydrolysed with sodium hydroxide (2.5 $mol.dm^{-3}$) and the free amines separated[31].

trans-3-aminocyclohexanol was obtained as the white crystalline hydrogen oxalate and cis-3-aminocyclohexanol as the gum of its hydroperchlorate salt.

It was found from PMR spectra that low pressure hydrogenation did not work very well as most of the product was still aromatic. The high pressure hydrogenation gave good reduction but it proved impossible to separate the isomers.

cis and trans-4-aminocyclohexanols

This was prepared as a mixture by the high pressure hydrogenation of 4-acetamidophenol PMR indicated that reduction was complete. The acetamidocyclohexanols were refluxed with sodium hydroxide (6 $mol.dm^{-3}$) for five days and then extracted by continuous extraction with chloroform.

The literature states that the trans isomer separated first by fractional recrystallisation from acetone.

However, it proved impossible to isolate the isomers in a pure state. CMR spectra showed a mixture of cis and trans isomers. The product was also very hygroscopic.

Preparation of Raney Nickel catalyst

Sodium hydroxide (32.5 g) was dissolved in water (125 cm^3) in a three-necked flask cooled in running water until the temperature fell to 50°C.

The Raney Nickel alloy (25 g) (Ni/Al) was added in small portions (1-2 g) to the rapidly stirred solution, keeping the temperature at 50°C ± 2°C. The foaming was controlled by adding a few drops of ethanol. When the alloy has been added keep the flask and contents at 50°C for a further hour by passing steam into a funnel around the three-necked flask. After this time the catalyst was washed by decantation with 2 $mol.dm^{-3}$ sodium hydroxide (100 cm^3) and twice with distilled water (100 cm^3). The mixture was then transferred to a Buchner funnel and tap water was passed through the funnel at the rate of 100 cm^3 per minute until the washings were neutral.

The catalyst was then quickly transferred to a wide-necked conical flask and stored under absolute alcohol.

Method for high pressure hydrogenation

1. Put pot into heater/cooler. Make sure that pot is in correct position (flat on pot by retaining block).
2. Place stirrer/thermometer/gas inlet lid onto pot, ensuring that lead washer is in reasonable shape (on underside of lid).
3. Screw on the clamping device which holds down the lid. Tighten this up by screwing down the six large screws with the Allen Key. (Screw down even left, i.e. opposite screw tightened alternately).
4. Put thermocouple leads into hole in lid.
5. Slide on the large electromagnetic over gas inlet pipe extending from lid.
6. Screw on the gas inlet manifold which has the bursting disc on top.

7. Connect up gas inlet line from cylinder.

8. Connect up power to heater, stirrer, temperature gauge.

9. Fill with gas to required pressure, set temperature and retire.

The methylcyclohexanols

1-methylcyclohexanol

This may be prepared using reactions of Grignard reagents with esters.

In the synthesis of 1-methylcyclohexanol pentamethylene di-Grignard reagent and methyl acetate are the reactants, e.g.

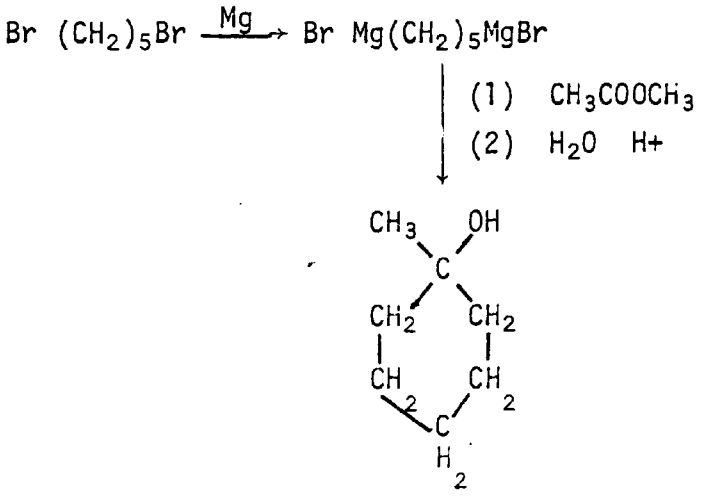

trans-2-methylcyclohexanol[33]

This compound may be prepared by the hydroboration of alkenes,

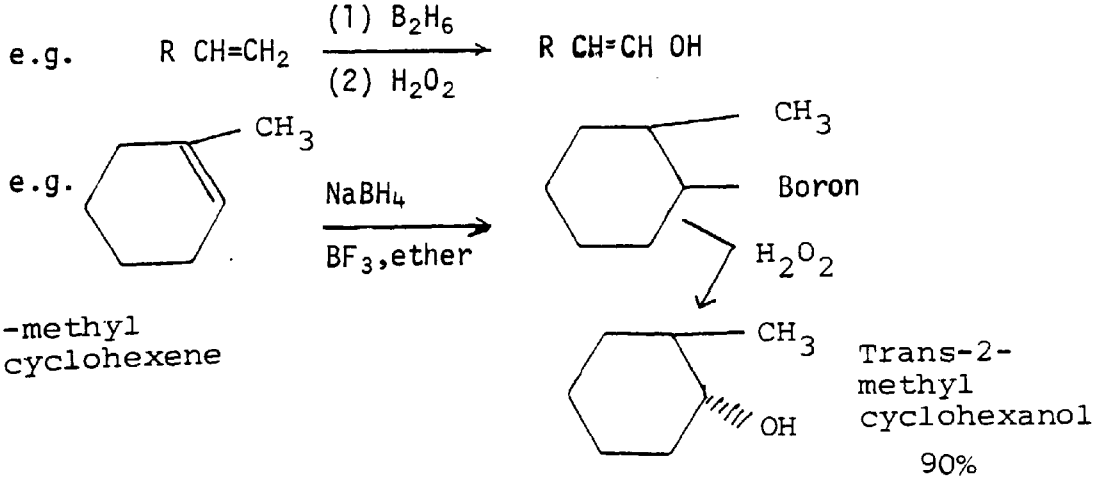

Diborane is best made in situ from sodium borohydride and boron trifluoride. The trialkylborane can be oxidised without isolation by hydrogen peroxide. The orientation is anti-Markovnikoff, the reaction is stereo specific, cis addition occurs to the least hindered side of the double bond and oxidation with hydrogen peroxide occurs with retention of configuration.

cis-2-methylcyclohexanol[34]

The compound is prepared by the protodesilylation of hydroxysilane (Homo-Brock rearrangements).

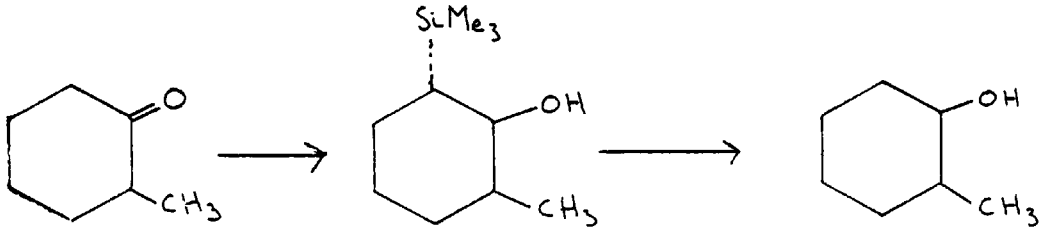

2-methyl-cyclohexanone | α-hydroxysilane | cis-2-methyl-cyclohexanol

α-hydroxysilane was prepared by the addition of trimethylsilyl lithium to 2 methylcyclohexanone (54 %) yield. The stereochemistry was initially assigned by assuming predominant attack of the silyl reagent trans to the methyl group. When this compound was treated with a solution of the potassium salt of 2-methylpropan-2-ol (5 %) in a mixture of dimethylsulphoxide in water (19:1) at room temperature, the reaction was complete in one hour giving the protodesilylation product (97 % cis).

Protodesilylation takes place with complete retention of configuration.

cis-3-methylcyclohexanol and trans-4-methylcyclohexanol[35]

Sodium borohydride is a relatively mild reducing agent whereas lithium tri-sec-butyl-borohydride (L Selectride Aldrich) is an exceptionally powerful and highly stereoselective reducing agent.

The stereoselective reduction of cyclic ketones depends critically on the steric bulk of alkyl substituents on the boron atom. The bulky trialkyl borohydride, lithium tri-sec-butyl borohydride approaches the ketones from the equatorial side, producing the less stable axial isomers with greater than 90 % stereoselectivity.

The reducing agent used was generated from n-butyl lithium and borane-dimethyl sulphide complex in equimolar ratio in toluene-hexane (or tetrahydrofuran-hexane).

The reductions in toluene-hexane or tetrahydrofuran-hexane at -78°C took two to four hours.

4-methylcyclohexanone is reduced to trans-4-methylcyclohexanol with 94 % stereoselectivity.

3-methylcyclohexanone is reduced to cis-3-methylcyclohexanol.

This method can be used to reduce 2-methylcyclohexanone to trans-2-methylcyclohexanol with 92 % stereoselectivity.

trans-3-methylcyclohexanol[36]

Schwartz's reagent η^5 $(C_5H_5)_2Zr(H)Cl$, is a good one for reducing cyclic ketones. The reduction involves a preferential equatorial attack to give the corresponding axial alcohol.

The reagent will reduce 3-methylcyclohexanone to trans-3-methyl-cyclohexanol.

cis-4-methylcyclohexanol[37]

This may be produced from 4-methylcyclohexanone by reduction with sodium borohydride-mandelic acid complex. This is a new reducing agent prepared from sodium borohydride; it is milder than sodium borohydride. It reduces unhindered cyclohexanones with the opposite stereoselectivity to lithium aluminium hydride giving 75.92 % of axial alcohols.

Boiling points of methylcyclohexanol isomers

1-methylcyclohexanol	168°C
trans-2-methylcyclohexanol	167.2 - 167.6°C
cis-2-methylcyclohexanol	168°C (166 - 168°C)
trans-3-methylcyclohexanol	169°C
cis-3-methylcylcohexanol	170°C
trans-4-methylcyclohexanol	174°C
cis-4-methylcyclohexanol	172 - 173°C

Figure 2(12)

Preparation of samples for T_1 measurement

The samples used during the experimentation were trans and cis 1,2, 1,3 and 1,4 methylcyclohexanols.

Some work was also carried out on 1-methylcyclohexanol.

Different carbons will not only exhibit different chemical shifts but also different rates of spin-lattice relaxation, hence different T_1 values.

Generally, the smaller the molecule size, the longer the T_1, and the larger the molecules, the shorter the T_1.

The T_1 of carbon atoms directly bonded to hydrogen atoms is relatively short. The greater the substitution of a carbon centre, the longer its T_1: e.g.

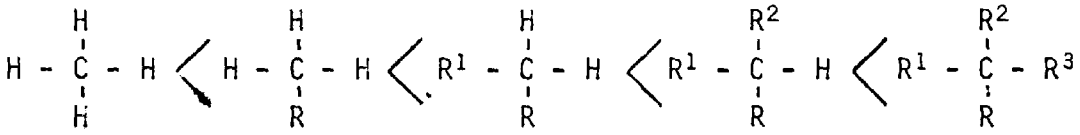

The literature results are not absolute, that is the T_1's may only deemed accurate for a particular set of conditions. In this one the temperature was set at 300 K.

Sample preparation

Approximately 2 $mol.dm^{-3}$ solution of the methylcyclohexanols were made up using a deuterated chloroform solvent ($CDCl_3$) e.g. 1.15166 g of trans-4-methylcyclohexanol was placed in a 5 ml graduated flask, deuterated chloroform was added up to the 5 ml mark.

Molar mass of trans-4-methylcyclohexanol = 114.19 g.

$$mol.dm^{-3} = \frac{wt\ dm^{-3}}{Mr} = \frac{1.15166 \times 200}{114.19}$$

$$= 2.017\ mol.dm^{-3}$$

Of primary importance in accurate relaxation time determination is the elimination of paramagnetic substances primarily oxygen dissolved in the sample. The oxygen has come from diffusion from the atmosphere and its presence in a sample even in concentrations of a few ppm can drastically reduce H relaxation time and broaden the observed lines, obeying the equation:

$$\Delta \nu_{\frac{1}{2}} = \frac{1}{\pi T_2}$$

where $\Delta \nu_{\frac{1}{2}}$ is the observed line width, clearly dependent on the transverse relaxation time, T_2.

Paramagnetic species have the effect of increasing dipole-dipole intermolecular relaxation rates by providing enhanced dipoles. The following technique was used to eliminate most of the oxygen from the samples:

DE-GASSING

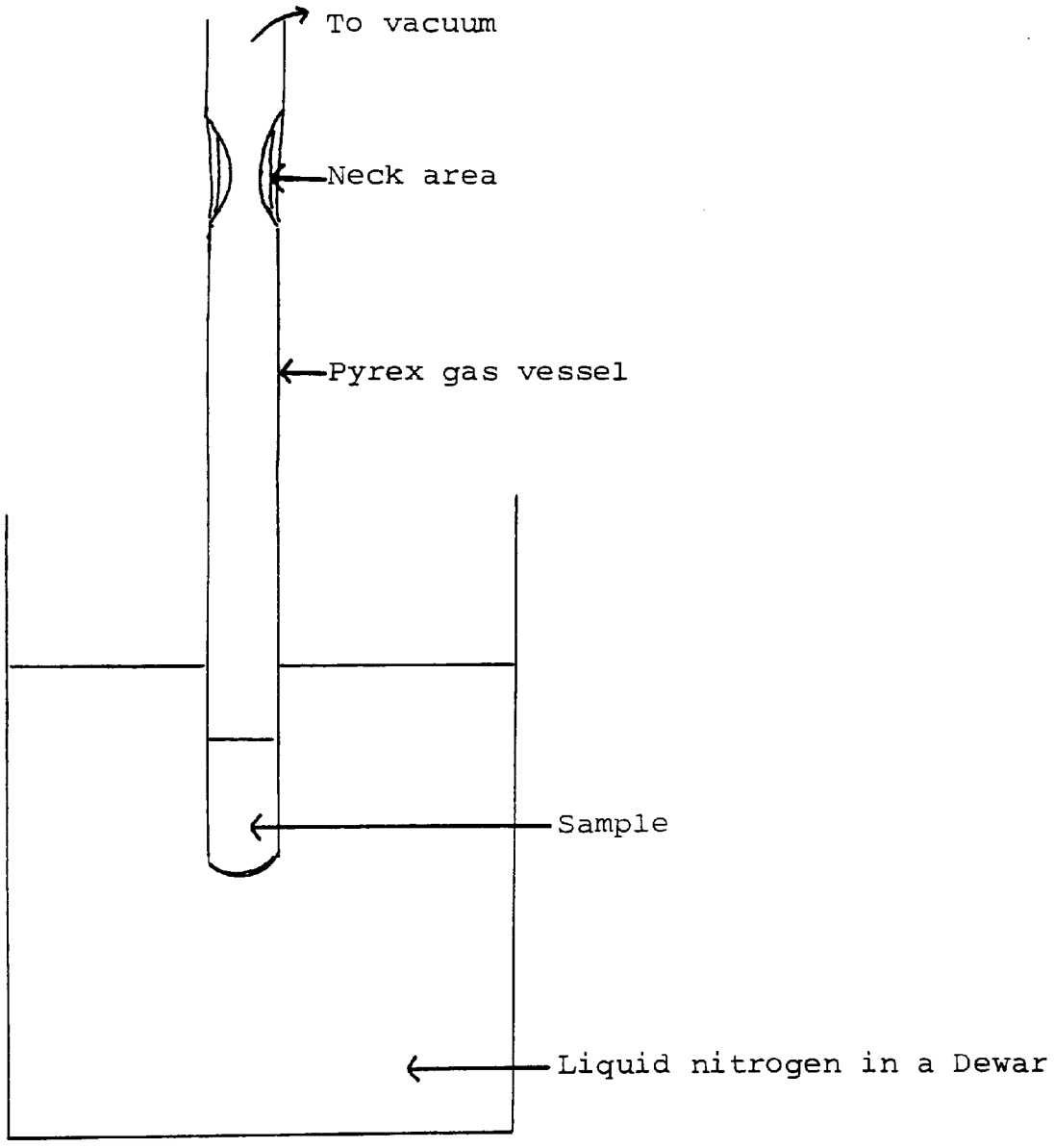
To vacuum
Neck area
Pyrex gas vessel
Sample
Liquid nitrogen in a Dewar

The de-gassing method employedwas a liquid nitrogen vacuum pump cycle. The methylcyclohexanol was contained in a glass tube. The tube was thoroughly washed with acetone and dried in a heater oven before use. The tube was then connected via a polythene tube to a vacuum pump and all joints were sealed as efficiently as possible with lengths of 'cling-film' wrapped tightly over them.

The system was put under vacuum ($\simeq$ 4 mm Hg) and the tube was gently lowered into a Dewar containing liquid nitrogen, and held there for three minutes. The tube was taken and the frozen sample was thawed by gently stroking the tube with fingers. As the sample thawed gas was seen to bubble out of the solution and was drawn off by the vacuum. The above procedure was repeated a further two times in order to draw off as much gas as possible.

Important aspects of sample technique

Low magnetic solvents for such experimentation are vital, deuterated solvents such as $CDCl_3$ are recommended, although the proton impurities must be below 1 % or proton impurity resonance will tend to interefere with NOE.

The cell is of high importance. The shape must be cylindrical and the flatter the camber the better the ultimate resolution. Spinning a non-straight tube in the magnetic field may give rise to troublesome sidebands and for the same reason the thickness of the walls should be uniform. The size of the cell is also important to maintain sample concentration at a constant level. The signal to noise ratio increases regularly with tube diameter as a greater number of nuclei are detected.

In order to attain optimum conditions, tight magnetic coupling is essential between the sample molecules and the coil. A vital consideration is the filling factor, η, which conditions the signal intensity.

$$\eta = \int_{\text{sample volume}} \frac{B_1^2}{\int_{\text{all space}} B_1^2 \, dv}$$

i.e. signal to noise ratio is proportional to η - so it is important to maximise η.

For cylindrical cells

$$\eta = \frac{ds^2}{2Dc^2}$$

where ds = internal tube diameter

Dc = coil diameter.

Taking into account the wall thickness, the filling factor is expected to decrease rapidly with tube size.

Filling the cell is very important, care should be taken to select a convenient height of liquid above the receiving coil. This is to minimise distraction of the magnetic field resulting from susceptibility differences between the sample and surrounding air, height of liquid should not be less than six to eight times the coil radius.

It was sometimes useful to employ a clean teflon vortex suppressor to counteract these fringe effects.

PMR and ^{13}CMR spectra, graphs and coding sheets are in Appendix A.

APPENDIX A

SUPPLEMENTARY INDEX FOR APPENDIX A

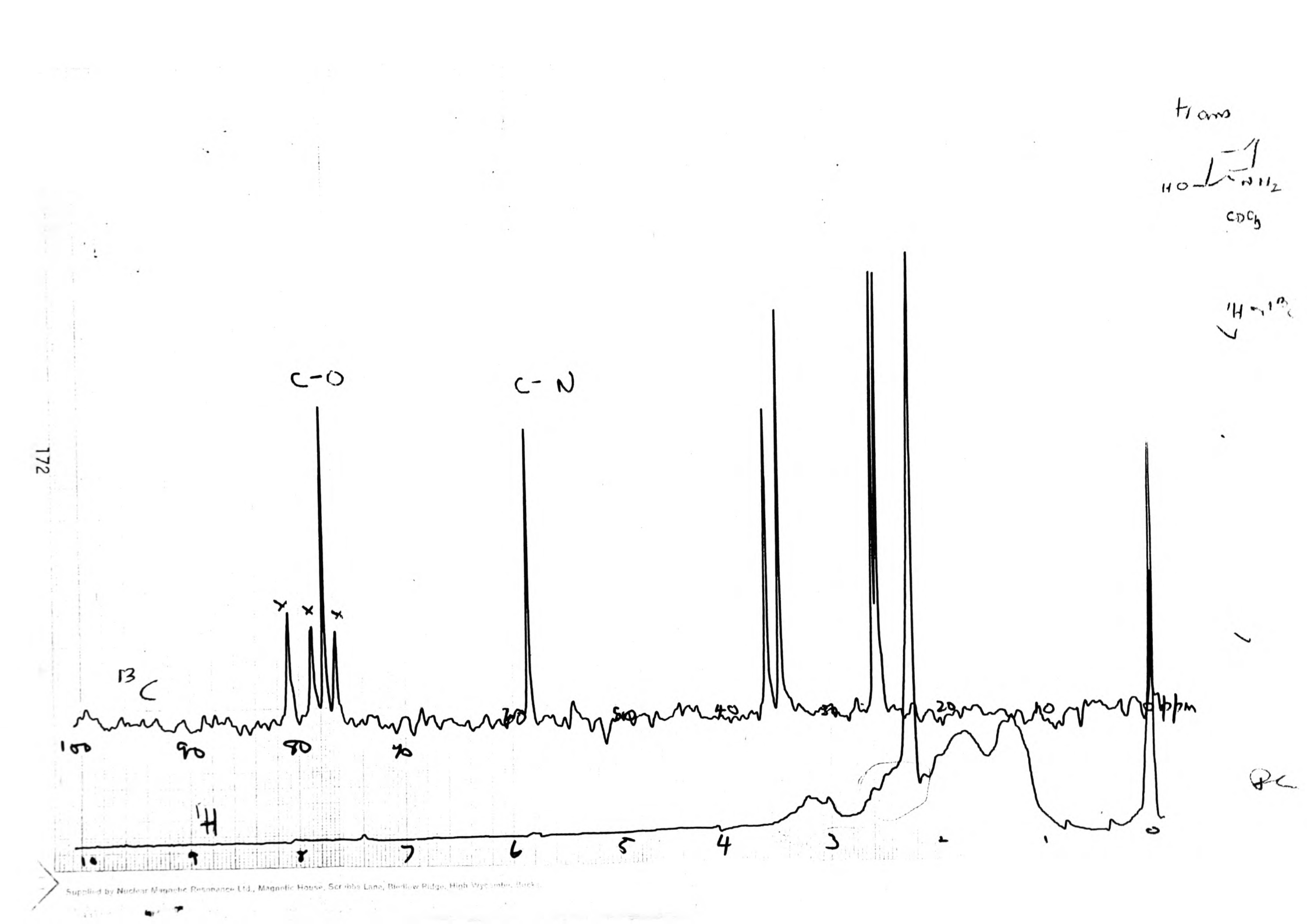
trans
HO
NH2
CDCl3
C-O
C- N
X
X
X
13C
100
90
80
70
60
50
40
30
20
10
0 ppm
1H
10
9
8
7
6
5
4
3
2
1
0
172
Supplied by Nuclear Magnetic Resonance Ltd., Magnetic House, Scribbs Lane, Bledlow Ridge, High Wycombe, Bucks.

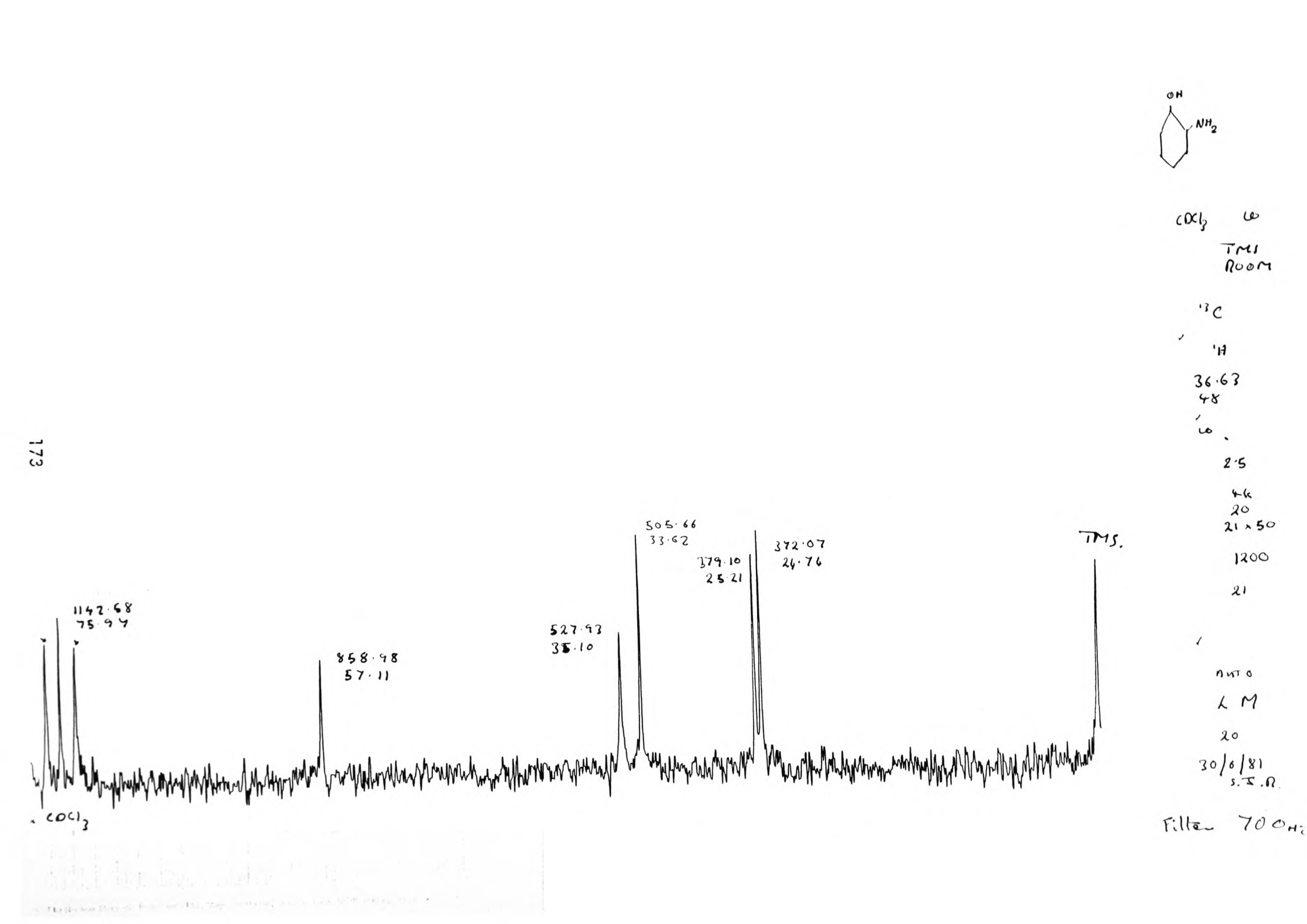
OH
NH2
CDCl3
TMS
ROOM
13C
1H
36.63
48
2.5
20
21 x 50
1200
21
30/6/81
S.I.R.
Filter 700 Hz
1142.68
75.94
858.98
57.11
527.93
35.10
505.66
33.62
379.10
25.21
372.07
24.76
TMS.
CDCl3

TMS
ROOM
13 C
1 H
30.13
48.02
2
4k
20
220.10
4500
20
AUTO
11
20
21 | 5.5.12.
CDCl3
37.5
30.8
48.0
53.0
69.6
125.7
124.5
130.3
154.0
169.3
170.2

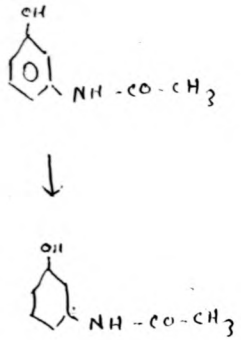

Very little starting material remaining

2 main products most likely in roughly equal proportions

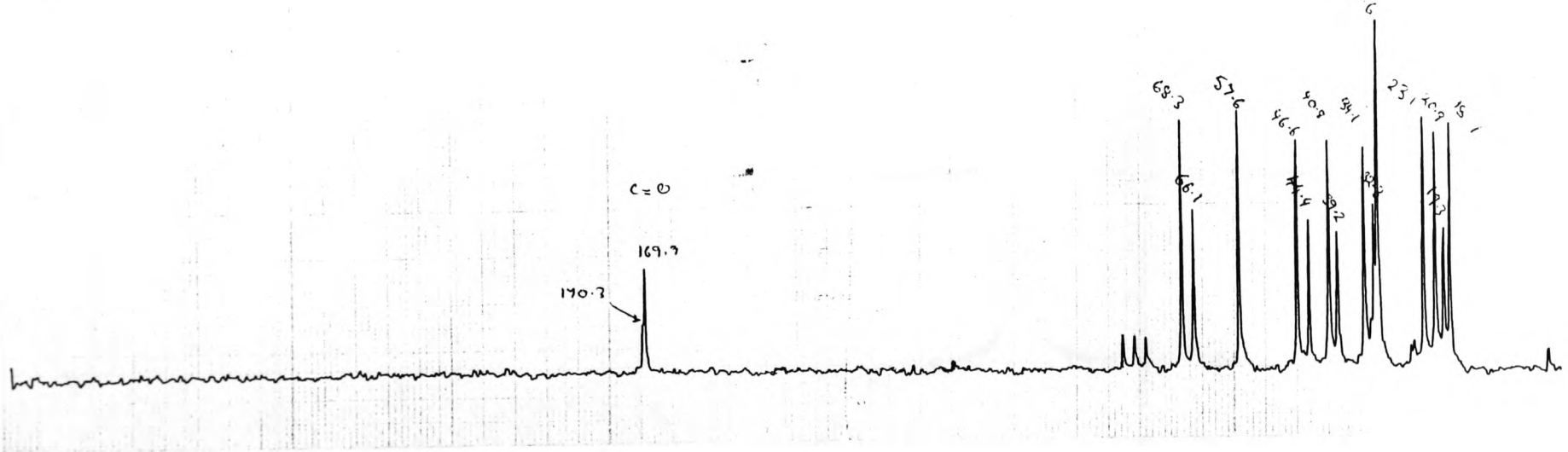

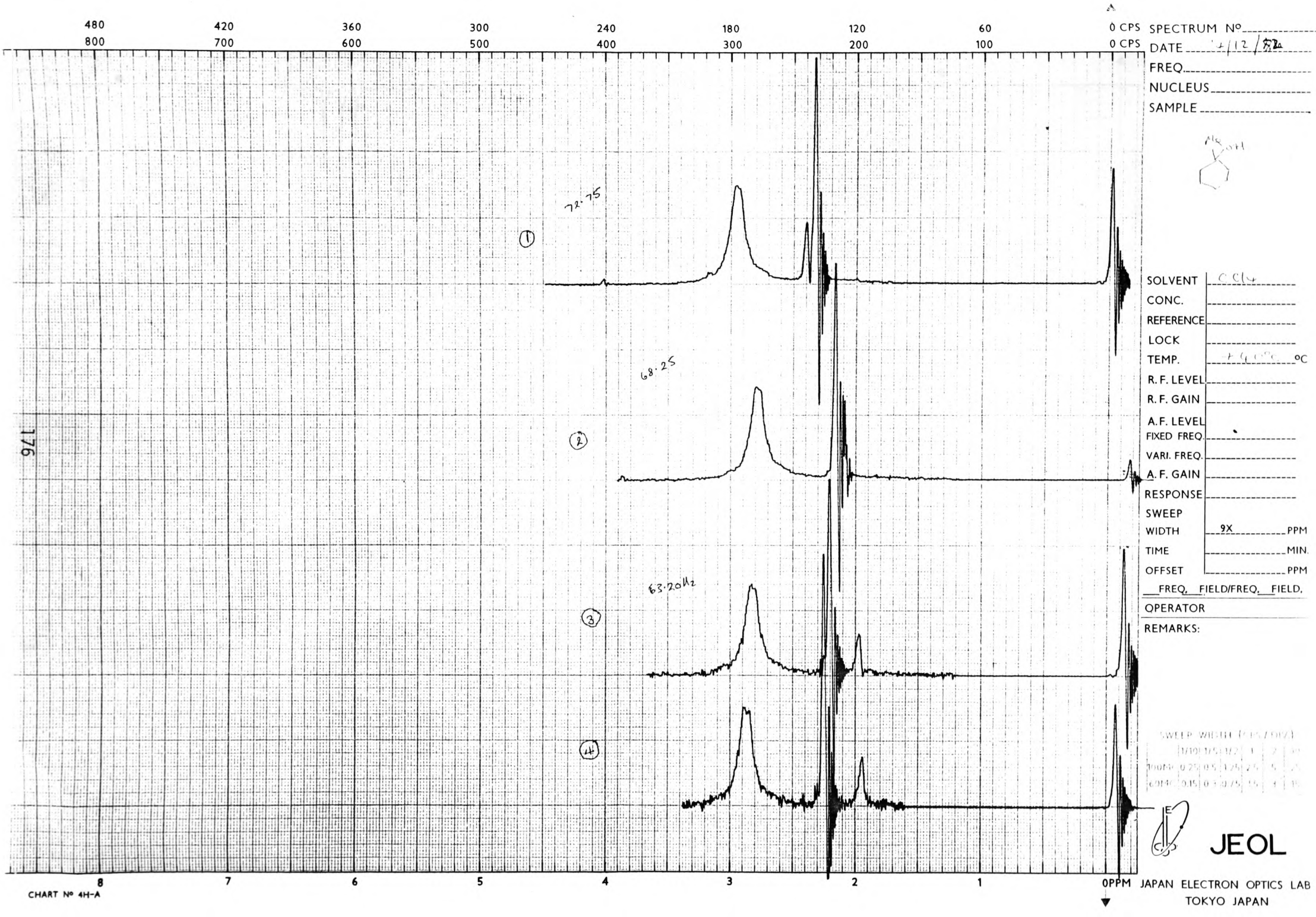
480
800
420
700
360
600
300
500
240
400
180
300
120
200
60
100
0 CPS
0 CPS
72.75
68.25
63.20Hz
8
7
6
5
4
3
2
1
0PPM
176
SPECTRUM Nº
DATE 4/12/82
FREQ.
NUCLEUS
SAMPLE
SOLVENT CCl4
CONC.
REFERENCE
LOCK
TEMP. +60°C °C
R. F. LEVEL
R. F. GAIN
A. F. LEVEL
FIXED FREQ.
VARI. FREQ.
A. F. GAIN
RESPONSE
SWEEP
WIDTH 9X PPM
TIME MIN.
OFFSET PPM
FREQ. FIELD/FREQ. FIELD.
OPERATOR
REMARKS:
CHART Nº 4H-A
JEOL
JAPAN ELECTRON OPTICS LAB
TOKYO JAPAN

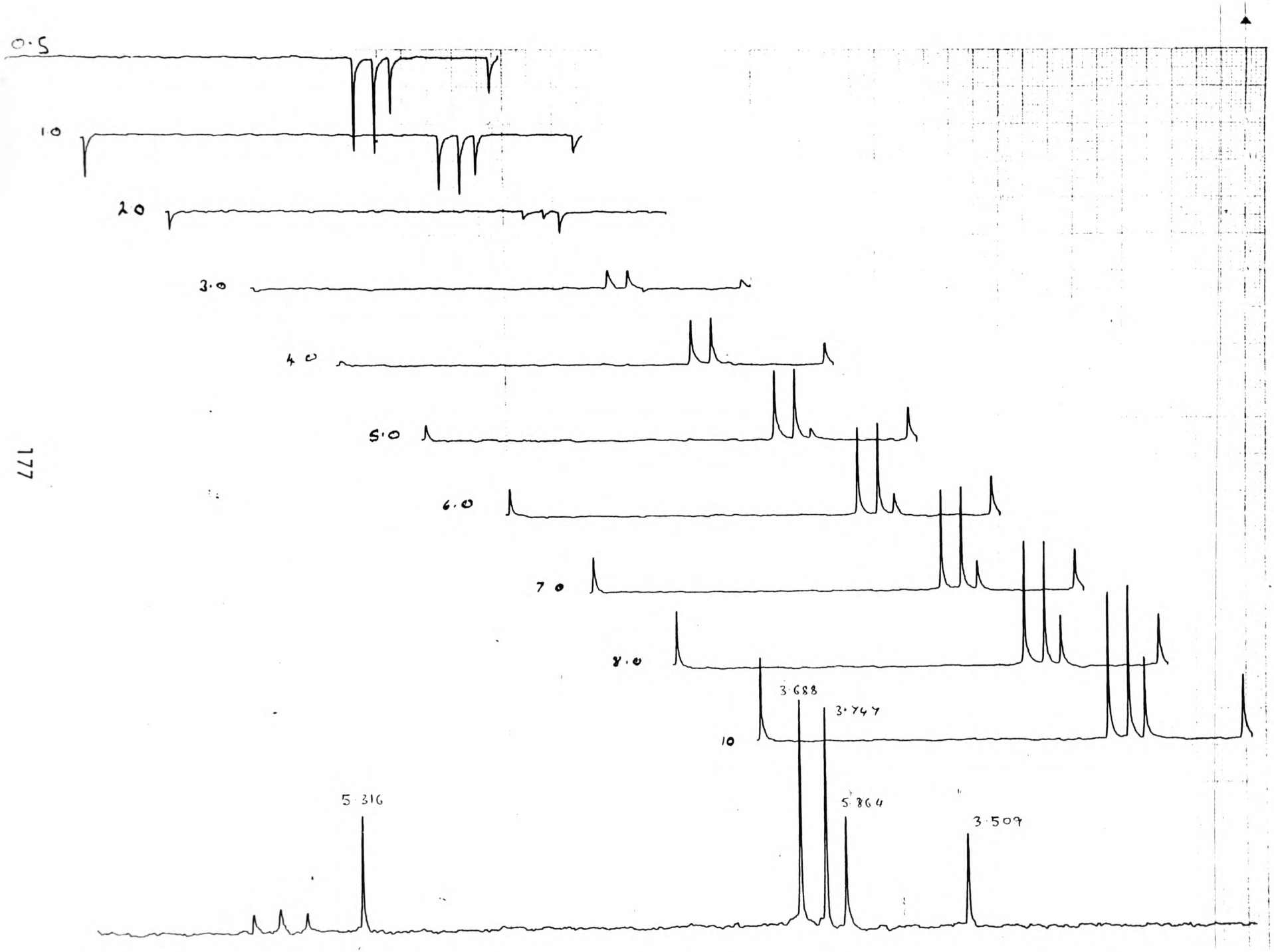

29.9.82.

FX

CHART NO.

SAMPLE T_1

trans 4 methyl-cyclohexanol

$CDCl_3$ TUBE 100

TMS

ROOM

^{13}C

^{1}H

36·66

48

60

8k

20

DUMMYS 5

1

15⁰⁰

AUTO

29/9/82

S.T.R.

177

29.9.82

T1

trans 4 methyl - cyclohexanol

$CDCl_3$ 10

ROOM

^1H

47.5

20

8h

0

2

1

600

AUTO

29/9/82

S.T.

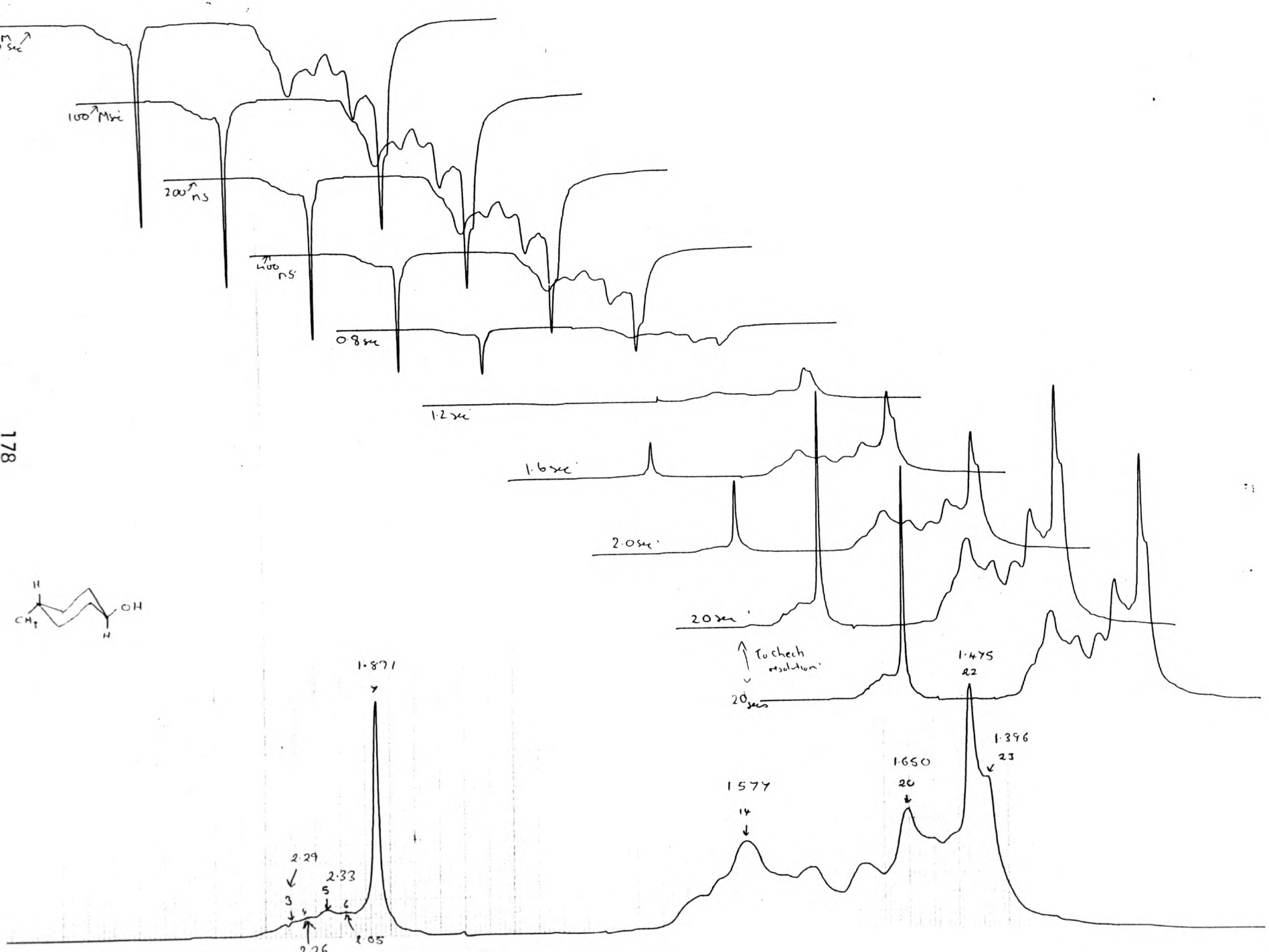

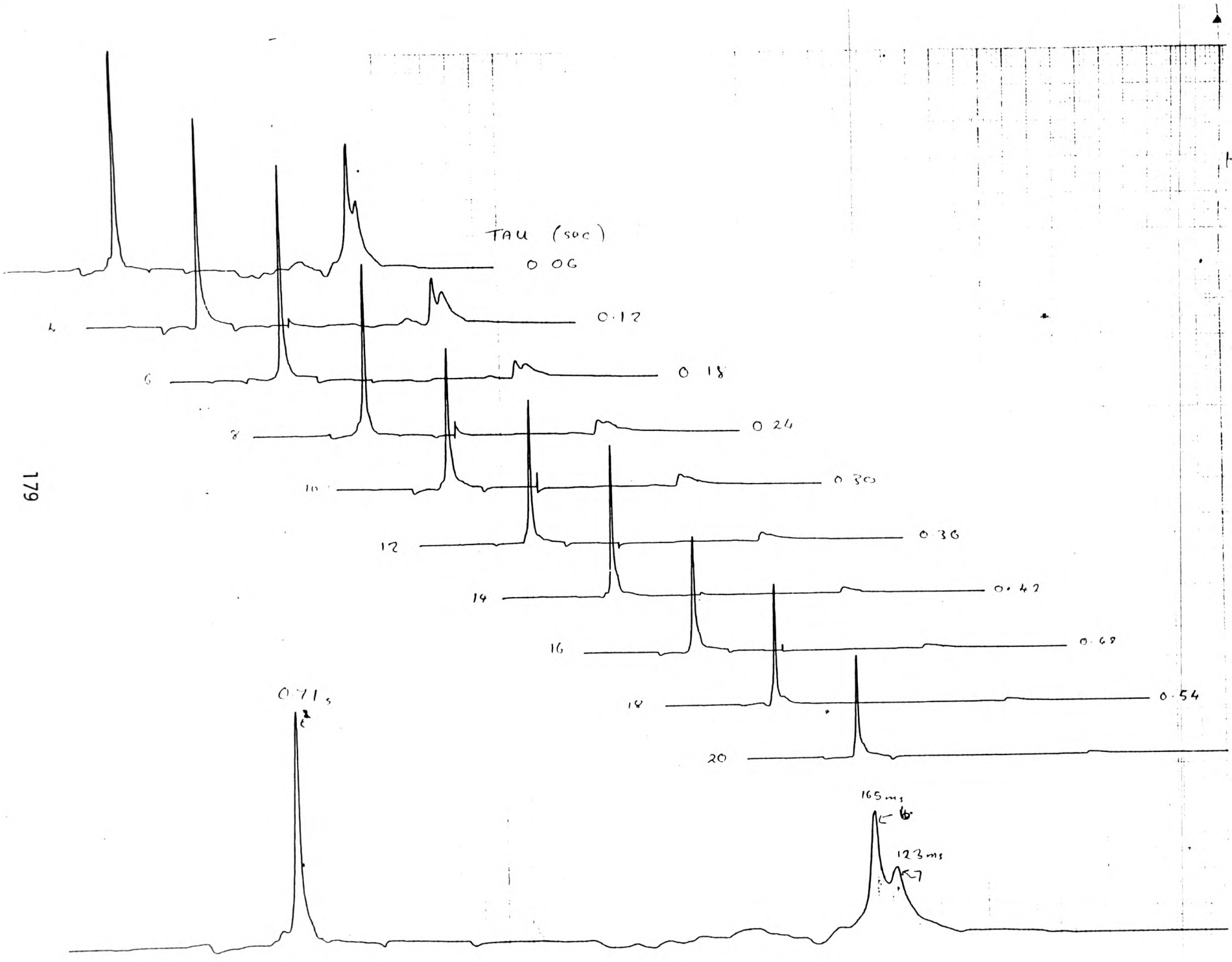
FX
CHART NO.
T 12
trans-4-methyl-
cyclohexanol
TAU (sec)
0 06
0·12
0 18
0 24
0 30
0 36
0·42
0·48
0·54
4
6
8
10
12
14
16
18
20
0·71 s
165 ms
123 ms
179
ROOM
15 ms
15
600
AUTO
24/7/32

Ti - FREEMAN HILL METHOD

CONCENTRATION 2·017 mol dm^{-3}

PD = 40 s

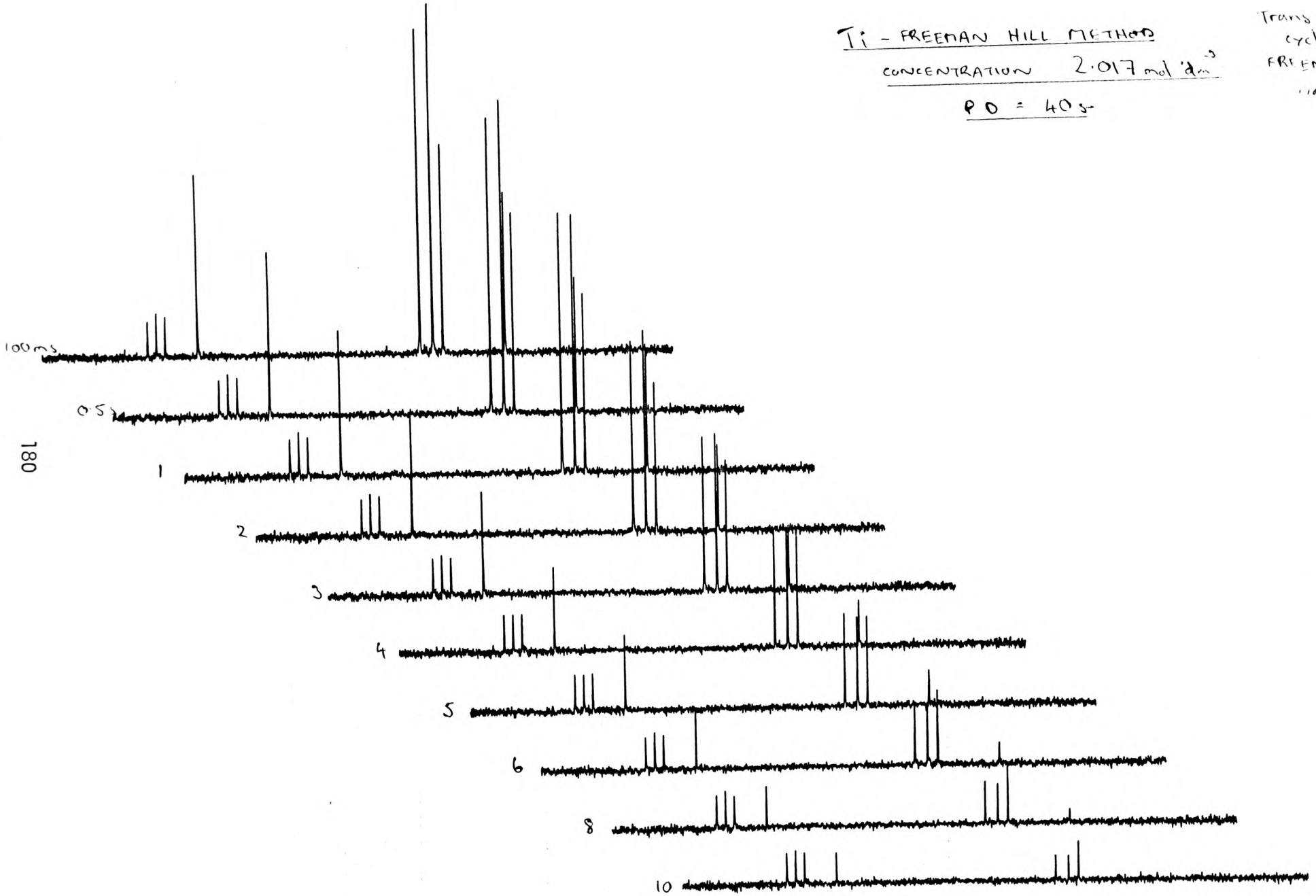

Trans-1,4-methyl cyclohexanol

FREEMAN-HILL

FIRST DATA SET

30.8

10

10

22.69

41.93

22.80

89.55

5.5

6

30/15

40

10

8

8

100

13.78 84

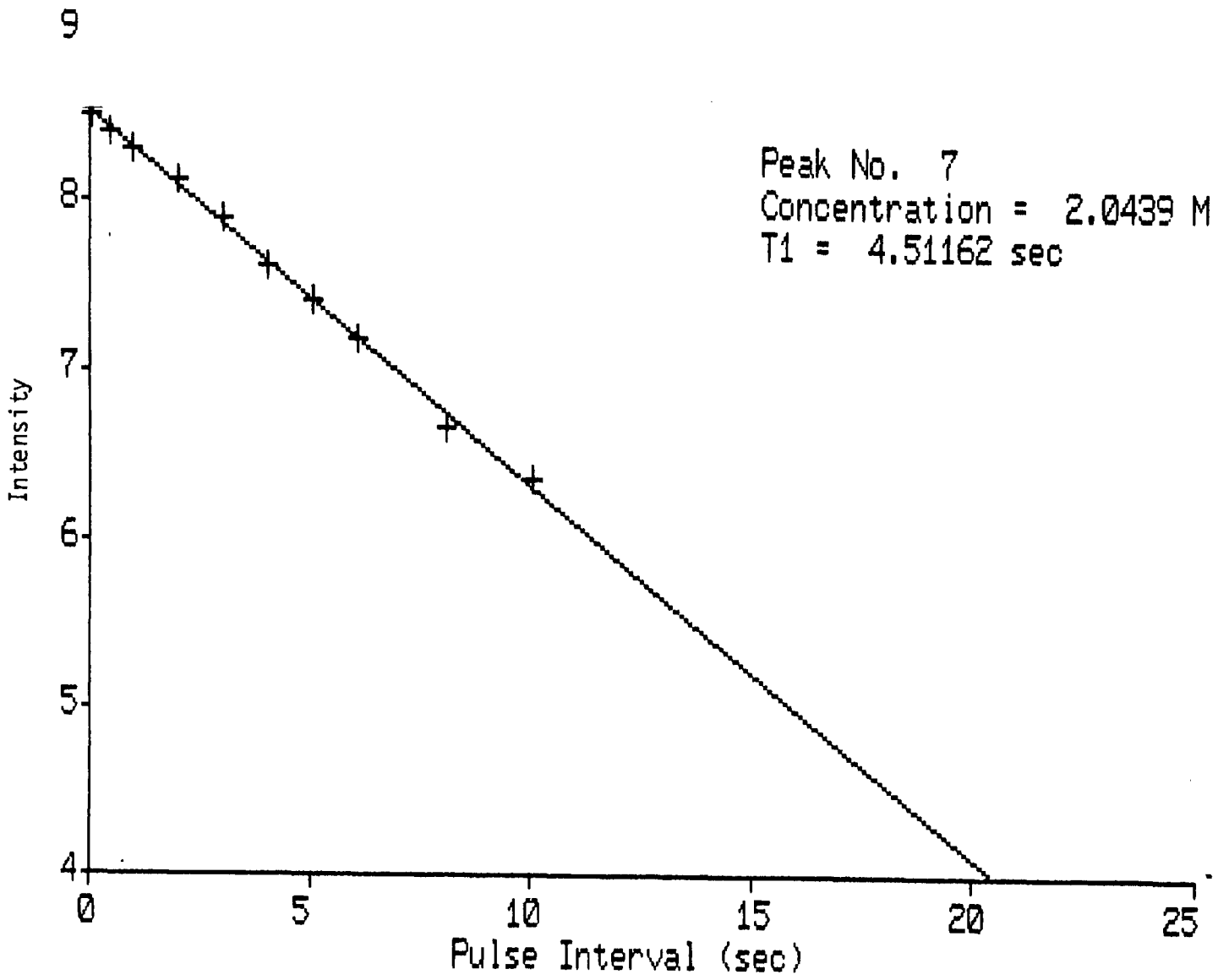

cis-2-methylcyclohexanol

11. CODING SHEET FREEMAN/HILL INVERSION RECOVERY SEQUENCE

Address	K	C	B	A	8	7	J	5	4	3	2	1	Command	Parameter No.	Comment
0	—	—	—	—	—	—	—	—	—	—	—	—	—	—	- SET
1													TIM	9	INITIAL WAIT (1SEC)
2					*										IRRADIATION GATE OPEN
3													TIM	7	PREDELAY (200 MS)
4					*							*			IRRADIATION + OBSERVATION OPEN
5													TIM	1	90° PULSE
6					*				*						PHASE RESET AT ZERO
7													TIM	5	DEAD TIME (50 μs)
8													PUL		SAMPLING TRIGGER
9													LD2	1	ANALOGUE → DIGITAL
10					*			*	*						RECEIVER GATE OPEN
11													TIM	6	DELAY
12					*	*		*	*						A-D TRIGGER [RECEIVER OPEN
13													INT	5	ACCUMULATION INTERVAL
14					*			*	*						RECEIVER OPEN
15													INT	5	ACCUMULATION INTERVAL
16													JC 2	12	CONDITIONAL JUMP TO 12
17				*											HOMOSPOIL PULSE
18													TIM	10	SPOIL (10 S)
19	—	—	—	—	—	—	—	—	—	—	—	—	—	—	CLOSE GATES
20													TIM	4	90 = ST1 WAIT TIME
21													TIM	9	INITIAL WAIT (1SEC)
22	—	—	—	—	—	—	—	—	—	—	—	—	—	—	- SET
23												*			OBSERVATION GATE OPEN
24													TIM	2	180° PULSE
25											*				CHANGE PHASE
26													TIM	3	T(P1) SAMPLE INTERVALS
27					*						*				OPEN IRRADIATION GATE + PHASE
28													TIM	7	PREDELAY (200 MS)
29					*						*	*			OBSERVATION OPEN - PHASE CHANGE
30													TIM	1	
31					*										NO PHASE CHANGE

Address	K	C	B	A	8	7	J	5	4	3	2	1	Command	Parameter No.	Comment
	EXT.IV	EXT.III	EXT.II	EXT.I	Irradiation gate	AD trigger	EXT.V	Receiver gate	Phase reset	0° or 90° phase	0° or 180° phase	Observation gate	TIM (Table 1) JMP LD1 (Table 2) JC1 LD2 (Table 2) JC2 PUL INT (Table 1)		

Address	K	C	B	A	8	7	J	5	4	3	2	1	Command	Parameter No.	Comment
32													TIM	8	DEAD TIME (50 μs)
33													PUL		SAMPLE TRIGGER
34													LD2	1	A-D CONVERSION
35					*			*	*						RECEIVER GATE OPEN
36													TIM	6	DELAY
37					*	*		*	*						A-D TRIGGER
38													INT	5	INTERVAL
39					*			*	*						RECEIVER GATE OPEN
40													INT	5	INTERVAL
41													JC2	37	CONDITIONAL JUMP TO 37
42				*											PHOTOEROIL PULSE
43													TIM	10	EROIL (1MS)
44															SET
45													TIM	4	PD = 5 T_1 WAIT
46													JMP	2	UNCONDITIONAL JUMP TO 2
47													JMP	0	END
48															
49															
50															
51															
52															
53															
54															
55															
56															
57															
58															
59															
60															
61															
62															
63															

Address	K	C	B	A	8	7	J	5	4	3	2	1	Command	Parameter No.	Comment
	EXT·IV	EXT·III	EXT·II	EXT·I	Irradiation gate	AD trigger	EXT·V	Receiver gate	Phase reset	0° or 90° phase	0° or 180° phase	Observation gate	TIM (Table 1) JMP LD1 (Table 2) JC1 LD2 (Table 2) JC2 PUL INT (Table 1)		

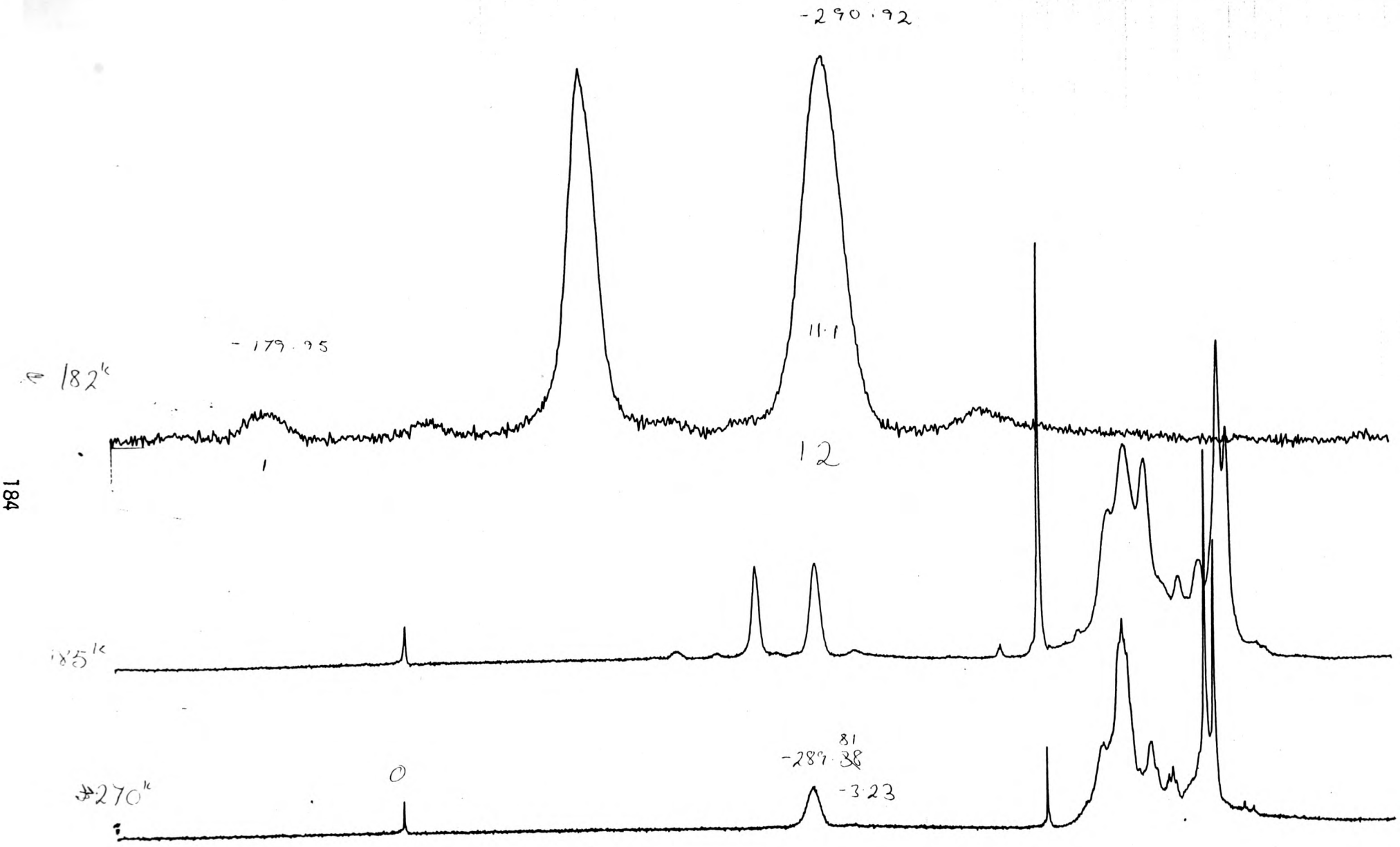
-290.92
-179.95
11.1
182K
1
12
185K
270K
0
81
-289.38
-3.23

REFERENCES

REFERENCES

1 J.E. Kilpatrick, K.S. Pitzer, R. Spitzer, J. Am. Chem. Soc., 1970, 69, p.2483.

2 H. Sachse, Z. Physik. Chem., 1892, 10, p.203.

3 E. Mohr, J. Prakt. Chem., 1918, 98, p.315.

4 F.R. Jenson, D.S. Noyce, C.H. Sederholm, A.J. Berlin, J. Am. Chem. Soc., 1962, 84, p.386.

5 N.L. Allinger, L.A. Freiberg, J. Am. Chem. Soc., 1960, 82, p.2393.

6 S. Winstein, N.J. Holness, J. Am. Chem. Soc., 1955, 77, p.5562.

7 E.L. Eliel, J. Chem. Ed., 1960, 37, p.126.

8 Pimentel and McClellan, The Hydrogen Bond (Freeman, San Francisco, 1980)

9 W.G. Schneider, H.J. Bernstein, J.A. Pople, J. Chem. Phys., 1958, 28, p.601.

10 E.D. Becker, U. Liddel, J.N. Schoolery, J. Mol. Spec., 1958, 2, p.1.

11 R.J. Ouellette, G.E. Booth, K. Liptak, J. Am. Chem. Soc., 1965, 87, p.3436.

12a C.H. Bushweller, J.A. Beach, J.W. O'Neil, G.U. Rao, J. Org. Chem., 1970, 35, p.2086.

12b W. Pauli, Naturwisschaften, 1924, 12, p.741.

13 W.J. Duffin, Electricity and Magnetism, McGraw-Hill (3rd Ed.), p.1080.

14 L.I. Bleaney and B. Bleaney, Electricity and Magnetism, Oxford Univ. Press (3rd Ed.), 1978.

15 J.W. Emsley et al., High Resolution NMR Spectroscopy, Pergamon Press, 1967, 1, pps. 15-16.

16 N.F. Ramsey, Phys. Rev., 1956, 103, p.20.

17 R.R. Ernst and W.A. Anderson, Review of Scientific Instruments, 1966, 37, p.93.

18 T.C. Ferrar, E.D. Becker, Pulse and Fourier Transform NMR, Academic Press, 1971, pps. 43-45.

19 I.M. Armitage, H. Huber, D. White, W. Pearon and J.D. Roberts, Magn. Reson., 1974, 15, p.142.

20 G.C. Levy, J.D. Cargioli, F.A.L. Anet, J. Amer. Chem. Soc., 1973, 95, p.152.

21 R. Freeman and H.D.W. Hill, J. Chem. Phys., 1969, 54, p.3140.

22 E.L. Eliel, Stereochemistry of Carbon Compounds, McGraw-Hill Book Co. Inc., N.Y, 1962, pps. 219-234.

23 J.A. Pople, W.G. Schneider and H.J. Bernstein, High Resolution Nuclear Magnetic Resonance, McGraw-Hill, N.Y, 1959, p.166.

24 E.L. Hahn, Phys. Rev., 1950, 80, p.580.

25 H.Y. Carr and E.M. Purcell, Phys. Rev., 1954, 94, p.630.

26 Freifelder et al, J. Org. Chem., 1965, 30, pps. 2485-2486.

27 V.S. Hartmann, Patent 2, 152, 960, 1939.

28 Brunnel, Ann. Chimm., 1905, (8), (6), p.253.

29 G.E. McCasland and D.A. Smith, J. Am. Chem. Soc., 1950, 72, pps. 2190-2195.

30 A.G. Renwick, R.T. Williams, Biochem. J, 1972, 129, pps. 857-867.

31 U. Burckhardt, C.A. Grab and H.R. Kiefer, Helv. Chim. Acta., 1967, 50, pps. 231-244.

32 Roberts and Caserio, Basic Principles of Organic Chemistry, Publs. W.A. Benjamin, 1965, pps. 354-355.

33 Roberts and Caserio, Basic Principles of Organic Chemistry, Publs. W.A. Benjamin, 1965, p.417

34 P.F. Hudrlik, A. Hudrlik, A.K. Kulkarni, J. Am. Chem. Soc., 1982, 104 (24) pps. 6809-6811.

35 Kim Sunggak, Moon Young Choon, Aln, Kyotton, J. Org. Chem., 1982, 47 (17), pps.3311-3315.

36 E. Cesarrotti, A. Chiesa, S. Maffi, R. Ugo., Inorganic Chim. Acta., 1982, 64 (4), pps. 207-208.

37 Nasipuri Dhanonjoy, Sarkar Ashis, Kenar-Samirk, Ghosh Amlt A Bha, Indian J. Chem., Sect. B., 1982, 21 (B) (3), pps. 212-215.